FOSSIL ENERGY

DOE/BC/15112-4
(OSTI ID: 792223)

# OPTIMIZATION OF SURFACTANT MIXTURES AND THEIR INTERFACIAL BEHAVIOR FOR ADVANCED OIL RECOVERY

Final Report
September 30, 1998-September 29, 2001

By:
Prof. P. Somasundaran

Date Published: March 2002

Work Performed Under Contract No. DE-AC26-98BC15112

Columbia University in the city of New York
New York, New York

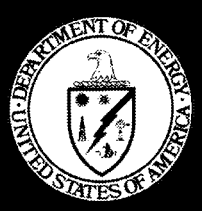


**National Energy Technology Laboratory**
**National Petroleum Technology Office**
**U.S. DEPARTMENT OF ENERGY**
**Tulsa, Oklahoma**

DOE/BC/15112-4
Distribution Category UC-122

# Optimization of Surfactant Mixtures and Their Interfacial Behavior for Advanced Oil Recovery

By
Prof. P. Somasundaran

March 2002

Work Performed Under DE-AC26-98BC15112

Prepared for
U.S. Department of Energy
Assistant Secretary for Fossil Energy

Jerry Casteel, Project Manager
National Petroleum Technology Office
P.O. Box 3628
Tulsa, OK 74101

Prepared by
Columbia University in the city of New York
Box 20, Low Memorial Library
New York, NY 10027

# TABLE OF CONTENTS

# LIST OF FIGURES

# LIST OF TABLES

# ABSTRACT

The objective of this project was to develop a knowledge base that is helpful for the design of improved processes for mobilizing and producing oil left untapped using conventional techniques. It was our aim to develop and evaluate mixtures of new or modified surfactants for improved oil recovery. In this regard, interfacial properties of novel biodegradable n-alkyl pyrrolidones and sugar-based surfactants have been studied systematically. Emphasis was on designing cost-effective processes compatible with existing conditions and operations in addition to ensuring minimal reagent loss.

The research involved a multi-pronged approach combining macroscopic measurements of phase behavior, interfacial tension, adsorption, electrokinetics, wettability and spectroscopic probing of adsorbed layers using fluorescence, electron spin resonance (ESR) and FTIR techniques. Solution and interfacial properties of n-alkyl pyrrolidones and sugar-based surfactants have been systematically investigated. Solution behavior of surfactant mixtures has been treated using regular solution theory to develop general guidelines for mixed surfactant systems. The adsorption of sugar-based surfactants on solids has been characterized and mechanisms explored. Mixtures of sugar-based surfactant with other surfactants used in the oil industry have been studied with parameters such as solid types, surfactant structure characteristics and solvent properties relevant to flooding sequence incorporated. Packed-column tests were conducted in order to determine the dynamics of surfactant adsorption. Theoretical modeling of the adsorption of surfactant molecules at the air-liquid interfaces both below and above the critical micelle concentration has also been developed. Through this integrated approach, a practical guide for designing innovative surfactant flooding schemes, using novel surfactants can be developed. It could help to effectively reduce interfacial tension between oil and flooding phase as well as lower the adsorption of surfactants on reservoir rocks.

# EXECUTIVE SUMMARY

The major aim of this research was to systematically investigate the micro and nanocharacteristics of alkyl pyrrolidones and sugar-based surfactants in solutions and at interfaces, especially in mixtures with other components, as a function of various parameters relevant to enhanced oil recovery (EOR), so that their interfacial behavior as surfactants in EOR processes can be optimized. During the three years, the interfacial behavior of these surfactants and their mixtures with other surfactants have been studied.

Alkyl pyrrolidones is a class of biodegradable surface active agents with low vapor pressure and low toxicity, which are miscible with water and oil. They possess all the characteristics required for oil flooding surfactants. Sugar-based surfactants are made from renewable resources, nontoxic and biodegradable. These environmentally benign surfactants feature high surface activity, good salinity and temperature tolerance, and unique adsorption behavior. This group of surfactants also has the potential for replacing currently used surfactants in oil recovery.

In the study of phase behavior and surface activity of N-hexyl 2-pyrrolidone (HP), it is found that HP and water are partially miscible above a lower consolute temperature (LCT) of 19.1 °C. HP is surface active at the air/solution interface and forms micelles in solutions at all temperatures. Another pyrrolidone surfactant, N-cyclohexyl-2-pyrrolidone (CHP), was found to form small micelles in water at a relatively high c.m.c. (0.45 M). The two-dimensional second virial coefficient of the adsorbed monolayer of CHP at the air/water interface suggests increasing attraction between chains with increase in temperature. Implications of increase in temperature in enhanced oil recovery (EOR) on adsorption due to this should be noted.

At solid/liquid interfaces, sugar-based surfactants have been found to absorb strongly on alumina, hematite and titania, but much less on silica. This behavior of alkyl maltoside on hydrophilic solids is exactly opposite to that of alkyl polyethylene oxide surfactants, although both groups of surfactants are nonionic in nature. This unique behavior of the sugar-based non-ionic surfactant has practical implications in controlling adsorption. Through systematic studies, it was concluded that hydrogen bonding between hydroxyl groups on the surfactants and alumina surface hydroxyl species is the primary force for the adsorption of alkyl polyglucosides on alumina.

Sugar-based surfactants have also been studied in mixtures with other surfactants to explore possible synergism or antagonism between these under various conditions. In solutions, sugar-based surfactants show synergy with cationic and anionic surfactants, the magnitude of such interactions follows the order anionic/nonionic > cationic/nonionic > nonionic/nonionic. At solid-liquid interfaces, depending on the solid types and the solution conditions, there are various interactions that decide synergy or antagonism. For example, dodecyl maltoside and sodium dodecylsulfate mixtures showed strong synergy on alumina/water interface at pH 6, but had antagonistic interactions at pH 11. The ratios of surfactant components on solids varied as a function of surfactant structure and concentration. These results have useful implications for the oil industry as weak adsorption of surfactants is essential for them to be cost effective in chemical flooding operations for enhanced oil recovery (EOR).

Packing columns studies have been carried out to study the kinetics of surfactant adsorption/desorption under situations close to oil recovery operations. The deaggregation of NP-15 hemimicelles from silica surface can enhance the desorption of NP-15. The adsorption of nonionic NP-15 on alumina is facilitated by the co-adsorbing anionic dodecyl sulfate and this co-adsorption can be a prolonged process. All such co-adsorption as well as desorption can have

marked effects on surface properties such as wettability.

A theoretical model for the adsorption of surfactant molecules at the air-liquid and solid-liquid interfaces has been developed. This model was developed for the kinetics of surfactant adsorption, i.e., surfactant adsorption from the bulk solution as a function of time. A pendant bubble setup to measure dynamic surface tension of $C_{14}E_6$ solutions above the CMC has been carried out in order to test this model. The experimental results are compared with the theoretical predictions. Indeed there is a need to develop a universal model that can predict interfacial behavior in terms of surfactant structure, solid properties and the medium.

# INTRODUCTION

Nearly 40% of all the energy consumed in the United States is derived from the oil and notably, more than 50% of this oil is currently imported. The latter figure is expected to grow in the coming decades increasing the dependence of this country on imports. From the point of view of national economy and energy security, effort must therefore be directed towards maximizing domestic oil production through increased application of adequate enhanced technologies. Domestic oil reservoirs are not fully exploited primarily because of the high costs as well as associated environmental concerns. While the probability of discovering new large oil fields in the United States is limited, nearly 300 billion barrels out of a possible 500 billion barrels of oil remain unrecovered in U.S. reservoirs. For a majority of these reservoirs, the use of improved extraction techniques is required to mobilize and produce oil remaining after secondary processes have been applied. However, the chemicals considered currently for the recovery techniques are expensive rendering the process often uneconomical. It is therefore critical to develop cost-effective chemical schemes to increase oil recovery from domestic oil reservoirs.

The benefits of secondary recovery techniques such as water flooding and steam flooding have been demonstrated in various field projects since the early part of this century. However, the presence of substantial quantities of oil in the reservoir, even after a successful waterflood, has prompted development of tertiary oil recovery methods to recover a third crop of oil. Miscible flooding has the potential to fully displace the oil in place, the main obstacle being the forces which bind the oil to the rock. The oil in the reservoir can be displaced if the interfacial tension between the oil and the driving fluid can be reduced and the micellar flood is effective in doing this due to the presence of highly surface active materials. The residual oil saturation of a reservoir is a strong function of low oil-water interfacial tension. Following the micellar slug, a low salinity

water/polymer solution is injected to control the mobility and to push the micellar slug uniformly through the formation. The efficiency and feasibility of the miscible flooding process are governed by several factors including accessibility of the surfactant to the oil in the reservoir pores, loss of the surfactant and/or polymer by adsorption and precipitation, interactions between the polymer and the surfactant in the slug, competitive or synergistic interactions among surfactant components in the slug that are invariably mixtures of many surfactants, and irreversible degradation of the reagents under high shear forces.

Among these factors, loss of surfactants and polymer by adsorption on reservoir minerals or precipitation with dissolved ions is a crucial problem determining the utilization of micellar flooding for oil displacement. Hence the study of adsorption/desorption and precipitation of oil flooding surfactants of diverse characteristics has been a major focus of current research. Significant progress has been made in understanding the adsorption/desorption behavior of single surfactants on reservoir minerals. However there are very few studies to understand the interfacial behavior of surfactant mixtures even though commercial surfactants are invariably mixtures of several surfactants. Work is clearly needed with surfactant mixtures and solids relevant to enhanced oil recovery. Moreover, no information exists on the dynamics of adsorption/precipitation in mixed surfactant systems. Clearly, study of mixed systems is imperative for designing surfactant mixtures for innovative reagent schemes for advanced oil recovery.

Further more, there are new classes of surfactants such as alkyl polyglucosides and alkyl pyrrolidones which have attracted attention recently due to their environmentally benign characteristics and high surface activities. Sugar based alkyl polyglucosides surfactants are manufactured from natural products and are biodegradable making them environmentally benign. They have many unique solution and interfacial properties such as highly surface activity, high salt

tolerance and no cloud point, as the solubility of such surfactants is a result of the hydroxyl groups and not ether oxygens (as in ethoxylates).[1-4] The greater stability of these surfactants at high temperatures and high salinity makes them suitable for use in the enhanced oil recovery. In addition, sugar-based surfactants have unique adsorption properties. Their affinity towards siliceous oxides is very low. This property could serve well in oil recovery applications since the reservoir minerals are predominantly silica based.

Another new class of agents currently under investigation are N-alky-l-pyrrolidones. N-alkyl-2-pyrrolidones comprise a class of biodegradable surface active agents with low vapor pressure and low toxicity, which are partially or completely miscible with water, depending on the chain length and the temperature. These molecules are very polar, with dipole moments close to 4 debye and will dissolve a variety of electrolytes.[5-6] They are highly surface active with increasing effectiveness at high temperatures, miscible with water and oil, compatible with inorganics and effective cosurfactants with anionics. Thus, they possess all the characteristics required for oil flooding surfactants. A knowledge of adsorption processes in mixed systems and interactions using such surfactants should enable us to design combinations of benign surfactants for optimum performance.

It was the aim of this research to seek solutions for the ways to minimize adsorption of surfactants on reservoir minerals by using appropriate surfactant combinations, to develop means to control the adsorption and micellization behavior in terms of the properties of the surfactant components, the solid, mixing ratios etc., to determine the attenuation in adsorption of surfactants due to cosurfactants, electrolytes and solution pH. It is also the aim to determine the role of mixed micelles and their structural changes on the behavior of surfactants at interfaces and the role of any changes in salinity, reservoir water hardness and high temperature conditions on the

adsorption/desorption of mixed surfactants on minerals. Most important, we aimed to investigate novel application of surfactants (sugar-based surfactants and N-alkyl pyrrolidones) which are highly surface active, salt tolerant, efficient at high temperatures and biodegradable, and mixtures of sugar-based surfactants and other surfactants commonly used in EOR. Finally, the basic parameters required for modeling the behavior of surfactant mixtures in solution and at the solid-liquid interfaces are being identified and a predictive model for their performance is being developed.

# MATERIALS & METHODS

## MATERIALS

*Surfactants:*

Several typical ionic and nonionic surfactants were selected for this study. Anionic sodium dodecyl sulfate (SDS) of greater than 99% purity purchased from Fluka chemicals and cationic dodecyl trimethyl ammonium bromide (DTAB) of greater than 99% purity purchased from TCI Chemicals, Japan were used as received. Nonionic ethoxylated surfactants covering a wide range of hydrophobic and hydrophilic chain lengths including ethoxylated alcohols ($C_nH_{2n+1}(CH_2CH_2O)_mH$ or $C_nEO_m$ ) and nonyl phenols were purchased from Nikko Chemicals.

Non-ionic sugar-based surfactant, n-alkyl-β-D-glucosides and n-alkyl-β-D-maltosides from Calbiochem and dodecyl polyglucoside from Henkel Corp., were also used as received. Dodecyl polyglucoside was an industrial sample with various headgroup configurations and glucose unit distributions, while n-alkyl-β-D-glucosides and maltosides were relatively pure ( at least >95% purity by TLC) and served as a model compound for alkyl polyglucosides. The structures of n-dodecyl-β-D-maltoside and dodecyl polyglucoside are shown in Figure 1.

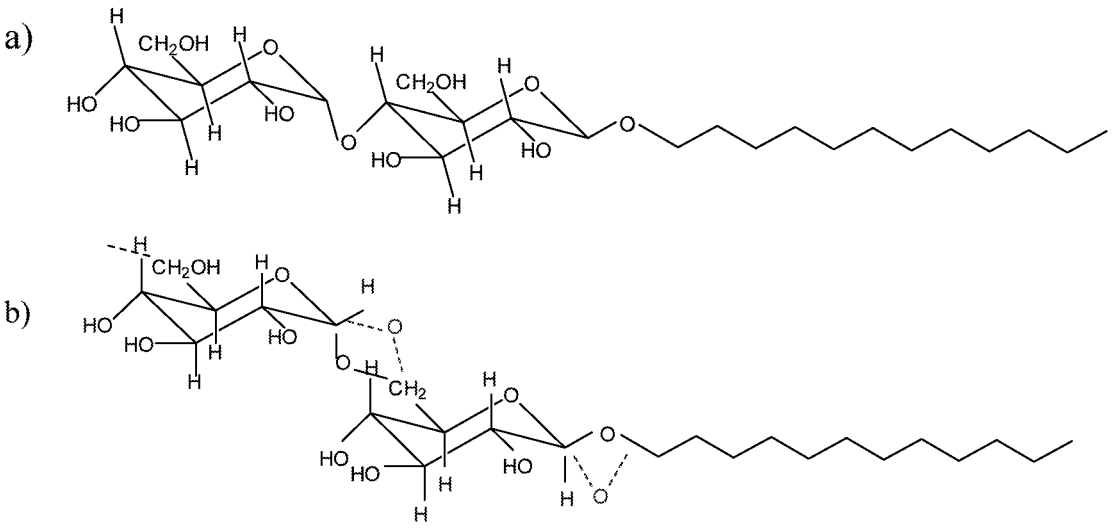


**Figure 1. The Chemical Structures of a) n-dodecyl-β-D-maltoside, and b) dodecyl polyglucosides**

All surfactants used for the study are listed in table I.

**Table 1. Surfactants used and their formulas**

| Surfactant | formulas |
|---|---|
| Sodium dodecylsulfate | $C_{12}H_{23}SO_4Na$ |
| Dodecyltrimethylammonium bromide | $[CH_3(CH_2)_{11}N(CH_3)_3]Br$ |
| Polyethoxylated alcohol | $C_nH_{2n+1}(CH_2CH_2O)_mH$ |
| Polyethoxylated nonyl phenol | $C_9H_{19}(C_6H_4)(CH_2CH_2O)_nH$ |
| n-octyl-β-D-glucopyranoside | $CH_3(CH_2)_7[C_6H_{10}O_5]OH$ |
| n-nonyl-β-D-glucopyranoside | $CH_3(CH_2)_8[C_6H_{10}O_5]OH$ |
| n-decyl-β-D-glucopyranoside | $CH_3(CH_2)_9[C_6H_{10}O_5]OH$ |
| n-dodecyl-β-D-glucopyranoside | $CH_3(CH_2)_{11}[C_6H_{10}O_5]OH$ |
| n-octyl-β-D-maltoside | $CH_3(CH_2)_7[C_6H_{10}O_5]OH$ |
| n-decyl-β-D-maltoside | $CH_3(CH_2)_9[C_6H_{10}O_5]OH$ |
| n-dodecyl-β-D-maltoside | $CH_3(CH_2)_{11}[C_6H_{10}O_5]OH$ |
| n-tetradecyl-β-D-maltoside | $CH_3(CH_2)_{13}[C_6H_{10}O_5]OH$ |
| Dodecyl polyglucoside | $CH_3(CH_2)_{11}[C_6H_{10}O_5]_nOH$ |

*N-alkyl-2-pyrrolidones*

In this work, N-ethyl, butyl, hexyl, octyl, and dodecyl-2-pyrrolidones were used. The structure of the pyrrolidone is shown in Figure 2.

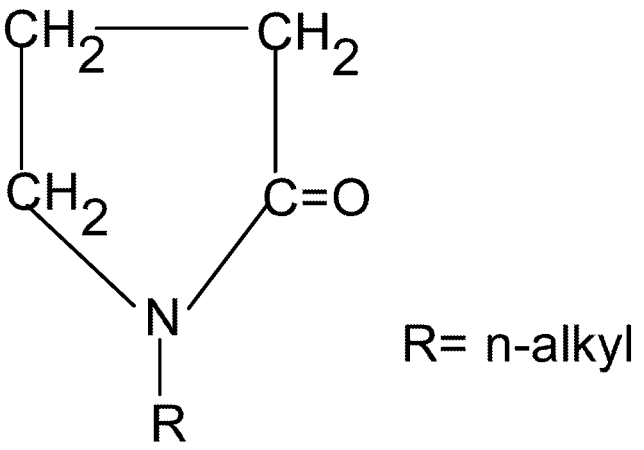


**Figure 2. The Structure of N-alkyl-2-pyrrolidone**

These compounds were analyzed by GLC. Purity of all the N-alkyl-2-pyrrolidones was greater than 99.6%. All the materials were provided by International Speciality Products Inc.

*Mineral Samples:*

Solid substrates selected for this study are alumina, hematite, titania, silica and graphite which have been well characterized in the past. These solids were chosen because of their low solubility, and relatively surface homogeneity with considerable amounts of information available in the literature. They are listed in Table 2.

**Table 2. List of Solids Used**

| Name | isoelectric point (iep) | mean particle size (μm) | specific surface area ($m^2/g$) | Source |
|---|---|---|---|---|
| Alumina (AKP-50) | 8.9 | 0.2 | 10.8 | Sumitomo |
| Alumina | 9.0 | 0.3 | 14 | Praxair |
| Silica | 2 | 0.2 | 5.8 | Johnson-Matthey |
| Silica | 2 | 0.3 | 12.21 | Geltech |
| Silica gel | 2 | 40 - 100 | 25 | Spherosil |
| Titania | 2 | 2 | 2.133 | Alfa Products |
| Kaolinite | -- | -- | 8.2 | Univ. of Missouri |

*Other Chemicals:*

HCl and NaOH, used for pH adjusting, were of A.C.S. grade certified (purity > 99.9%) and from Fisher Scientific Co.. Maltose was from Calbiochem, dimethyl sulfoxide from Sigma Chemical Co. and Urea from Fisher Scientific Co. To study the salt effects on surface tension, micellization and adsorption, LiCl, NaCl, KCl, $CaCl_2$, $AlCl_3$, NaF, NaSCN, $Na_2SO_4$, and $Na_3PO_4$ from Fisher Scientific Co.; RbCl from Alfa Products; NaBr and NaI from Aldrich Chemical Company, Inc.; and sodium citrate from Amend Drug & Chemical Company were used as received. They are all A.C.S. certified.

Water used in all the experiments was triple distilled, with a specific conductivity of less than $1.5\mu\Omega^{-1}$ and tested for the absence of organics using surface tension measurements.

Pyrene was obtained from Aldrich Chemicals and recrystallized from ethanol. All solutions were prepared in triply distilled water and at constant ionic strength as mentioned in later sections.

## METHODS

*Adsorption*:

Adsorption experiments were conducted in capped 20 ml scintillation vials. Solid samples of 2 gram were mixed with 10 ml of triple distilled water for 2 hours at room temperature. The pH was adjusted as desired and then 10 ml of the surfactant solution was added and equilibrated further for 16 hours with pH adjustment. The suspensions were then centrifuged at 3000-4000 rpm for 30 minutes and the supernatant analyzed for the residual concentration. Adsorption was calculated based upon surfactant depletion from the solutions.

*Desorption:*

After adsorption, desorption tests were conducted by removing part of the supernatant and adding water to make up for the volume of the supernatant removed. The total volume and thus solid-liquid ratio remained constant. Adsorption density was calculated from the change in concentration of the surfactant.

*Analytical Techniques*:

Sodium dodecylsulfate (SDS) concentration was determined using a two-phase titration method.[7] Dodecyltrimethyl ammonium chloride (DTAB) concentration was determined by complexing the surfactant with excess SDS and measuring the non-complexed SDS using the two-phase titration. The concentration of ethoxylated alcohol ($C_nEO_m$) was determined either by total organic carbon (TOC) analysis or using high pressure liquid chromatography (HPLC) with a $C_{18}$ bonded silica column and a refractive index detector. The solvent used was a 90:10 mixture of acetonitrile and water. Pentadecylethoxylated nonyl phenol concentration was determined by UV absorption at 223 nm. Sugar-based surfactant concentration after adsorption was determined by measuring the total organic carbon (TOC) in the sample using a Shimazu Total Organic Carbon

Analyzer, or by colorimetric method through phenol-sulfuric acid reaction.[8] In surfactant mixtures, the total surfactant concentration was measured by TOC method, while the SDS or DTAB concentration was measured by the two-phase titration, NP-10 by UV-Vis method and sugar-based surfactant by the colorimetric method.

*Surface tension*:

Surface tension of the surfactant solutions was measured using a Wilhelmy plate made of platinum, or by drop volume method using a syringe.

*Electrokinetics*:

Zeta potential of the samples was determined using a Pen Kem Laser Zee Meter. After the surfactant adsorption, the sample was diluted with its own supernatant to make a dispersion of suitable solid concentration.

*Calcium Ion Measurement*:

The $Ca^{2+}$ ion concentration was measured by an Orion Research Microprocessor Ionalyzer (model 901) using a calcium electrode (Orion Research).

*FTIR Spectroscopy*:

A Perkin Elmer Paragon 1000 PC FTIR spectrometer was used to record the IR spectra for the attenuated total reflectance(ATR). ATR was conducted in-situ for solid/liquid slurries in a nine-reflection prism cell (ZnSe, 45°) supplied by Harrick scientific Co.

*Fluorescence spectroscopy*:

A Photon Technology International PTI LS-100 was used for fluorescence experiments. The

samples containing pyrene dissolved to its maximum solubility in water ($\approx 2x10^{-7}$ kmol/m$^3$) were excited at 335 nm and emission between 365 and 500 nm was recorded.

*Packing column test*

The setup is adapted from the high performance liquid chromatographic (HPLC) equipment. A column packed with silica gel (Fisher Science) or alumina powder (Pairax) is used in this study. The dimension of column was 4.5mm diameter x 250mm length. Surfactant solutions at desired concentrations were pumped through the packed column at a rate of 2 ml/min., and the changes in surfactant concentrations were monitored by a UV-vis detector as a function of time. The surfactant used for this tests was the nonionic pentadecylethoxylated nonylphenol (NP-15). The set-up for packing column test is schematically shown in figure 3.

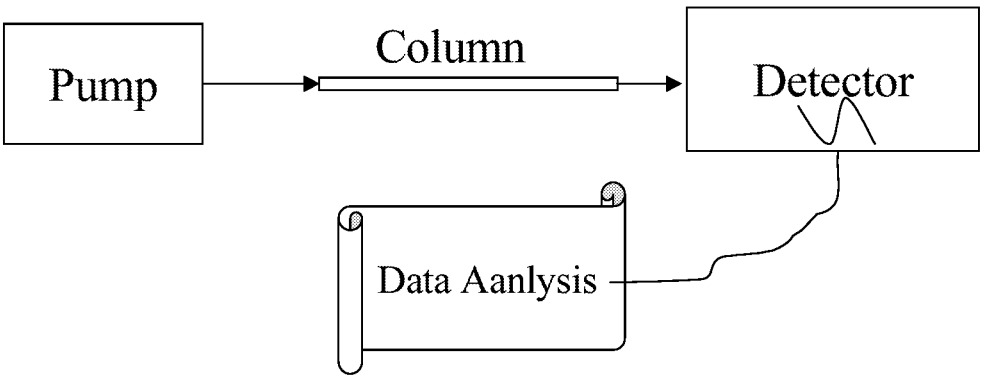


**Figure 3. Schematics of packed column test set-up**

# RESULTS & DISCUSSION

## 1. PHASE SEPARATION, SURFACE ACTIVITY AND MICELLIZATION IN MIXTURES OF N-HEXYL 2-PYRROLIDONE AND WATER

The N-alkyl-2-pyrrolidones comprise a class of biodegradable surface active solvents with low vapor pressure and low toxicity, which are partially or completely miscible with water depending on the chain length and temperature. These molecules are very polar, with dipole moments close to 4 Debye and liquid dielectric constants in the range of 32 (methyl) to 20 (dodecyl). The liquids are conducting and dissolve a variety of electrolytes. The molecules form a resonance hybrid of a nonionic and zwitterionic molecule.

To understand the interfacial and micellization behavior of pyrrolidones, tests were done with pyrrolidones of different carbon chain length and structures. For n-hexyl 2-pyrrolidone (HP), it has been found that it is fully miscible with water below 19.1 °C. Above this lower consolute temperature (LCT) two phases are formed (Fig.4).

The interfacial tensions ( $\sigma$ ) of the coexisting phases above the LCT are given in Fig.5, with the tension shown as zero at the LCT. Measurements of $\sigma$ close to $T_c$ were difficult with the spinning drop apparatus since the drop size varies substantially with temperature, which was controlled within ± 0.1 °C. The density difference between the co-existing phases is also small at temperatures well away from $T_c$, making precise values of $\sigma$ difficult to measure. The data were therefore inadequate for estimating the critical exponent for surface tension.

The surface tension at the air/solution interface at 18.°C (just below the LCT) across the whole miscible range of concentration shows a plateau region from approximately 5 to 70% (w/w), as seen in Fig.6. Above about 70 w/w% HP, the surface tension rises, indicating that water is positively adsorbed from very concentrated HP solutions. The plateau in Fig.6 indicates micellar

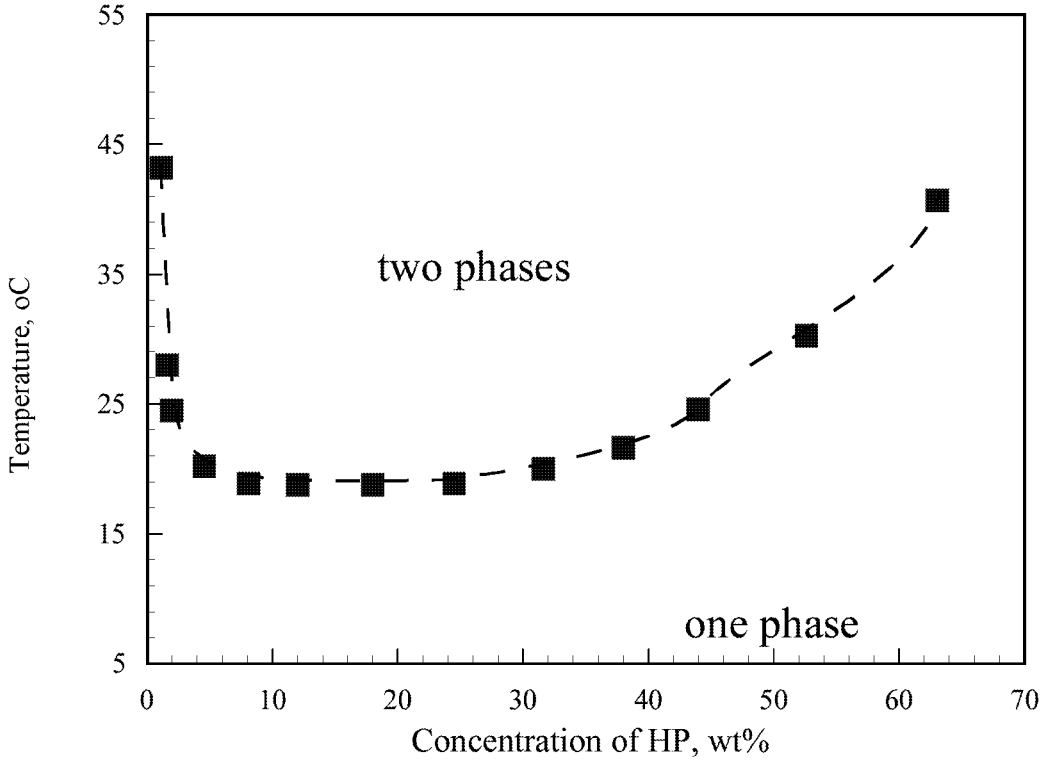


**Figure 4. Phase Diagram of Hexyl-Pyrrolidone with Water**

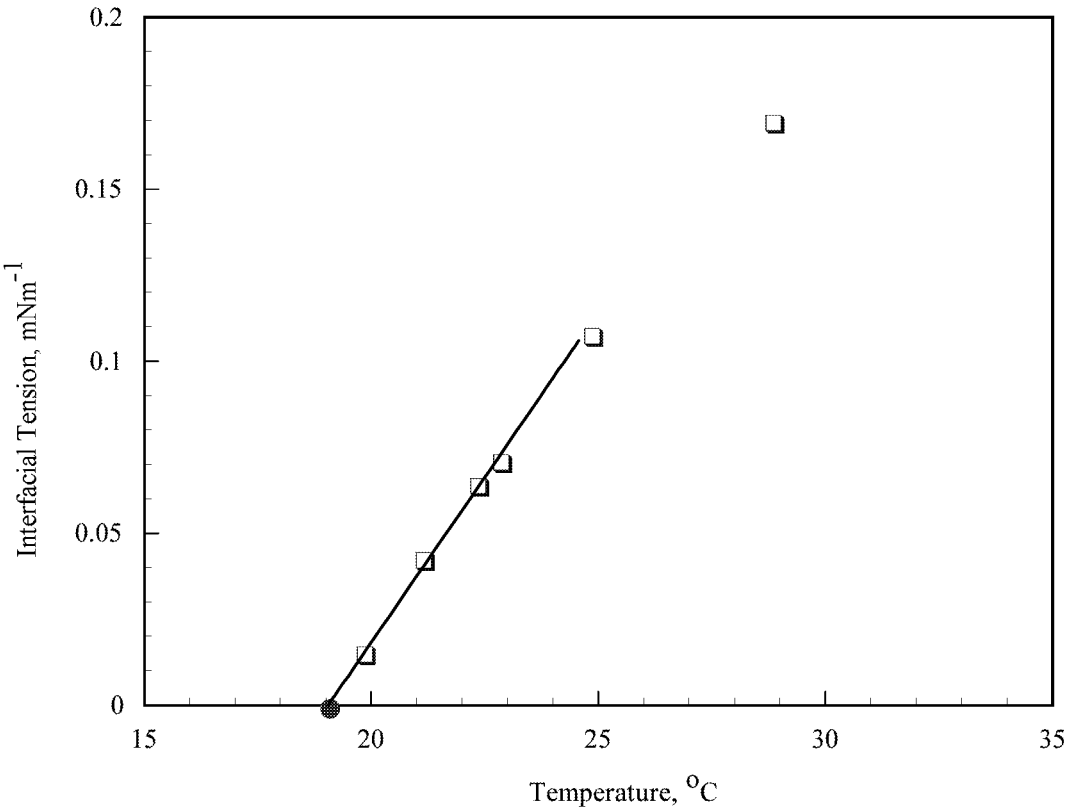


**Figure 5. Interfacial Tension in the N-Hexyl-2-Pyrrolidone/Water Two-Phase System at Different Temperatures. The LCT is indicated at zero tension.**

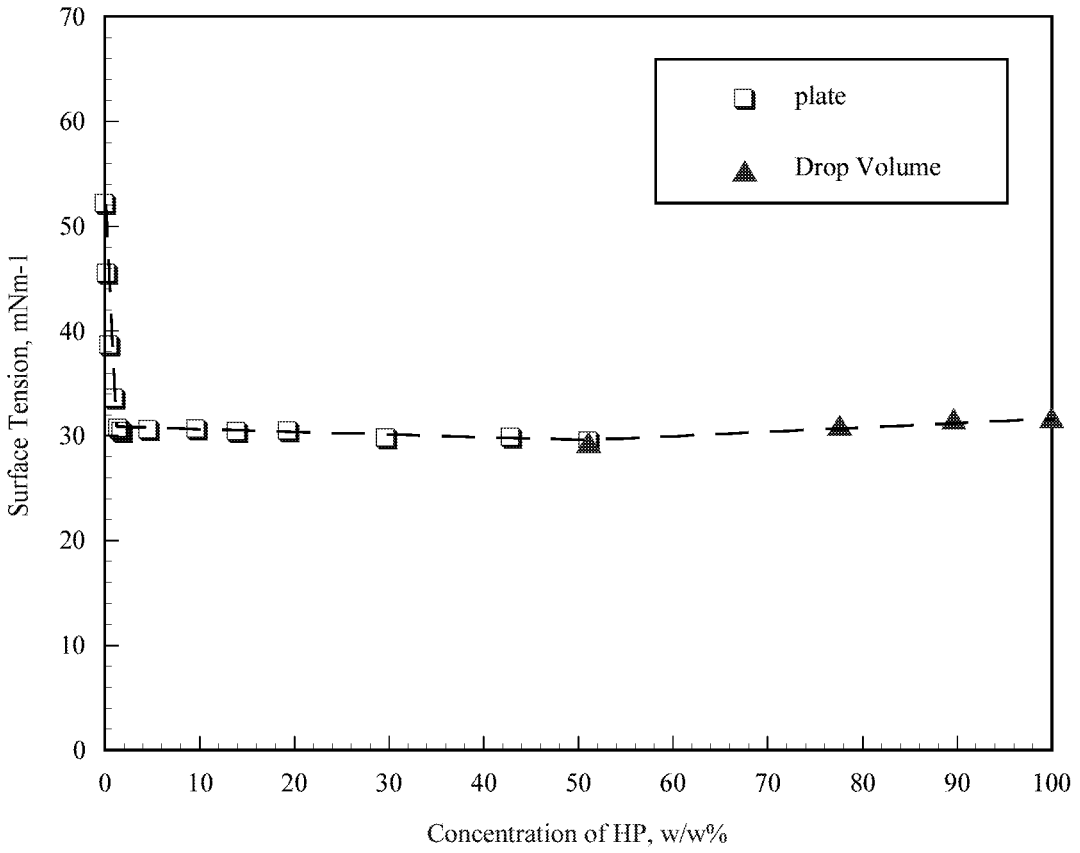


**Fig.6. Surface Tension of Solutions of N-hexyl-2-pyrrolidone in Water at 18 oC.**

aggregation in the solution. Micelle formation was confirmed by measurements of the freezing point depression ($\Delta T$) of water-rich mixtures, shown in Fig.7. The abrupt change in trend at 0.14 M (molal) strongly suggests micelle formation above this concentration. The aggregation number, as determined from the slope of $\Delta T$ against concentration above the CMC, may be estimated as 80 at the freezing point.

The formation of micelles was further probed by surface tension measurements at 15 °C, and also confirmed by the large increase in the solubility of pyrene above about 0.15 M in HP/water mixtures at 20 °C shown in Fig.8. At 25 °C, the surface tension results (Fig.10) suggest micelle formation just below the saturation limit. The phase diagram in the water-rich region including

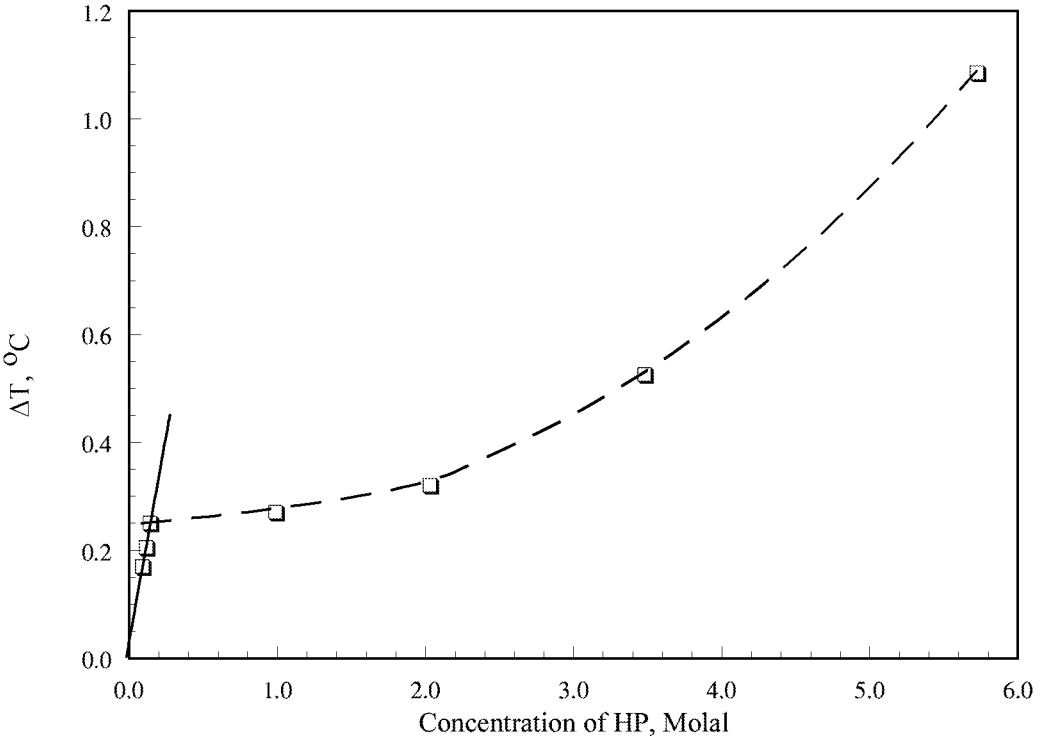


**Figure 7. Depression of the freezing point (DT) of N-hexyl-2-pyrrolidone solutions in water**

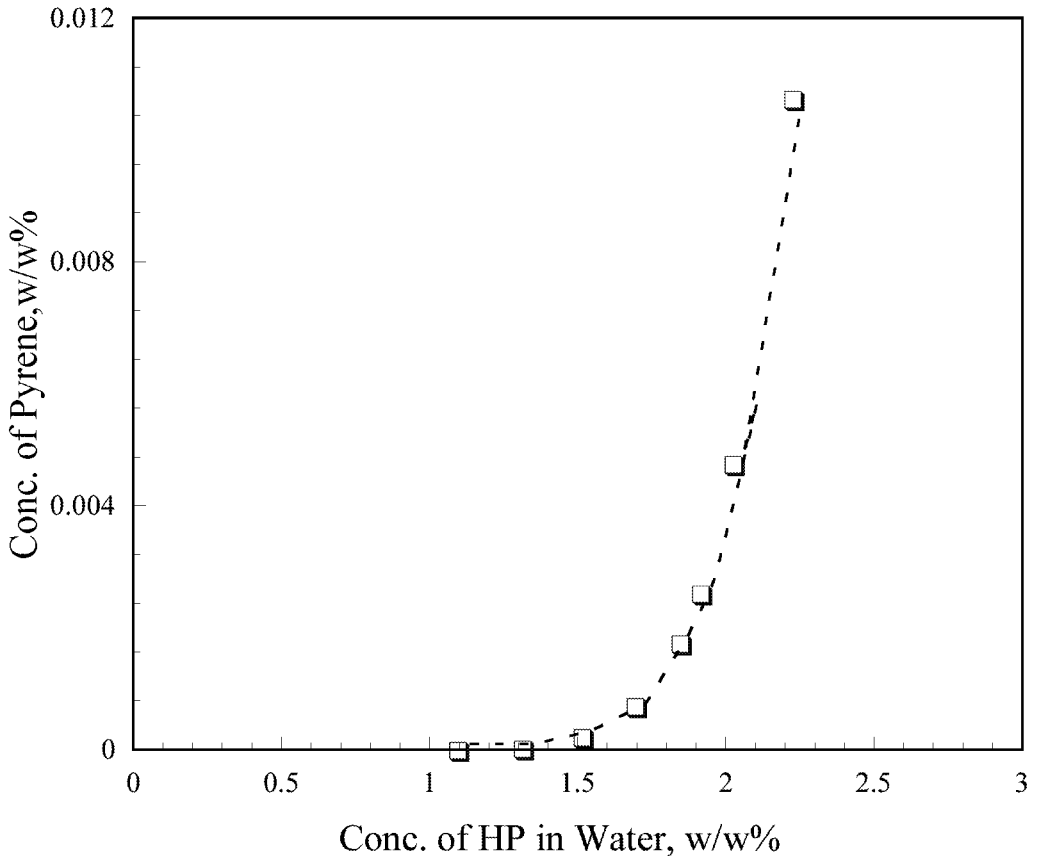


**Figure 8. Solubility of Pyrene in N-Hexyl-2-Pyrrolidone/Water mixtures at 20 °C**

micelle formation and ice separation is shown in Fig.9. The CMC-temperature relationship suggests a shallow minimum in the range 15-19 °C, corresponding to a zero heat of micellization. The solubility of HP in water as a function of temperature shows an inverse Kraft point, solubility increasing as T is lowered until micelle formation begins and the solubility increases rapidly with further lowering of the temperature.

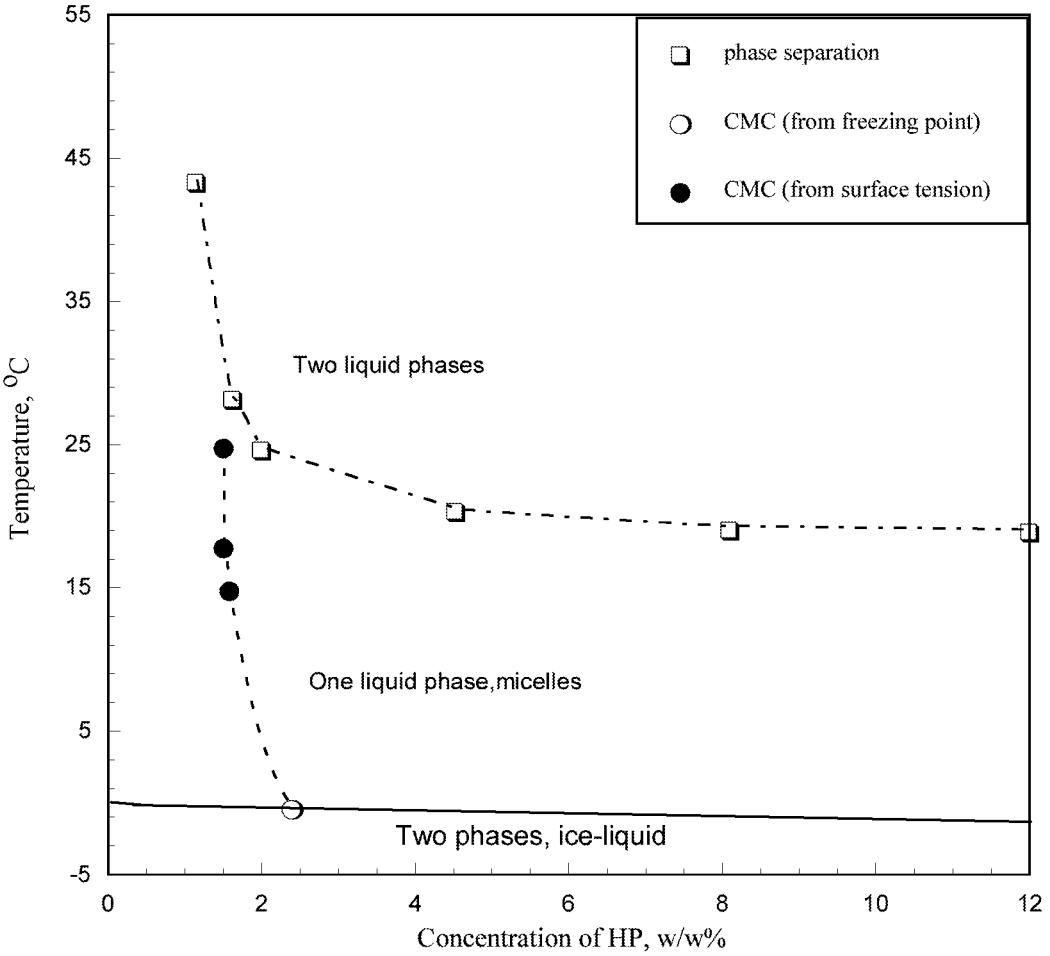


**Figure 9. Phase diagram of N-hexyl-2-pyrrolidone in water including micelle formation and ice separation**

From the air/water surface tension results shown in Fig.10, the excess surface density (Γ) of the adsorbed HP at 25 °C close to the phase separation boundary may be calculated from the Gibbs equation in the form

$$d\Pi/d\ln a = kT\Gamma = (d\ \Pi/d\ \ln c)(d\ \ln c/d\ \ln a) \quad (1)$$

where $\Pi$ is the surface pressure of the adsorbed HP monolayer, and a and c are the activity and concentration (molal) of HP in water. The activity coefficient (a/c) may be estimated from the freezing point results, assuming zero heat of dilution below the CMC. The osmotic coefficients (g) below the CMC are given within experimental error by $g = (1-\lambda c)$, where $\lambda$ is 0.5 ±0.05. The activity coefficient is related to g by $-\ln(a/c) = 2(1-g)$, so that

$$d\ \Pi/d\ \ln c = = kT\Gamma\ (1-2\lambda c) \quad (2)$$

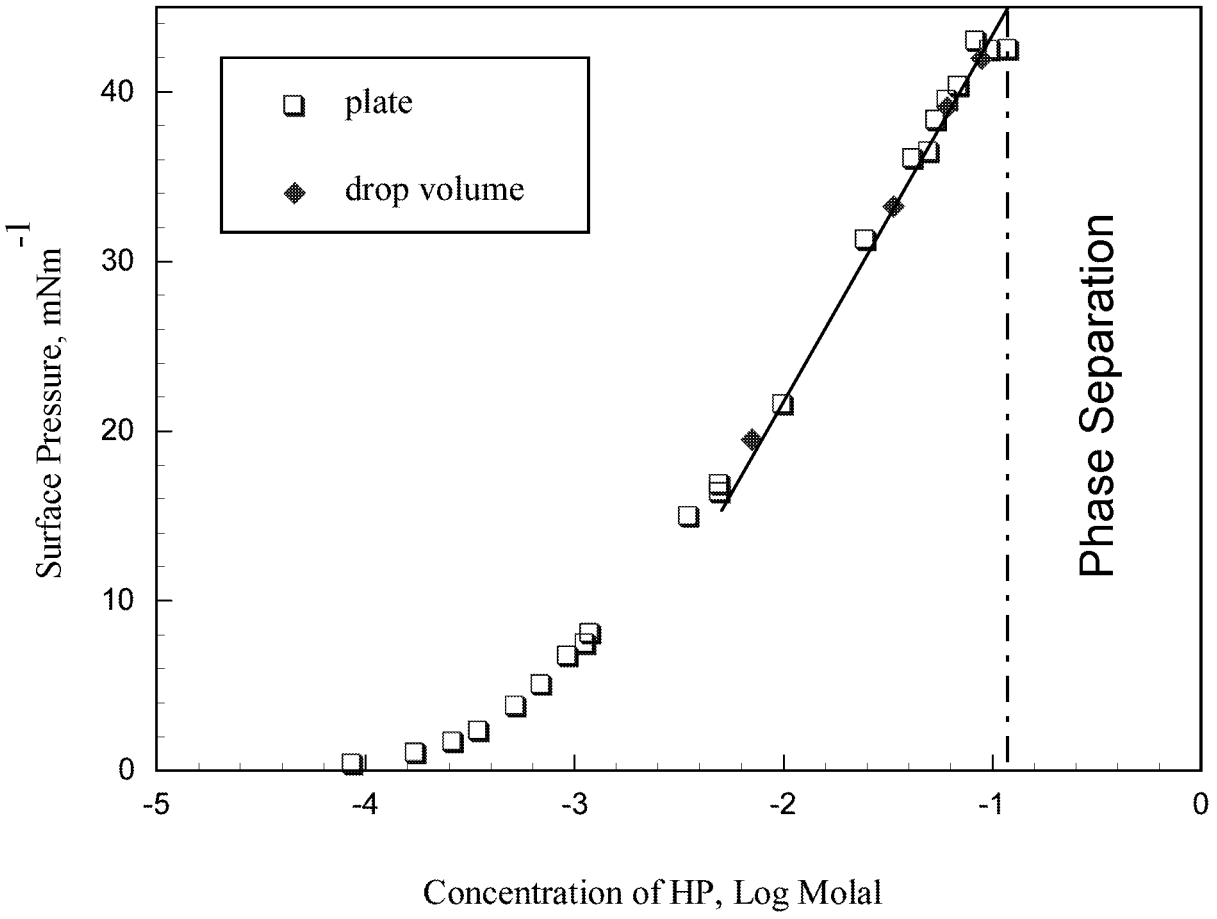


**Fig.10. Surface Pressure of Solutions of N-Hexyl-2-Pyrrolidone in Water at 25 oC**

In the Π-log c region close to the solubility limit at 25 °C, the activity coefficient is not lower than 0.9, and the adsorption of HP corresponds to an area/molecule of 0.38 $nm^2$/molecule for the N-octyl and N-dodecyl-pyrrolidones without using the activity correction at the much lower concentration required for these two homologs. The Π-A (area per molecule) isotherm at 25 °C at the air/solution interface for HP is shown in Fig.11. There is no evidence for saturation adsorption at higher pressures.

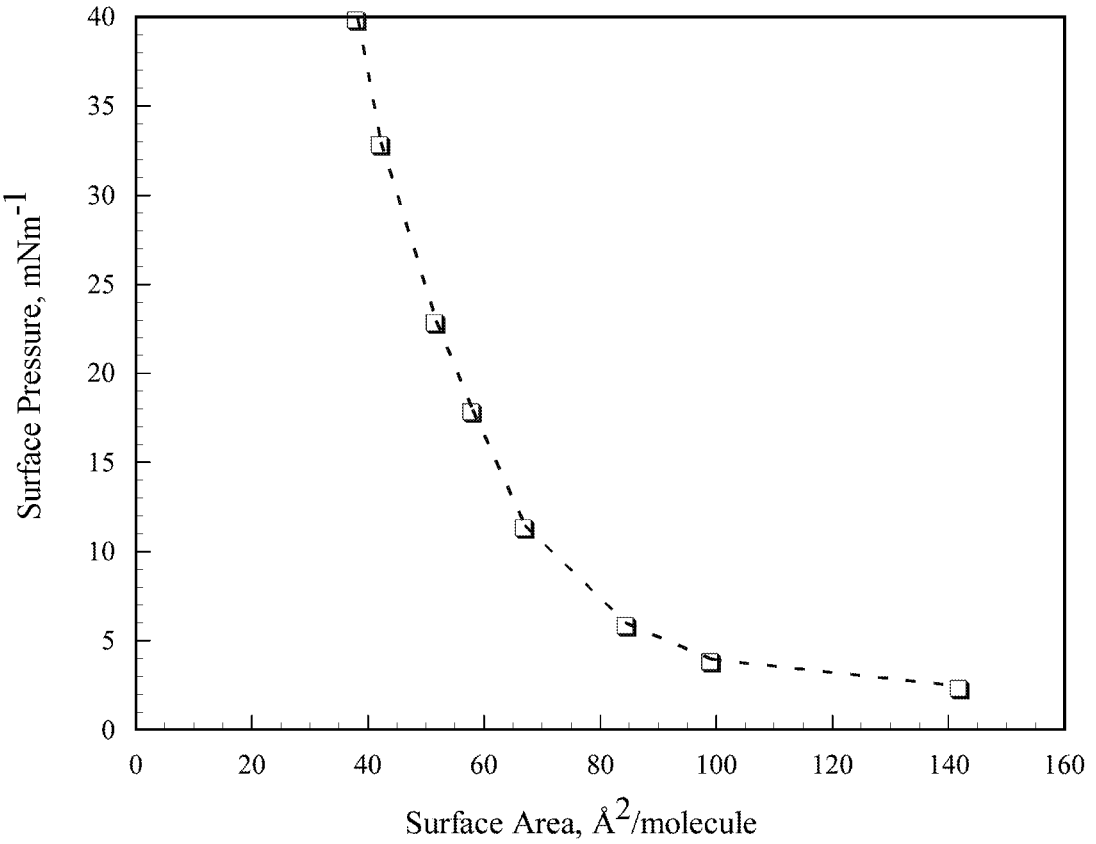


**Fig.11. Surface pressure-area isotherm for N-Hexyl-2-Pyrrolidone adsorbed from aqueous solution at 25 °C**

In summary, the principal findings of this part of the study are that N-hexyl 2-pyrrolidone in mixtures with water shows a lower consolute temperature and forms micelles over a wide concentration range. Unlike the widely studied non-ionic surfactants of the alcohol-polyoxethylene

type, the phase diagram shows no sign of a closed loop (Fig.4). The existence of micellar aggregates is clearly shown by the results for surface tension, freezing point and the pyrene solubility in HP/water mixtures. Micelles have been demonstrated at all temperatures between the freezing points and the LCT, and at temperatures up to about 25 °C in water-rich mixtures where the CMC is close to the two-phase boundary. The surface tension results for the entire concentration range below the LCT (Fig.4) show that micellar aggregates are also present in the mixtures up to about 70% HP by weight (0.2 mole fraction HP) below the LCT, and it is possible that these micelles are also present in the HP-rich one-phase region up to the phase separation temperature. At even higher concentrations of HP, the observations completed so far indicate that only water is positively adsorbed at the HP/air interface, without evidence for aqueous aggregates. Based on the high surface pressure data at the air/solution interface, the surface excess is in accord with what is expected from molecular models for the close packing.

The micellar behavior of HP and its relation to the phase diagram are similar to that found for 2-butylethanol/water mixtures, except that the HP/water phase diagram shows no closed loop for the miscibility as a function of temperature. Results obtained for the N-substituted 2-pyrrolidones show that micelles are formed with several compounds showing a lower consolute point with water, and that manipulation of the LCT by the addition of a third component modifies or induces micellization.

## 2. MICELLIZATION BEHAVIOR OF N-CYCLOHEXYL-2-PYRROLIDONE

Figure 12 shows the surface tension (measured by the drop volume method to avoid contact angle problems at high CHP concentrations) at 22 ± 0.5 °C across the whole concentration range. CHP is surface active, and the air/solution surface tension can be decreased to about 40 $mNm^{-1}$ at a plateau in the range from approximately 10-60% w/w. The results suggest the formation of aggregates of CHP in solution above about 7% w/w (0.45 M). Above 60% w/w, the surface tension decreases from the plateau value. This indicates clearly that the structure of mixtures above 60% CHP is no longer one of simple aggregates of CHP in water and that water is negatively adsorbed at high CHP ratios. Micelle formation with a critical micelle concentration (c.m.c.) of about 0.45 M is suggested clearly in Fig. 13, which shows the surface tension as a function of concentration at two temperatures.

Micelle formation of CHP molecules in aqueous solution was confirmed by measurements of the solubility of pyrene and of the polarity parameter ($I_3/I_1$ ratio) in CHP aqueous solutions. Fig. 14 shows the solubility of pyrene in CHP solutions. The solubility increases sharply above a concentration of about 6%, close to the c.m.c. value estimated from the surface tension results. The $I_3/I_1$ ratio of the pyrene spectrum as a function of CHP concentration in water is shown in Fig. 15 at a constant pyrene concentration of $3 \times 10^{-7}$ M. It is seen that the ratio initially increases slightly with concentration, but with a definite change in trend over a narrow concentration range at about 6% w/w% CHP to an almost constant value of about 0.72 at high CHP concentrations. This ratio is significantly lower than that for pyrene in SDS micelles (~0.9) and similar to the ratio for dilute pyrene in pure CHP ((0.73). This shows that the interior of the CHP micelle is more polar than those of the liquid paraffins which represent the interior of SDS micelles.

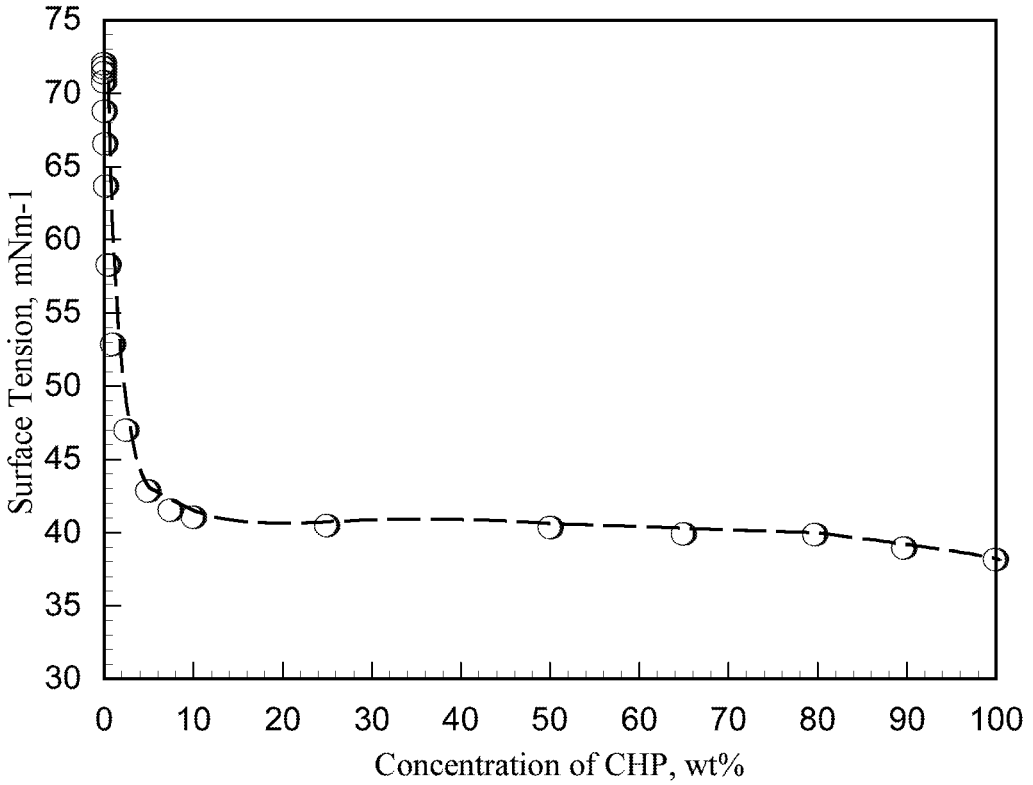


**Figure 12. Surface tension of CHP aqueous solutions at 21 °C using Drop Volume Method**

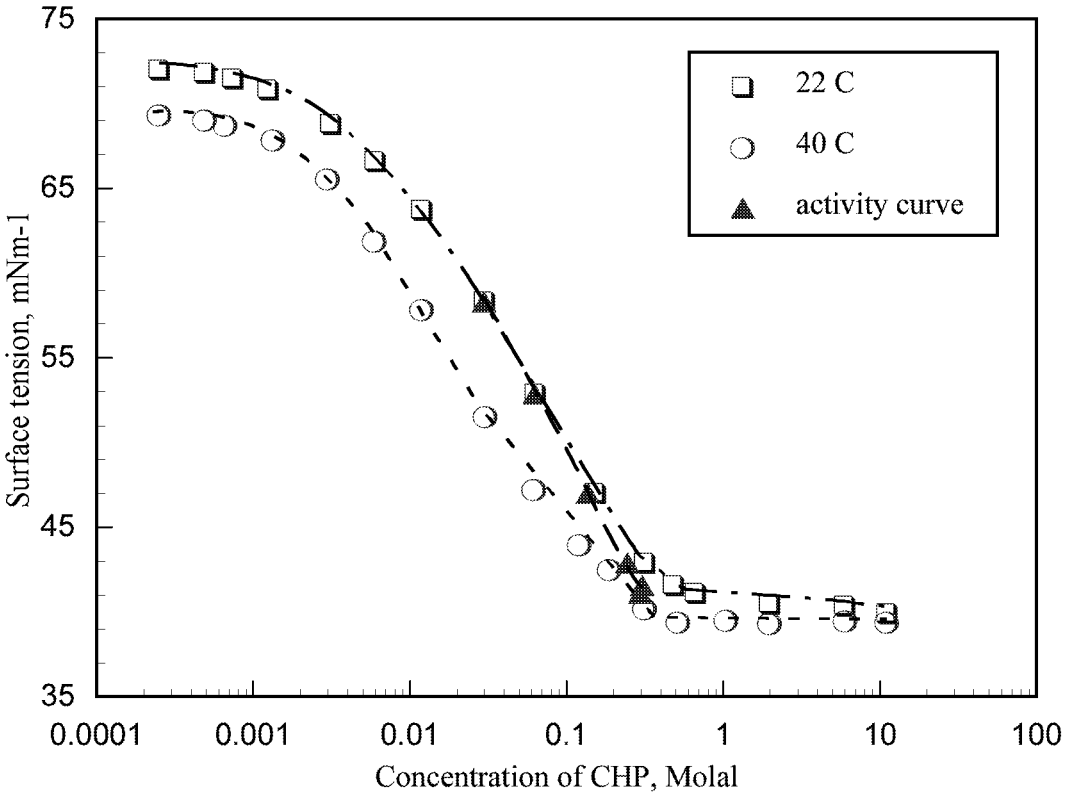


**Figure 13. Surface tension of CHP at different temperatures using plate and drop volume methods**

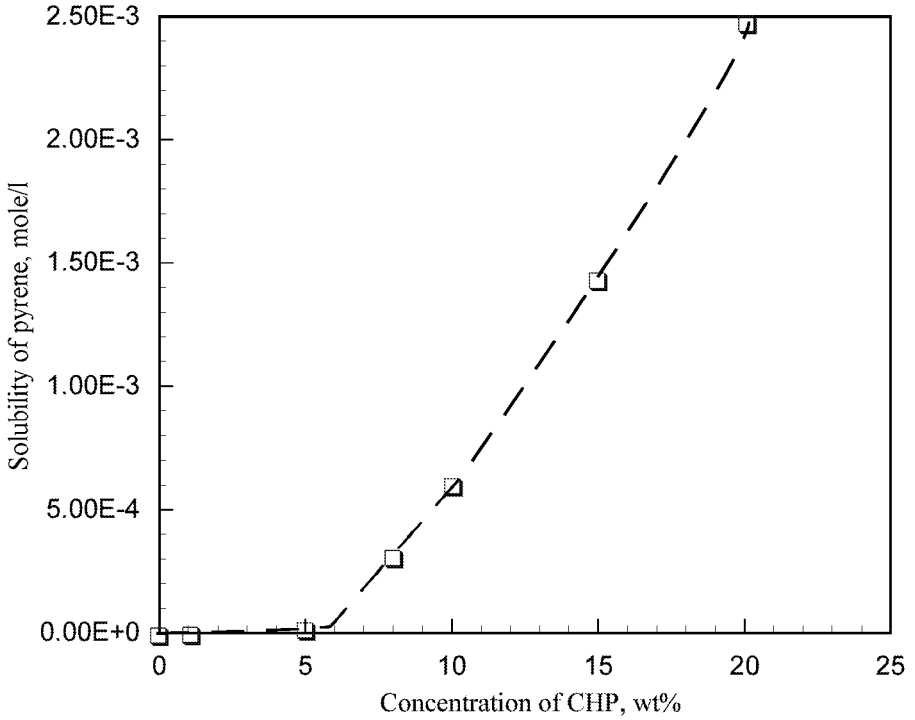


**Figure 14. Pyrene solubility in CHP/Water mixtures**

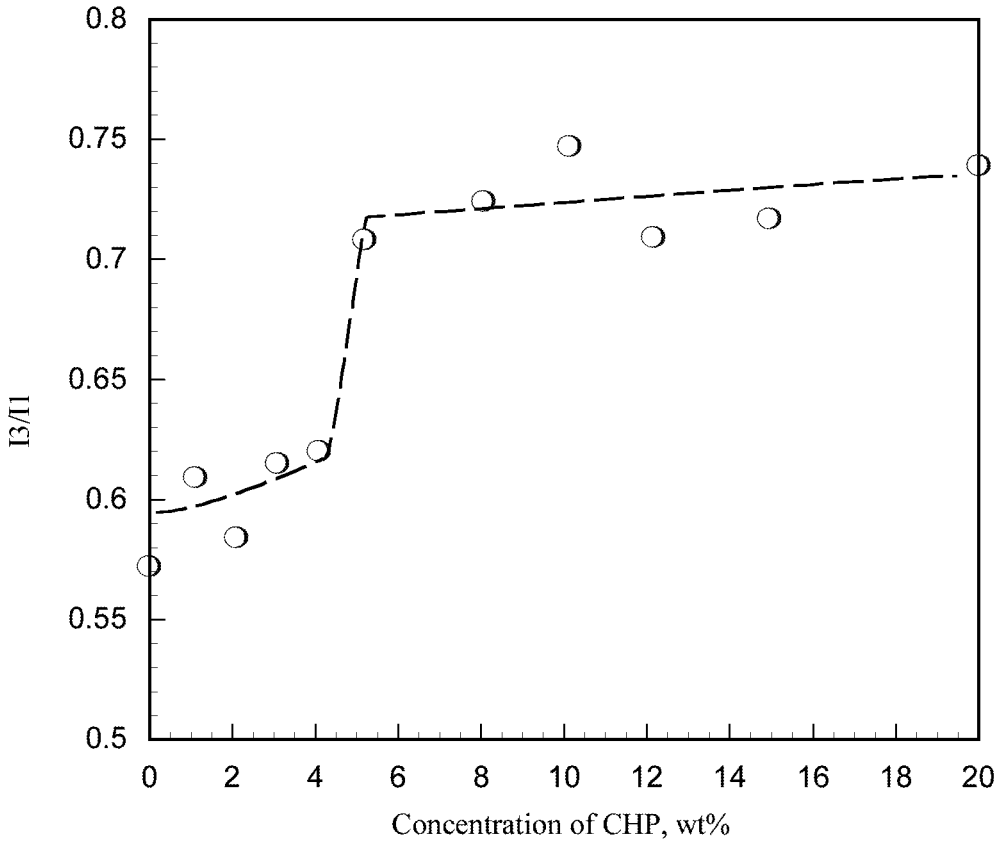


**Figure 15. $I_3/I_1$ ratio of pyrene fluorescence spectrum in cyclohexyl pyrrolidone aqueous solution**

Micelle formation is also confirmed by measurements of the freezing point depression ($\Delta T$) as a function of CHP concentration shown in Fig. 16. The change in trend at about 0.5 M again suggests micelle formation. The aggregation number, as judged from the slope of $\Delta T$ against concentration above the c.m.c., may be estimated as approximately 5 at the freezing point. Approximate aggregation numbers can also be estimated from the slopes of the surface tension plots of Fig. 13 above and below the micelle point, assuming that the adsorption is constant above the c.m.c. On this basis, the aggregation number is 20-25 at 22 °C and about 70 at 40 °C, close to the lower consolute temperature. These estimates, although approximate, indicate that aggregation

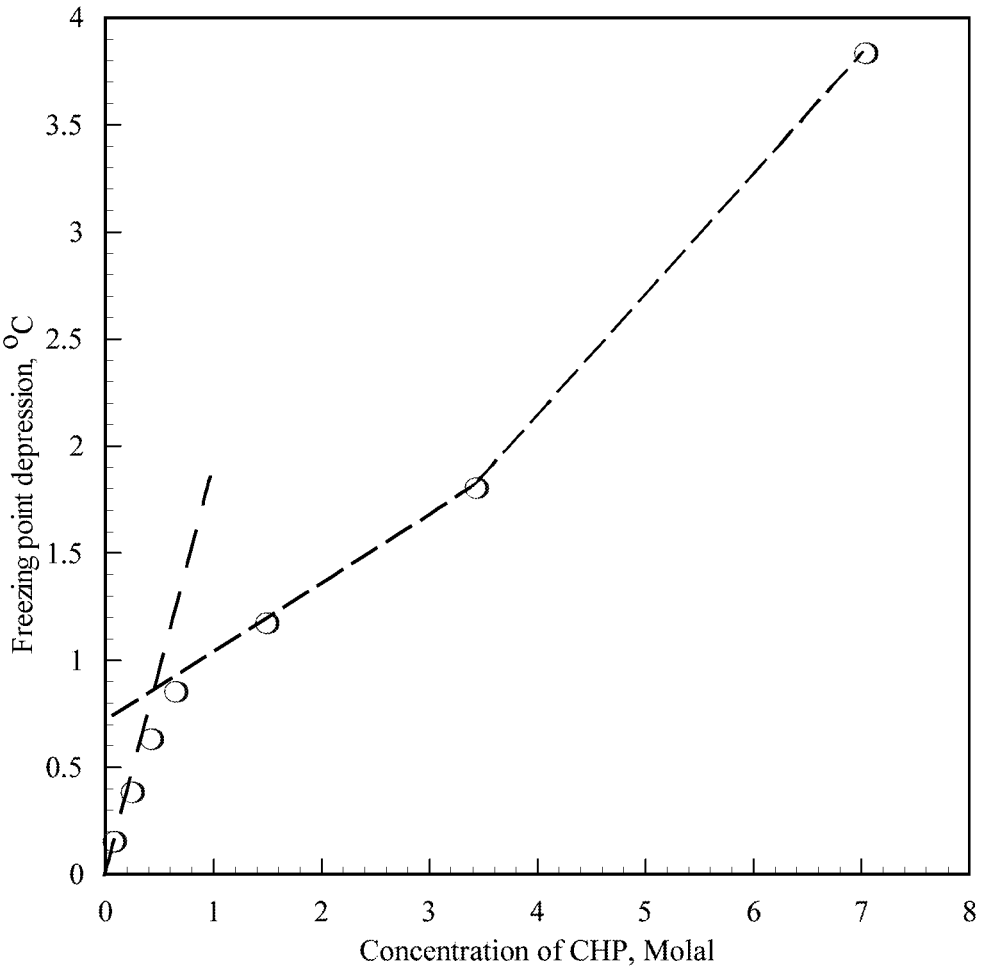


**Figure 16 Freezing point depression of cyclohexyl pyrrolidone aqueous solutions**

increases with temperature. Unlike many polyxyethelene surfactants which show lower consolute behavior, there is no "cloud point" with the alkyl pyrrolidones as the phase separation boundary is approached. The estimate of aggregation number from surface tension data at 22 °C is supported by a light scattering study using Zimm plots which gives a value of 20 at 23 °C.

***Adsorption Behavior N-cyclohexyl-2-pyrrolidone***

The surface tension results shown in Fig. 13 at 22 °C and 40 °C show clear evidence that micellization occurs over a range of concentrations and that the c.m.c. is not sharp. As described below, the activity coefficients for CHP at 22 °C in water were calculated from the freezing point and dilution heat results. The CHP activities are shown in Fig. 13 and allow direct calculation of the excess adsorption of CHP. At high surface pressures, close to the c.m.c., the adsorption corresponds to a molecular area of $54 \pm 2$ Å$^2$ /molecule. This area is significantly higher than the 38 Å$^2$/molecule at high pressures found for the N-n.hexyl-2-pyrrolidone, reflecting the effect of the cyclohexyl ring on the packing in the monolayer.

The surface pressure ($\Pi$) is shown in Fig.17 as a function of the concentration (c) of CHP in the dilute region, and the plot of $\Pi$/c as a function of c is shown in Fig. 18. For monolayers, the two-dimensional virial expansion may be expressed as

$$\Pi = kT ( \Gamma + B_2(T)\Gamma^2 + B_3(T)\Gamma^3 + ...) \qquad (3)$$

where $\Gamma$ is the surface density, B2(T), B3(T), etc. are the temperature dependent second, third, etc. virial coefficients, k is the Boltzman constant, and T is the temperature. For adsorbed monolayers, the appropriate $\Gamma$ is the surface excess density as given by the Gibbs Adsorption Isotherm. In the dilute concentration range as shown in Fig. 17, the CHP solutions are nearly ideal. The surface excess is therefore given by

$$kT\Gamma = c\, d\Pi/dc \quad (4)$$

Combining these equations, the second virial coefficients can be expressed as

$$B_2(T) = (-\beta/\alpha^2)kT \quad (5)$$

where $\alpha$ and $\beta$ are the initial slopes of the $\Pi$ - c and ($\Pi$/c) - c plots respectively when the concentration is close to zero.

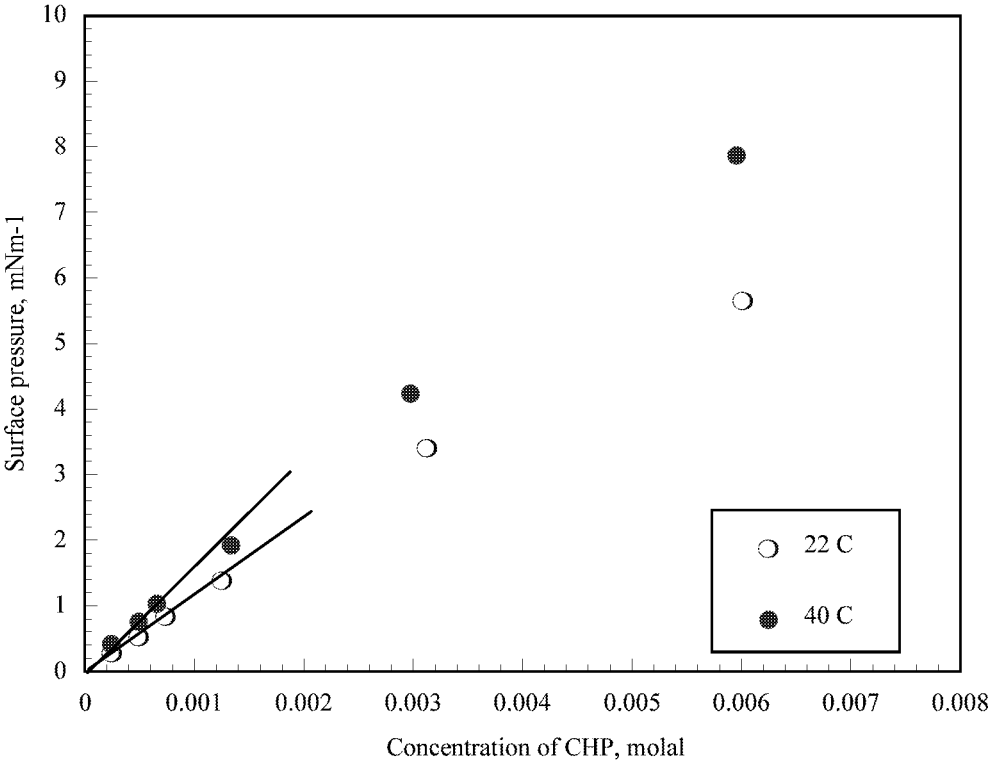


**Figure 17. Surface pressure of cyclohexyl pyrrolidone at the air/water interface**

Following the procedure discussed previously, the $\alpha$ and $\beta$ values from the lines as drawn in Figures 17 and 18 (noting that $\alpha$ is obtainable from either $\Pi$-c or $\Pi$/c-c plots) are used to obtain the positive $B_2(T)$ values at 22 ° and 40 °C of 10 Å$^2$ and 9 Å$^2$/ molecule respectively. The data at 5° and 60 °C showed greater scatter, making estimates of $B_2(T)$ unsatisfactory. It can be seen that the second virial coefficients become more negative with increase in temperature.

The values of $\alpha$ as a function of temperature allow estimation of the standard heat of

adsorption of ($\Delta H^{\circ}$) of CHP from the solution to the air/water interface, using the relation

$$d(\ln \alpha)/d(1/T) = - \Delta H^{\circ}/R \qquad (6)$$

Adsorption is endothermic with $\Delta H^{\circ}$ estimated as 11 ± 1 KJ/mole.

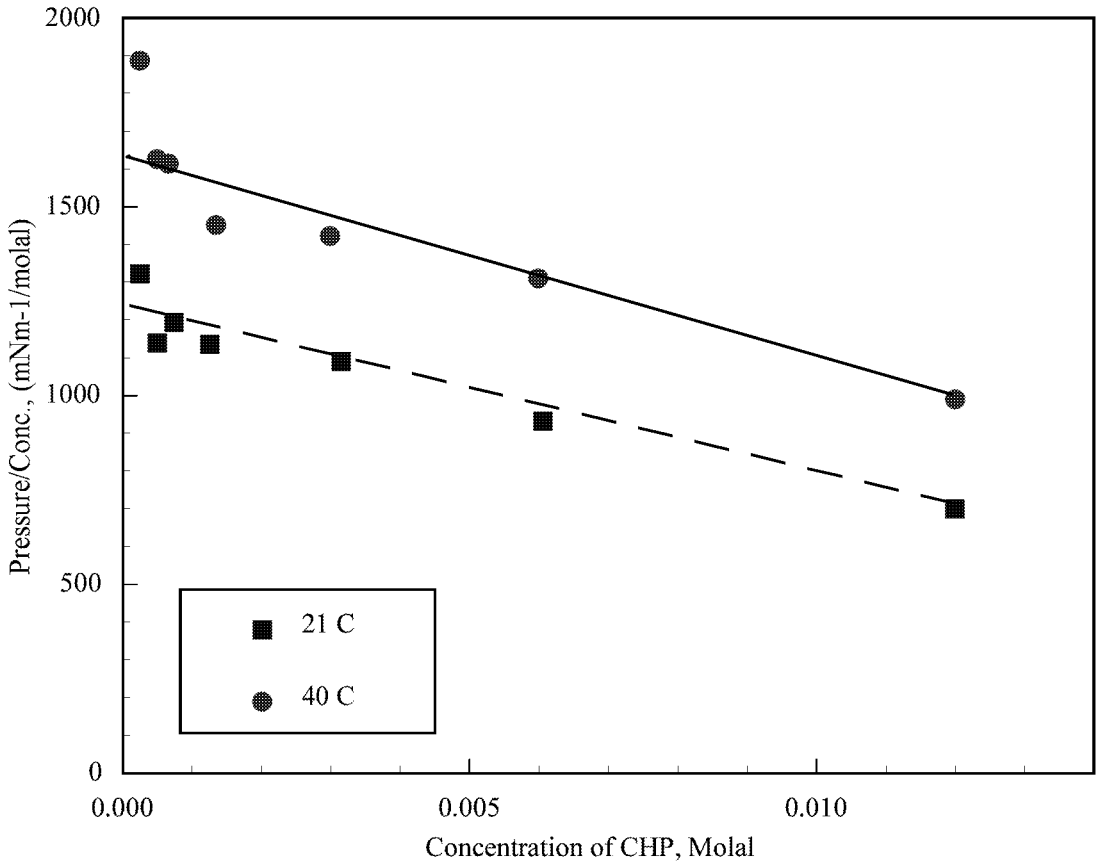


**Figure 18. Π/C as a function of concentration of cyclohexyl pyrrolidone in water**

***Calorimetry***

The heat capacities of CHP-$H_2O$ mixtures are shown in Fig. 19. The excess heat capacity of mixing is positive. The specific heat capacity of CHP is 1.7 J $g^{-1}K^{-1}$ (286 J $mole^{-1}$ $K^{-1}$ ), well below the specific heat capacities of the n-alkanes in the same molecular weight range (decane 2.21, dodecane 2.20 J $g^{-1}K^{-1}$), and close to cyclohexane (1.81), reflecting in part the restricted bond rotation in the CHP two-ring structure. In the pure liquid state the molecules of CHP, as with other

N-substituted pyrrolidones, interact strongly as shown by the high boiling point (154 °C at 7 mm Hg) and viscosity (~11.6 cp). This structuring, probably related to the interaction of the large molecular dipoles, is also reflected in the low heat capacity.

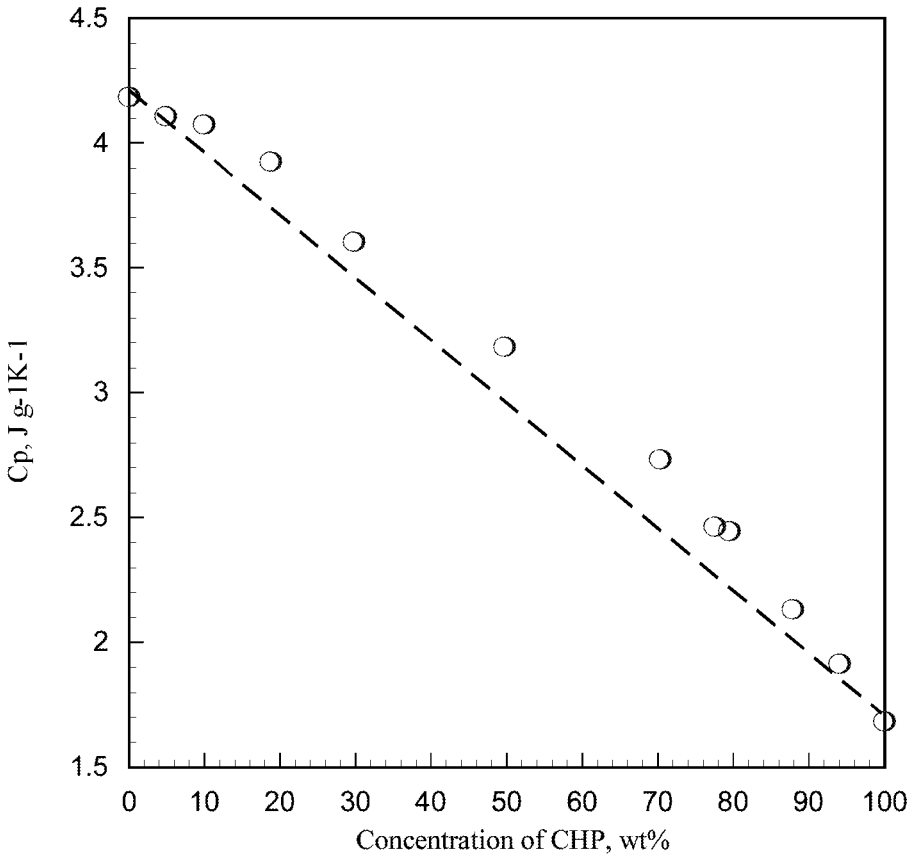


**Figure 19. Heat capacity of cyclohexyl pyrrolidone/water mixtures at 25 °C**

The calorimetric data for the heat of mixing of CHP with water at 24 °C are shown in Figs.20 and 21. For Fig.20, the heats of dilution obtained with dilutions in the range of CHP concentrations below 50% w/w using the LKB calorimeter are added to the heat of mixing of equal masses of CHP and water (56 J $g^{-1}$ CHP). The overlap between the two calorimetric methods is satisfactory. Also shown in Fig. 20 is the heat of dilution at high CHP ratios on a linear scale for the addition of water. The error introduced by the initial water content of the CHP (0.17% w/w) is minor (~1J/g CHP) in

reference to the precision of the measurements.

The heats of dilution show four district regions, best seen in Fig. 21 for the partial molar heats of dilution ($\Delta H_d$). At low water addition (up to 0.1 g $H_2O$/g CHP, which is close to the 1:1 mole ratio) the partial molar heat of dilution is constant, suggesting the formation of a CHP hydrate with a heat of formation of -2.4 KJ/mole. At higher water contents, but before the region of the surface tension plateau (the probable micellar range) $\Delta H_d$ falls sharply. Over the probable micellar range, $\Delta H_d$ decreases less sharply until entering the fourth region (dilute in CHP, no micelles) where $\Delta H_d$ falls to zero within the experimental error. The decrease in $\Delta H_d$ across the micellar range strongly indicates that the micellar aggregates are changing in structure and aggregation number on dilution. The value of $\Delta H_d$ just above the micelle point shows a heat of micelle breakdown corresponding to -9.9 KJ/mole CHP. This large heat of micellization agrees qualitatively with the change of c.m.c. with temperature (Fig. 13).

If it is assumed that both the heat capacity of CHP/water mixtures (Fig. 19) and the $\Delta H_d$ are constant over the range of experimental temperatures, the osmotic coefficients for CHP in water can be estimated at higher temperatures, and the solute activity coefficients may then be obtained. This procedure was used to calculate the CHP activities shown in Fig. 13 at 22 °C. The calculations were not repeated at 40 °C since the assumptions involved are less valid than at 22 °C.

***Viscosity***

The viscosity results (Fig. 22) show a maximum viscosity at 25 °C corresponding to a mole ratio of 0.75 CHP/water. The maximum may be further evidence of hydrate formation, though less definite than indicated from the calorimetric data. Hydrates of N-substituted pyrrolidones have been

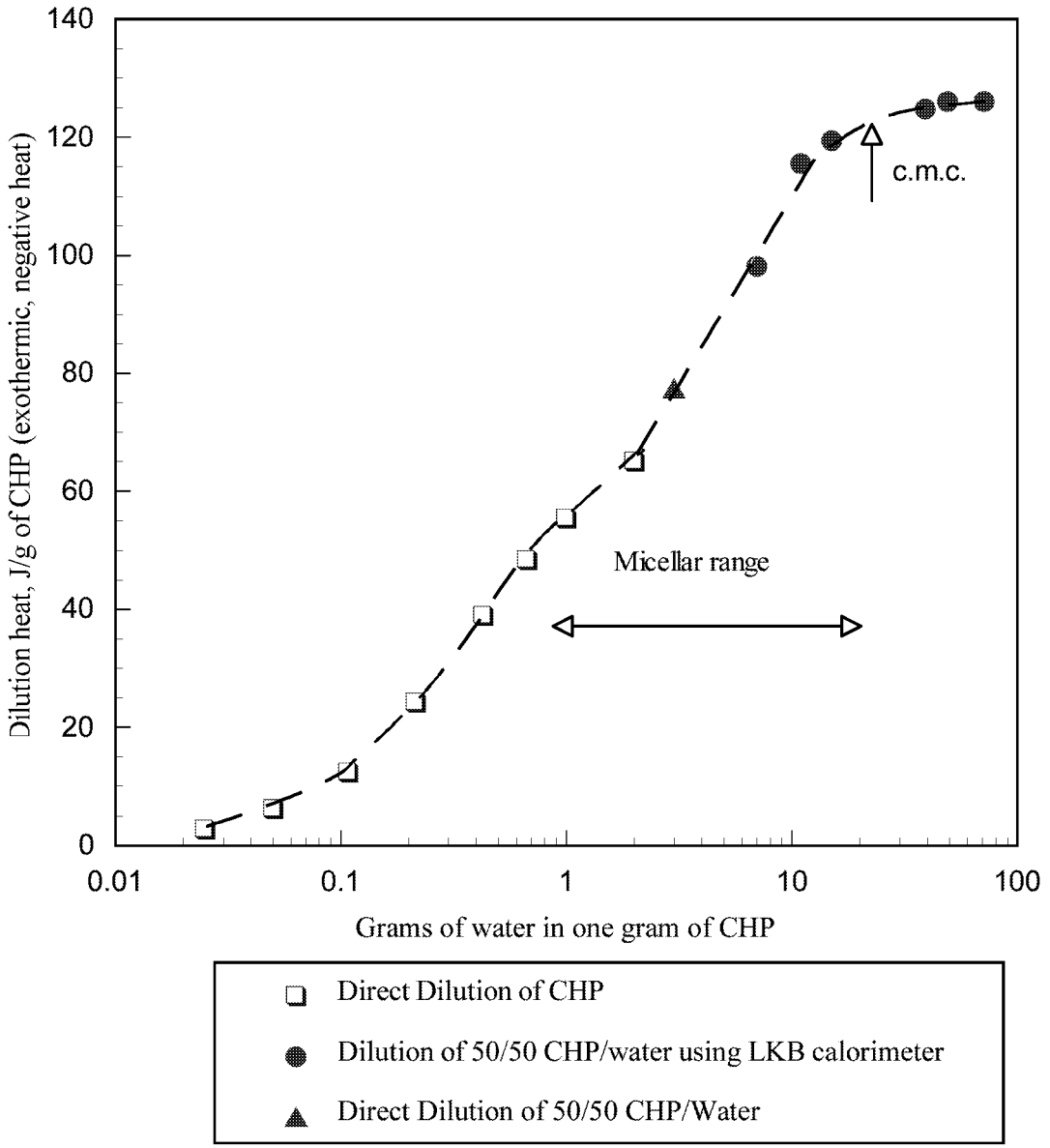


**Figure 20. Heat of dilution of cyclohexyl pyrrolidone in water**

suggested previously from spectroscopic evidence, but only two such hydrates are known to be sufficiently stable to show clearly on phase diagrams. 2-pyrrole forms a monohydrate with a melting point of 30.4 °C (compared to the melting point of 25 °C for 2-pyrrole itself), and the phase diagram shows two eutectics. N-methyl-2-pyrrolidone (NMP) forms a dihydrate melting at -22 °C, close to

the melting point of NMP, with two clear eutectics in the phase diagram. The spectroscopic evidence for a hydrate of N-vinyl-2-pyrrolidone (VP) was considered, who found only one eutectic in the phase diagram for melting of VP-water mixtures.

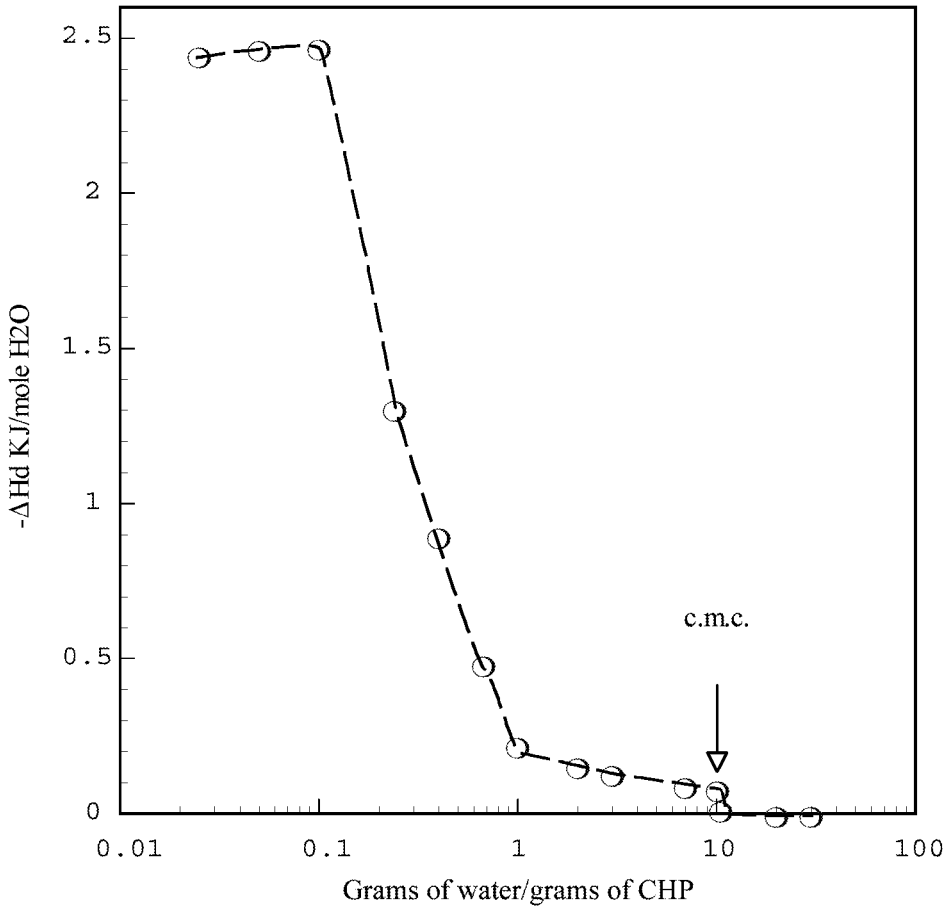


**Figure 21. Partial molar heat of dilution of cyclohexyl pyrrolidone in water at 24 °C**

N-cyclohexyl-2-pyrrolidone (CHP) forms micelles in water at temperatures in the miscibility region below or near the lower consolute temperature. The micelle points are not sharp and the aggregation numbers above but near the c.m.c. increase with temperature from about 5 at 0 °C to about 70 at 40 °C, close to the lower consolute temperature. No "cloud point" phenomenon is observed on approaching the phase boundary. At concentrations well above the c.m.c., the partial molar heats of dilution decrease as the CHP concentration decreases suggesting substantial changes

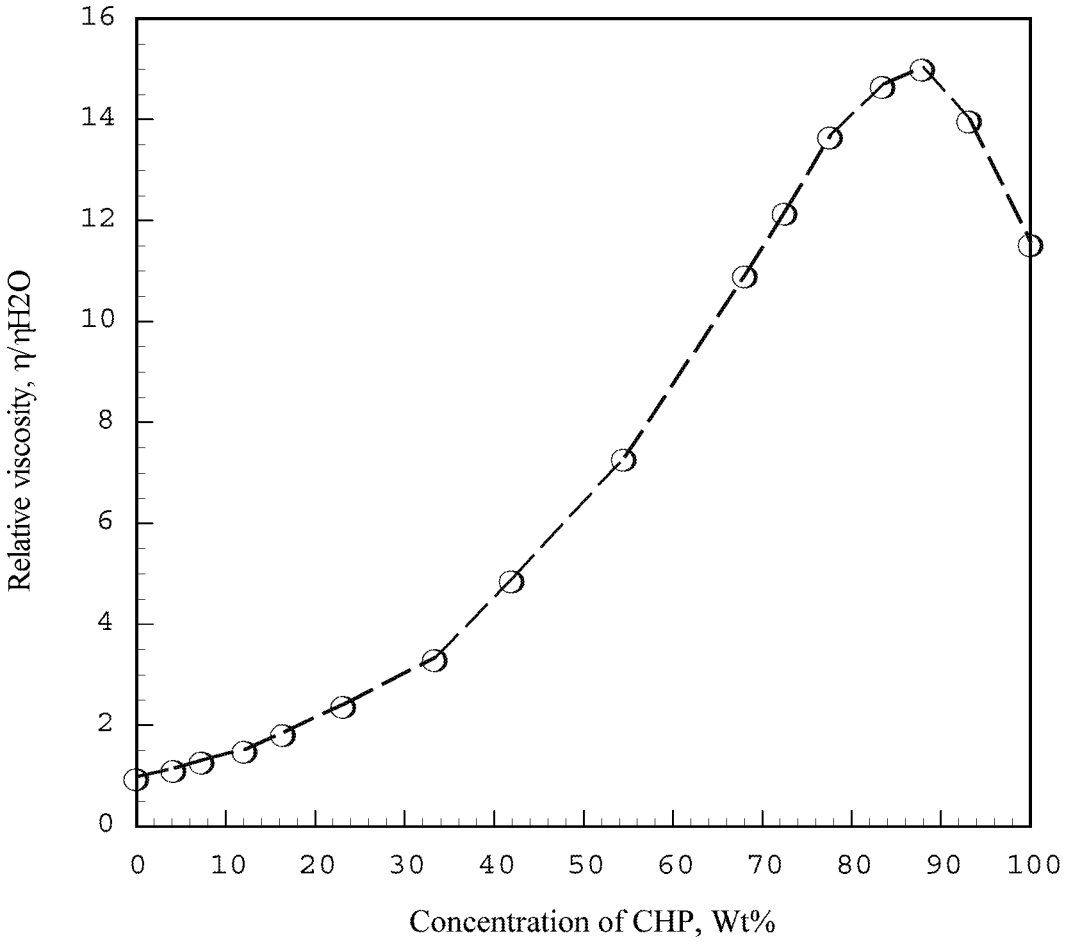


**Figure 22. Relative viscosities of CHP/water mixture at 25 °C.**

in the micelle structure. The micellar interior resembles pure CHP, as judged from fluorescence measurements with pyrene. CHP is surface active reaching a packing corresponding to 54 ± 2 $Å^2$/molecule at high surface pressure. This area is significantly larger than for the n-hexyl analog. From the data at low surface pressures the two-dimensional second virial coefficients at 22 and 40 °C. are shown to be positive but decreasing with temperature, as found for n-alkyl pyrrolidones. The second virial coefficient for the n-hexyl pyrrolidone is negative at 25 °C. This difference is in accord with the finding from the surface tension data that the cyclohexyl ring packs less efficiently on the interface than the n-hexyl compound.

## 3. SUGAR-BASED SURFACTANT AT THE SOLID/LIQUID INTERFACES

Sugar-based surfactants are a new group of nonionic surfactants. They have been known for more than 100 years, but economic production has been realized only in recent years. These surfactants are biodegradable, nontoxic, and synthesized from renewable material such as fatty alcohols and sugars.[9-12] These properties make them interesting substitutes for other surfactants that are potentially damaging for the environment. From ecological and toxicological points of view these surfactants have received attention as a new generation of non-ionic surfactants.

Alkyl glucosides (polyglucosides) are the most common sugar-based surfactants. Their solution and interfacial behaviors such as phase behavior, surface tension, micellar properties, etc. have been studied in the past.[1-4, 13-17] In these studies, alkyl polyglucosides were found to possess remarkable properties which, in some cases, differed clearly from those of other nonionic surfactants. These properties enable them to be utilized in a number of applications such as detergents, cosmetic products, emulsifiers. It was the aim of this study to find their application in enhanced oil recovery.

Sugar-based surfactant n-dodecyl-β-D-maltoside in solution and at air-solution interfaces have been studied in our previous research. It was found that pH and salt have little effect on their surface tension behavior. Also, metal ions such as $Ca^{2+}$ have no interaction with the surfactants. At the same ionic strength, different salts have different effects on the surface tension and the cmc of n-dodecyl-β-D-maltoside. For the same cation $Na^+$, the effect of anions on the depression of the cmc follows the order: $F^- > Cl^- > SO_4^{--} > Br^- > PO_4^{---} >$ citrate $> I^- > SCN^-$. Similarly, for the same anion $Cl^-$, the effect of cations is in the order: $K^+ > Na^+ > Rb^+ > Li^+ > Ca^{++} > Al^{+++}$. The effect of anions on the depression of the surface tension and cmc of n-dodecyl-β-D-maltoside in various salt solutions is interpreted by their influence on the water structure rather than on the surfactant.

However, the effect of cations is exactly opposite to those of anions and no general explanation is available, although this anomalous behavior of the cations is reflected in the Hofmeister series or the lyotropic series.[18]

There is very limited studies on the sugar-based surfactants at solid/liquid interfaces. It is the goal to study their behavior at solid-liquid interfaces and reveal the mechanism of interactions for the purpose of controlling surfactant loss due to adsorption in EOR.

*Adsorption of n-dodecyl-β-D-maltoside on Various Hydrophilic Solids*

Adsorption isotherms of n-dodecyl-β-D-maltoside on hydrophilic solids, alumina, silica, titania and hematite, at neutral pH and 25°C are shown in Figure 23. The surfactant is found to adsorb on alumina, hematite, and titania while it absorbs of significant less on silica, particularly in the high concentration range.

A three-stage adsorption phenomenon becomes evident upon examining these isotherms. In the first stage of adsorption, the surfactant adsorbs individually and sparsely on the surface and chain-chain interaction is not significant. A sharp increase in the adsorption density occurs in the second stage, and this is the result of the association of the surfactants into hemimicelles due to the chain-chain interaction. The adsorption isotherm reaches a plateau region at the onset of the third stage. The inflection point between stages II and III corresponds to the critical micelle concentration of the surfactant.

In the plateau region, the adsorption density is about $5.5 \times 10^{-6}$ mol/m$^2$ and the surface area per molecule adsorbed is calculated to be 30 Å$^2$ . Comparing with the value derived from the surface tension at the solution-air interface, which is 48.5 Å$^2$, the amount of surfactant adsorbed on the particles is more than that required to form a monolayer and is close to that required for a

bilayer. However, this value can be explained equally well by assuming adsorption of surface micelles since a wide range of values can be obtained depending on the shape of adsorbed micelles and its distribution on the surface.

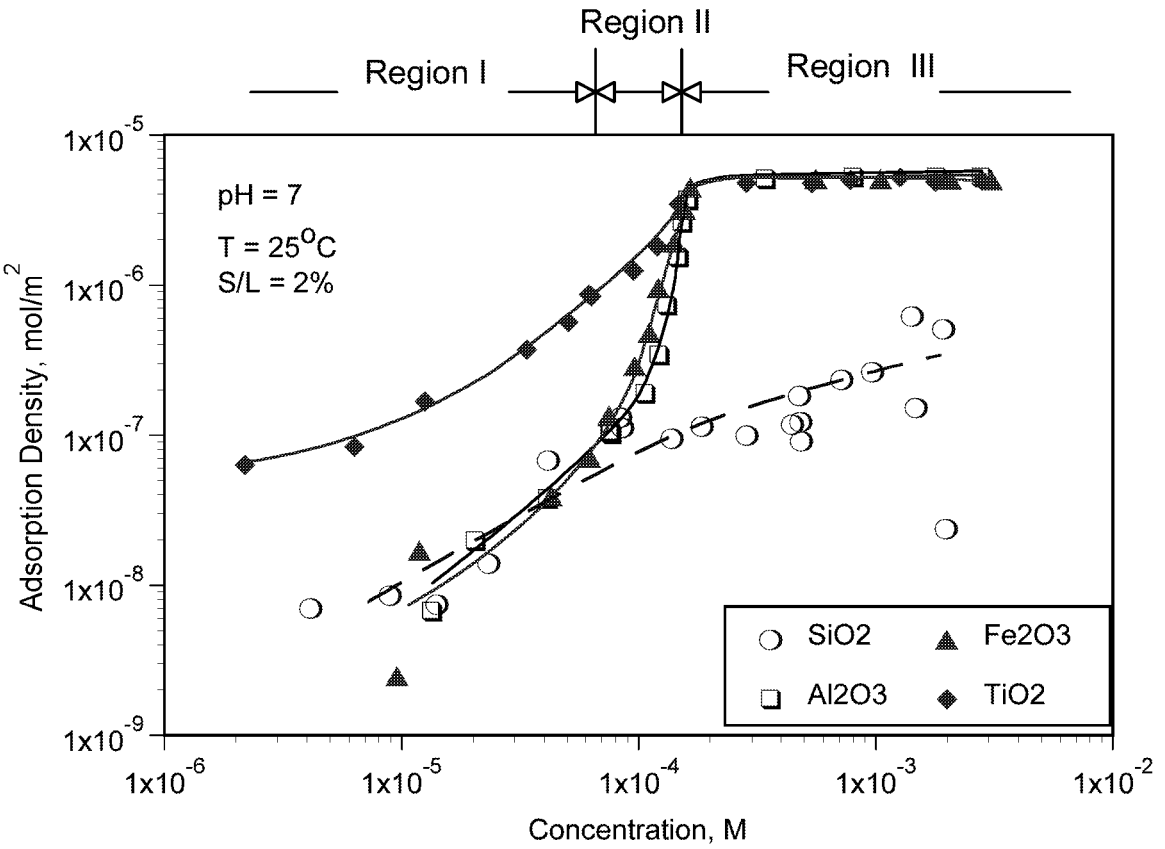


**Figure 23. Adsorption Isotherms of N-Dodecyl-β-D-Maltoside on Hydrophilic Solids**

As indicated above, n-dodecyl-β-D-maltoside adsorbs on alumina, hematite and titania, but much less on silica. Polysaccharide polymers such as dextrin and starch also behave in a similar manner. However, another group of nonionic surfactants, the ethoxylates, adsorbs on silica but not on alumina. This drastically different behavior of alkyl polyglucosides surfactants and ethoxylated surfactants may be due to the different interactions between surfactants and solids. Hydrogen bonding has been proposed as the driving force for the adsorption of ethoxylated surfactants on

oxides, the adsorption mechanism of alkyl polyglucosides on solids is likely to be different and will be explored in the future.

*Adsorption of Alkyl Glucosides and Alkyl Maltosides on Alumina*

To study the effect of important chemical structure variables, the hydrocarbon chain length and the glucose units, on the adsorption of alkyl glucosides and maltosides on solids, adsorption isotherms of octyl, decyl-β-D-glucosides and octyl, decyl, dodecyl, tetradecyl-β-D-maltosides were determined and the results obtained are shown in Figures 24 and 25. All the isotherms are similar in shape with the inflection point for each surfactant corresponding to its cmc value.

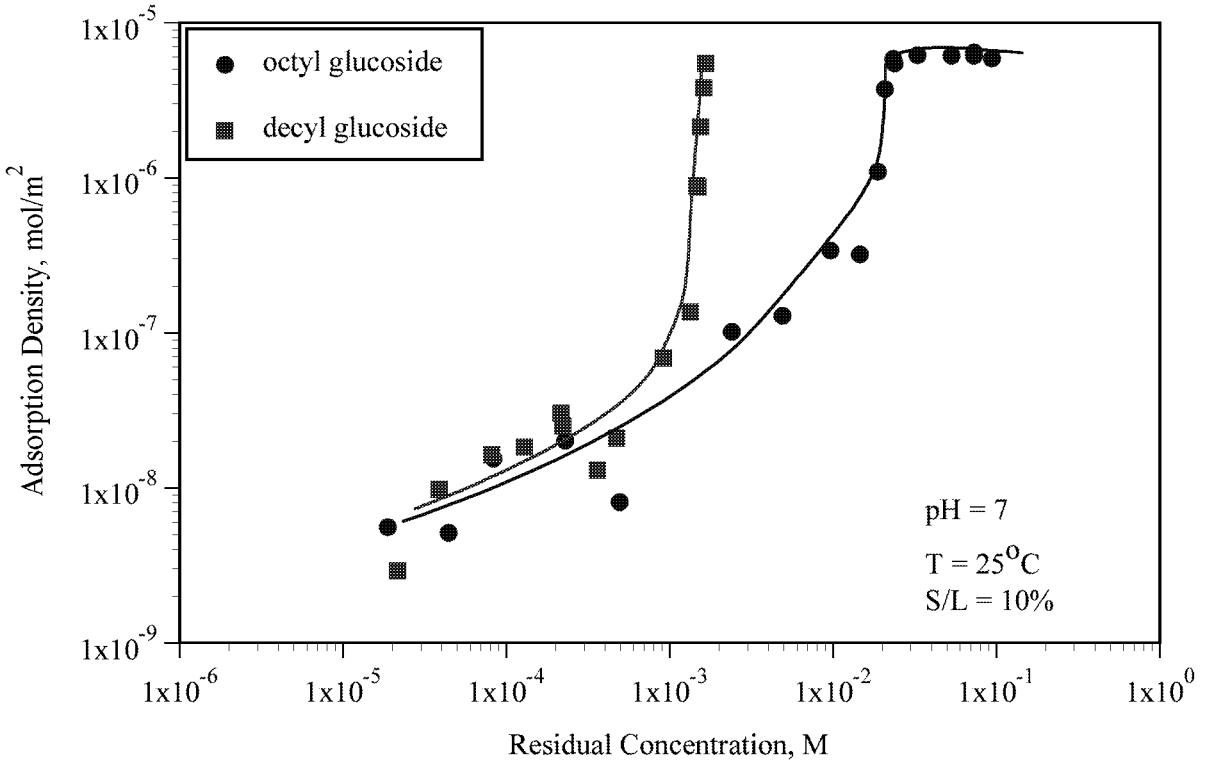


**Figure 24 Adsorption of N-Alkyl-β-D-Glucosides on Alumina**

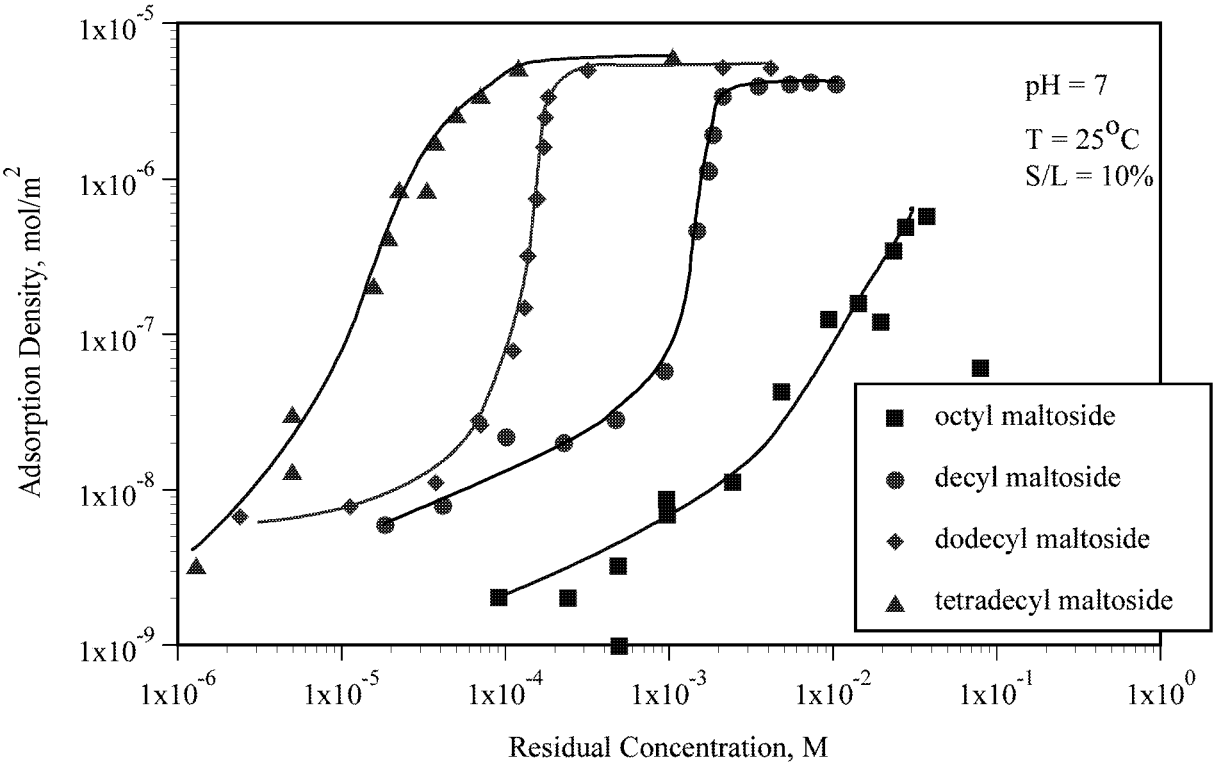


**Figure 25. Adsorption of N-Alkyl-β-D-Maltosides on Alumina**

It can also be seen from figure 25 that with the chain length increase, there is a small increase in the adsorption density in the plateau region. This suggests that packing for longer chain surfactant is more compact than that for the shorter chain ones, possibly due to the stronger hydrophobic interactions as chain length increases.

Also, glucosides have a higher maximum adsorption density than maltosides of the same chain length. This is due to the small size of glucosides, which requires less area for their packing than maltosides. Furthermore, as the number of glucose units increases, the hydrophobicity of the surfactant is expected to decrease, and this can also cause a decrease in adsorption density of the surfactant. Similar results have been obtained also for ethoxylated surfactants.

The isotherms are analyzed further in-situ to derive fundamental information on the interactions between the surfactants and the solids.

*Adsorption Kinetics of N-Dodecyl-β-D-Maltoside on Alumina*

The adsorption kinetics of n-dodecyl-β-D-maltoside on alumina is shown in Figure 26 for three surfactant concentrations. The adsorption is fast with the process almost complete in 1-2 minutes after the addition of the surfactant. The equilibrium is attained within 30 minutes. This is normal since this surfactant is small and can transport to surface rapidly unless there is a barrier such as that due to electrostatic repulsion.

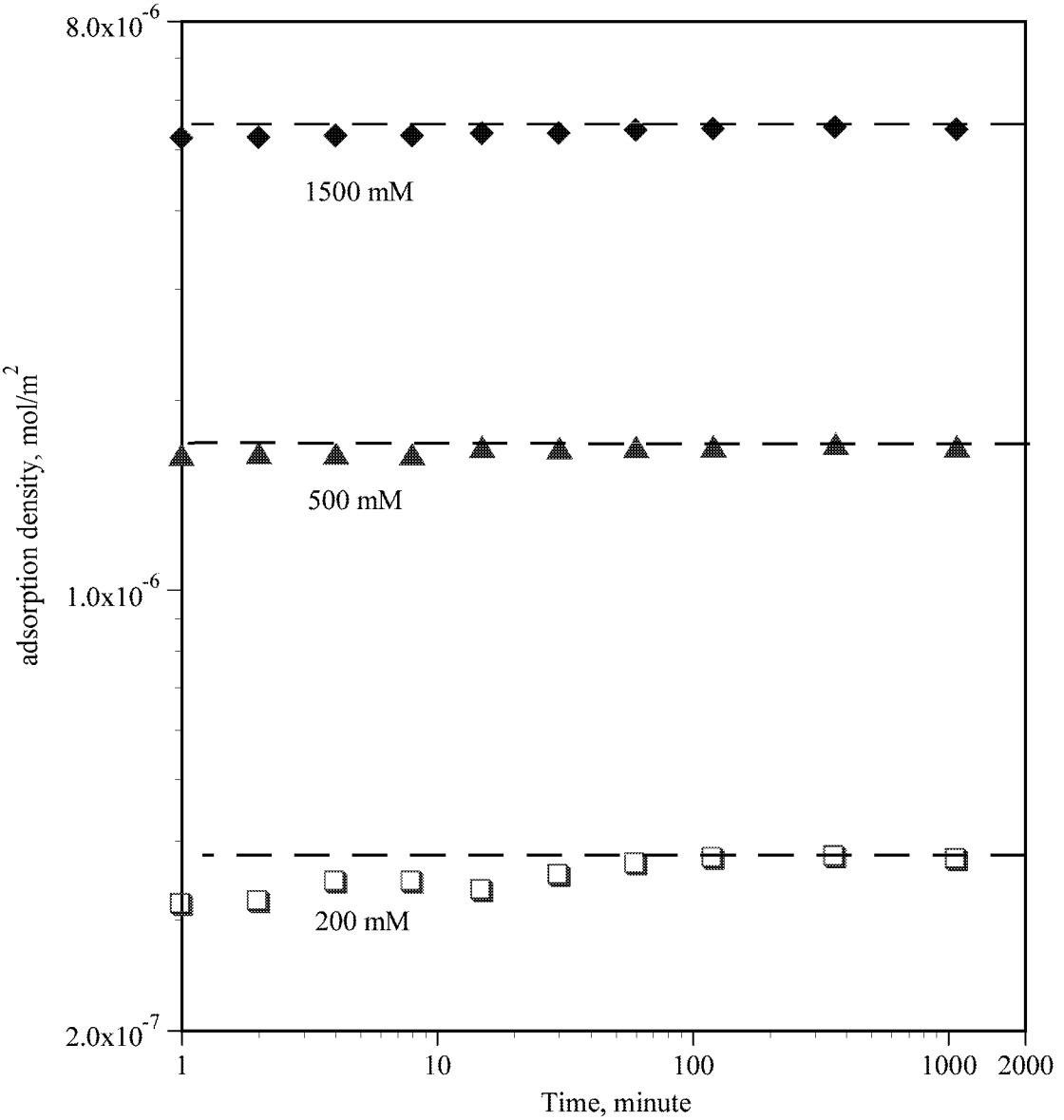


**Figure 26. Adsorption Kinetics of N-Dodecyl-β-D-Maltoside on Alumina**

*Effect of pH on the N-Dodecyl-β-D-Maltoside Adsorption*

The effect of pH on the adsorption of DM on alumina is shown in Figure 27. The maltoside adsorption is not affected by the change in pH in the range tested. Since the isoelectric point of AKP-50 alumina is 9, at the two pH conditions tested the zeta-potential of the alumina is very different. The identical adsorption isotherms obtained at the two pH conditions suggest that the electrostatic interaction is not a determining factor for the adsorption of n-dodecyl-β-D-maltoside on alumina.

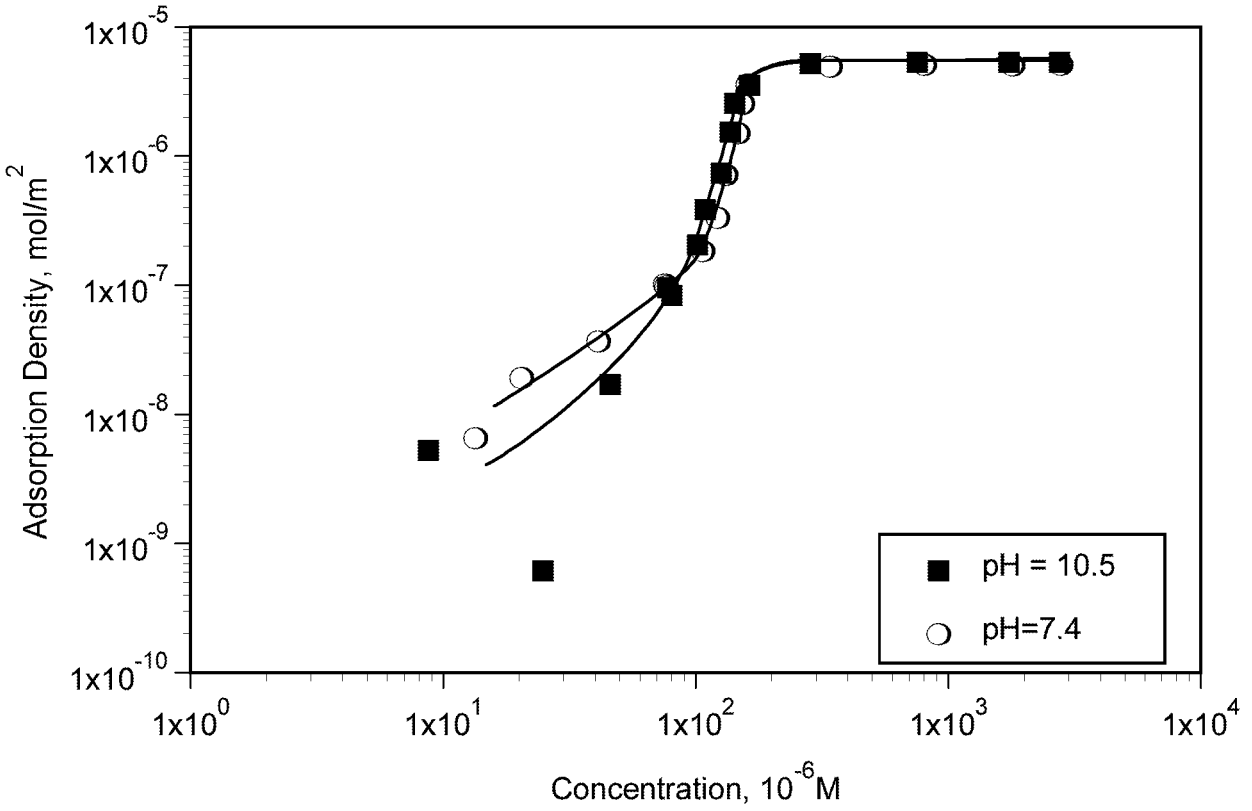


**Figure 27. Effect of pH on the Adsorption of N-Dodecyl-β-D-Maltoside on Alumina**

*Effect of Salt on the N-Dodecyl-β-D-Maltoside Adsorption*

The effect of $Na_2SO_4$ salt on the adsorption of n-dodecyl-β-D-maltoside on alumina is shown in Figure 28. The adsorption isotherm is found to shift to the left in the lower concentration region

and downwards at higher concentrations in the presence of salt. In the present case, $Na_2SO_4$ causes the inflection point to drop from $1.8 \times 10^{-5}$ mol/L to about $9 \times 10^{-6}$ mol/L. The surface tension measurements showed that at the same concentration of $Na_2SO_4$, the cmc of n-dodecyl-β-D-maltoside is reduced from $1.8 \times 10^{-5}$ mol/L to $9.4 \times 10^{-6}$ mol/L. The effect of the salt on surface tension has been attributed to the salting-out of the hydrocarbon chain of the surfactant. The comparable shifting of the inflection point on the adsorption isotherm suggests that the shifting of the adsorption isotherm due to $Na_2SO_4$ can be attributed primarily to changes in solution conditions rather than those on the solid surface. Similar results have been reported for the adsorption of an ethoxylated surfactant on silica in the presence of $Na_2SO_4$.

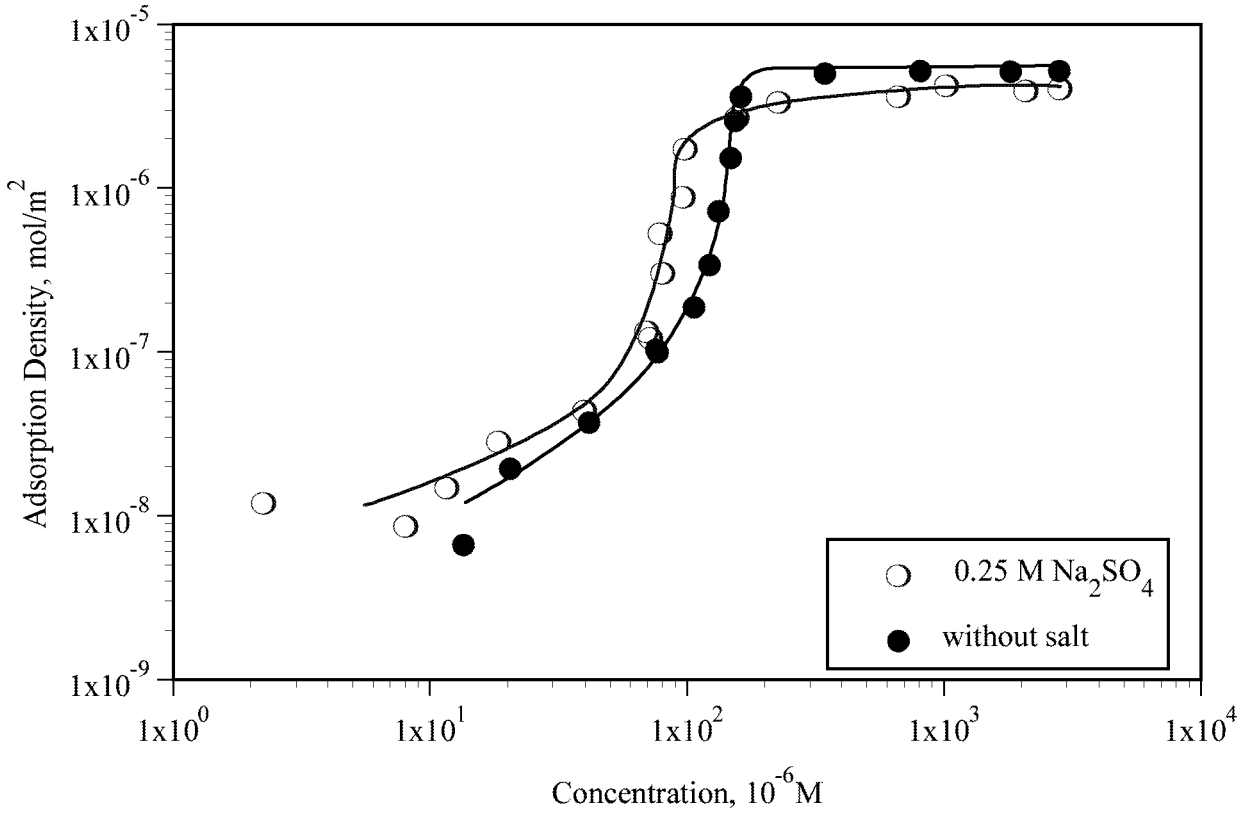


**Figure 28. Effect of Salt ($Na_2SO_4$) on the Adsorption of N-Dodecyl-β-D-Maltoside on Alumina**

*Fluorescence Spectroscopic Study of N-Dodecyl-β-D-Maltoside Adsorption*

To understand the nature of the above adsorption effects, microstructure of the adsorbed layer was probed using fluorescence spectroscopy. The fluorescence of pyrene is very sensitive to the medium in which it resides. The ratio of the intensities of the third and first peaks ($I_3/I_1$) on a pyrene emission spectrum can reveal the polarity of the aggregate environment.

Changes in the polarity parameter of pyrene at the alumina-water interface and in the supernatant are plotted in Figure 29 along with the adsorption isotherm of n-dodecyl-β-D-maltoside on alumina. A pyrene spectrum was detected in the solution at all concentrations studied. The polarity parameter changes sharply from ~0.66 to ~1.0 around the critical micelle concentration of the surfactant, suggesting surfactant aggregate formation in the solution. On the other hand, the pyrene spectrum was seen at the solid-liquid interface only above a certain adsorption density. This can be interpreted as due to the beginning of aggregate formation at the solid-liquid interface at this adsorption density. The concentration at which the increase in polarity parameter of surfactant at solid-liquid interface occurs corresponds to the increase in the adsorption density. In the adsorption plateau region, pyrene is present both in the surface aggregates at the solid-liquid interface and micelles in solution. It is reported that in alumina-sodium dodecyl sulfate system, pyrene is preferentially solubilized in solloids (surface colloids or aggregates) at the alumina-water interface rather than in SDS micelles in the supernatant. In contrast, in the alumina-tetradecyl trimethyl ammonium chloride (TTAC) system, pyrene is preferentially solubilized in the micelles than at the solid -liquid interface. The present study suggests that the solubilizing power of DM solloids is between those of SDS and TTAC.

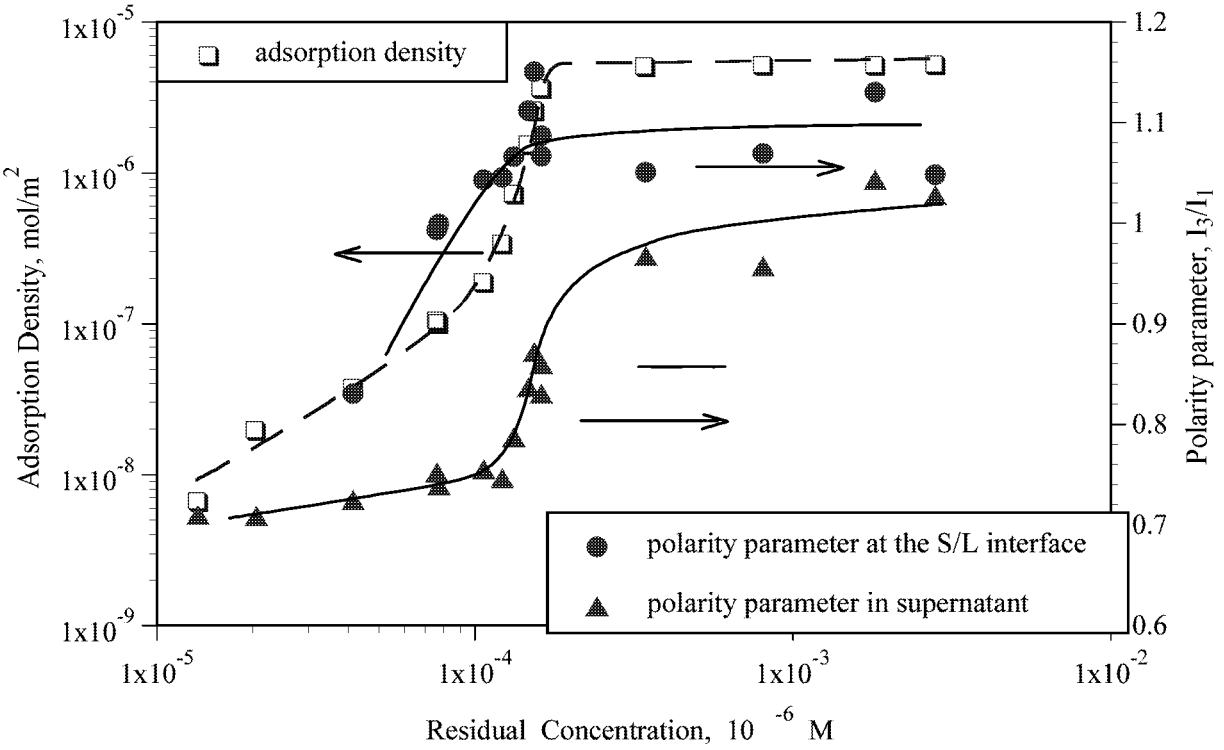


**Figure 29. Polarity parameters of Pyrene at the Alumina/Water Interface and in Supernatant As a Function of N-Dodecyl-β-D-Maltoside Adsorption**

In the adsorption plateau region, the polarity parameter of the solloid is higher than that of micelles. This means that packing of the surfactants at the solid-liquid interface is denser than that in micelles. This is attributed to the strong hydrophobic chain-chain interaction and inter-penetration of surfactant tails into solloids.

*Effect of Temperature on the Adsorption N-Dodecyl-β-D-Maltoside on Alumina*

Adsorption of nonionic surfactant is usually affected by the temperature. For ethoxylated surfactants, due to their dehydration at elevated temperatures, increase in temperature usually causes an increase in adsorption density. Considerable thermodynamic information on adsorption can be obtained by studying the effect of temperature on the adsorption process.

The effect of temperature on the adsorption of n-dodecyl-β-D-maltoside on alumina is shown in Figure 30. It can be seen that temperature has but only a small effect on the adsorption of n-dodecyl-β-D-maltoside. The maximum adsorption density is also not affected by the temperature

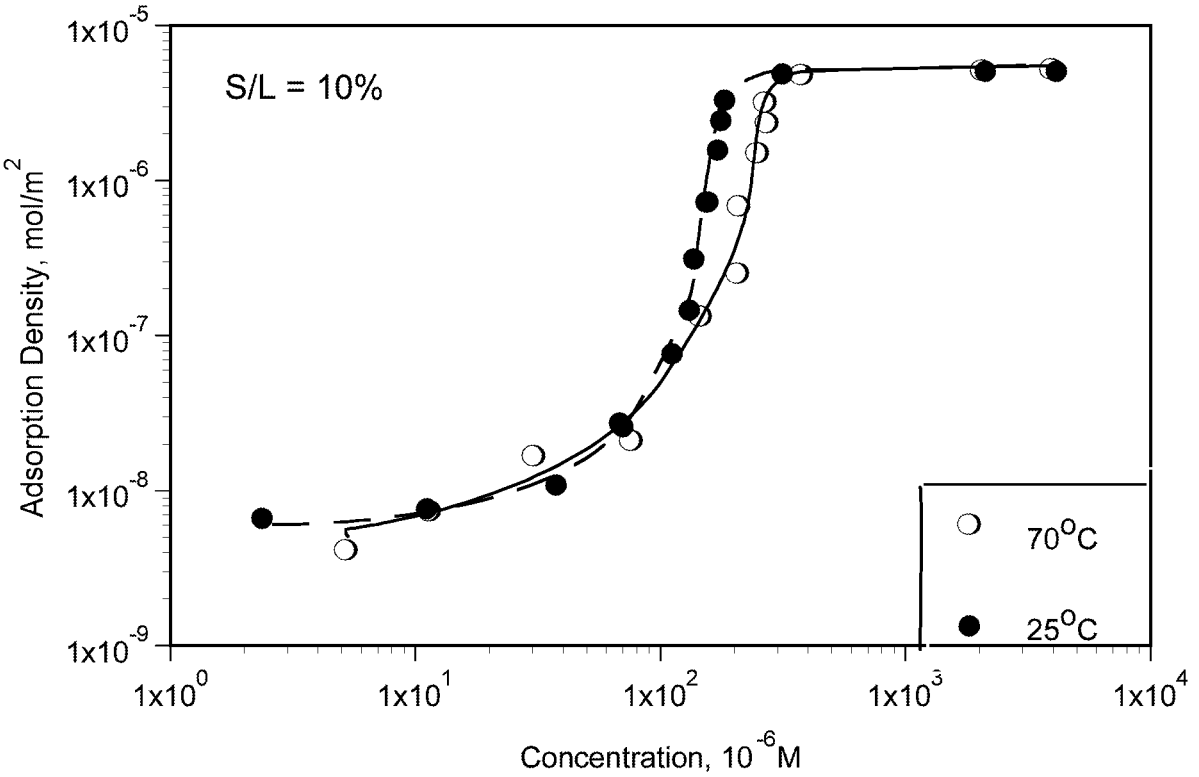


**Figure 30. Effect of Temperature on the Adsorption of N-Dodecyl-β-D-Maltoside on Alumina**

change. The shift in inflection point between region II and region III is mostly the result of the increase in critical micelle concentration of the surfactant with an increase in temperature. The small effect of temperature suggests that there is no chemical interaction between the surfactant and the solid.

*Hydrophobicity of Alumina with N-Dodecyl-β-D-Maltoside Adsorption*

Information on changes in relative hydrophobicity of the solid surface due to surfactant adsorption can give important information on the conformation of the surfactant on the solid and help to elucidate the mechanism involved. The effect of surfactant adsorption on the wettability of the alumina is illustrated in Figure 31 along with the adsorption isotherm. In the absence of the surfactant, the alumina exhibits complete hydrophilicity. With the onset of adsorption on alumina,

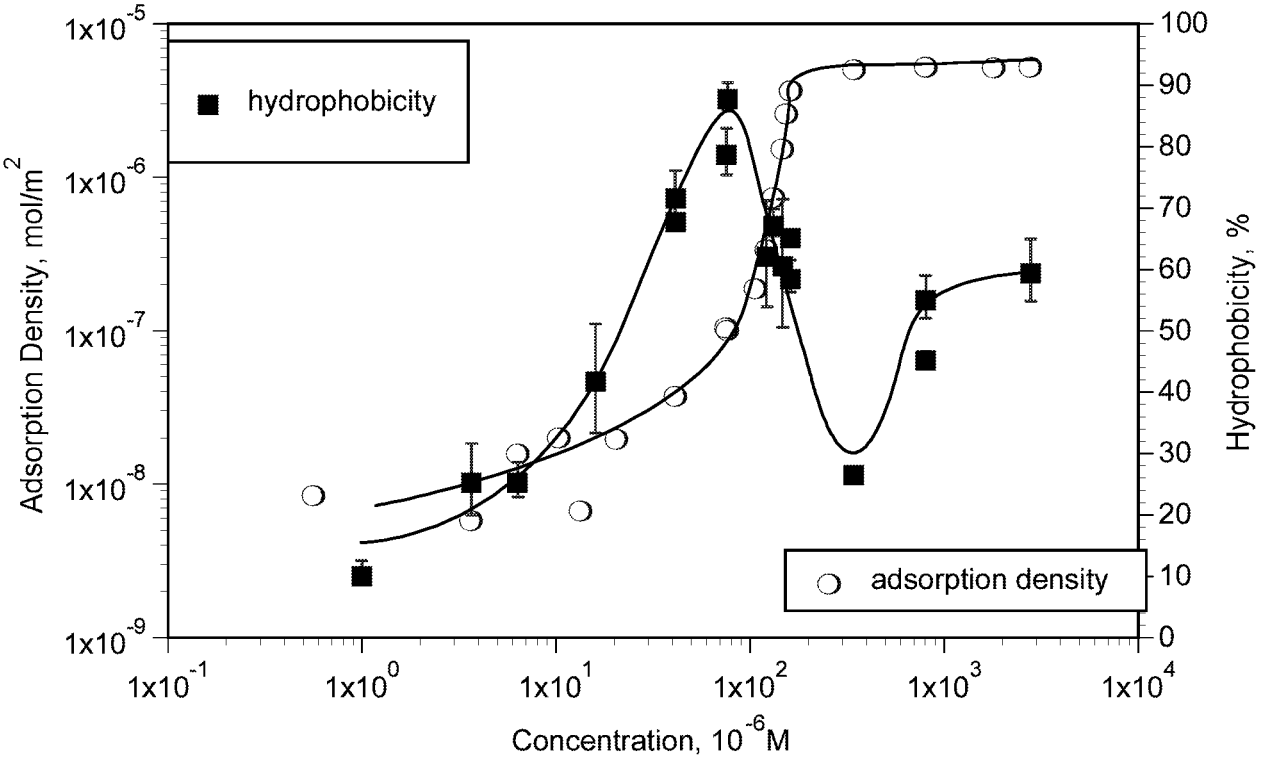


**Figure 31. Adsorption of N-Dodecyl-β-D-Maltoside and Its Effect on the Hydrophobicity of Alumina Particles as Determined by Two Phase Separation**

the surface becomes hydrophobic, suggesting increasing amounts of surfactant to be adsorbing with their hydrophobic tails oriented towards the bulk solution. The hydrophobicity reaches a maximum in the beginning of the region where adsorption density rises sharply. At higher adsorption density the hydrophobicity decreases. This decrease in hydrophobicity suggests that the chain-chain

interaction in this region occurs with some hydrophilic groups orienting towards the aqueous phase. The hydrophobicity of the alumina continues to drop in the region of plateau adsorption. The drop in hydrophobicity in the plateau region is proposed to be due to bilayer adsorption. Further variation in hydrophobicity in the plateau region is possibly related to the effect of high residual DM on the two phase separation that is used here to monitor hydrophobicity.

Similar conclusion can be drawn by examining the hydrophobicity of alumina particles as a function of the adsorption density of n-dodecyl-β-D-maltoside(Figure 32). At low adsorption densities, the hydrophobicity of alumina increases with the adsorption density and reaches a maximum at the adsorption density of $10^{-7}$mol/m$^2$. Further adsorption of the surfactant causes the hydrophobicity to decrease, suggesting reverse orientation of the surfactant at the solid/liquid interface.

It is to be noted that the bilayer conformation of n-dodecyl-β-D-maltoside on alumina may not be a regular homogenous bilayer. Due to the bulky nature of the maltose head group, close packing of the adsorbed layer will require the hydrocarbon chains of opposing surfactant to interpenetrate each other so that there is actually one layer of hydrocarbon chains with two layers of headgroups on each side. The cross-sectional area of the headgroup is 48.5 Å$^2$ while that of the paraffin chain is about 20 Å$^2$. Hence the arrangement proposed above can be considered to be a strong possibility.

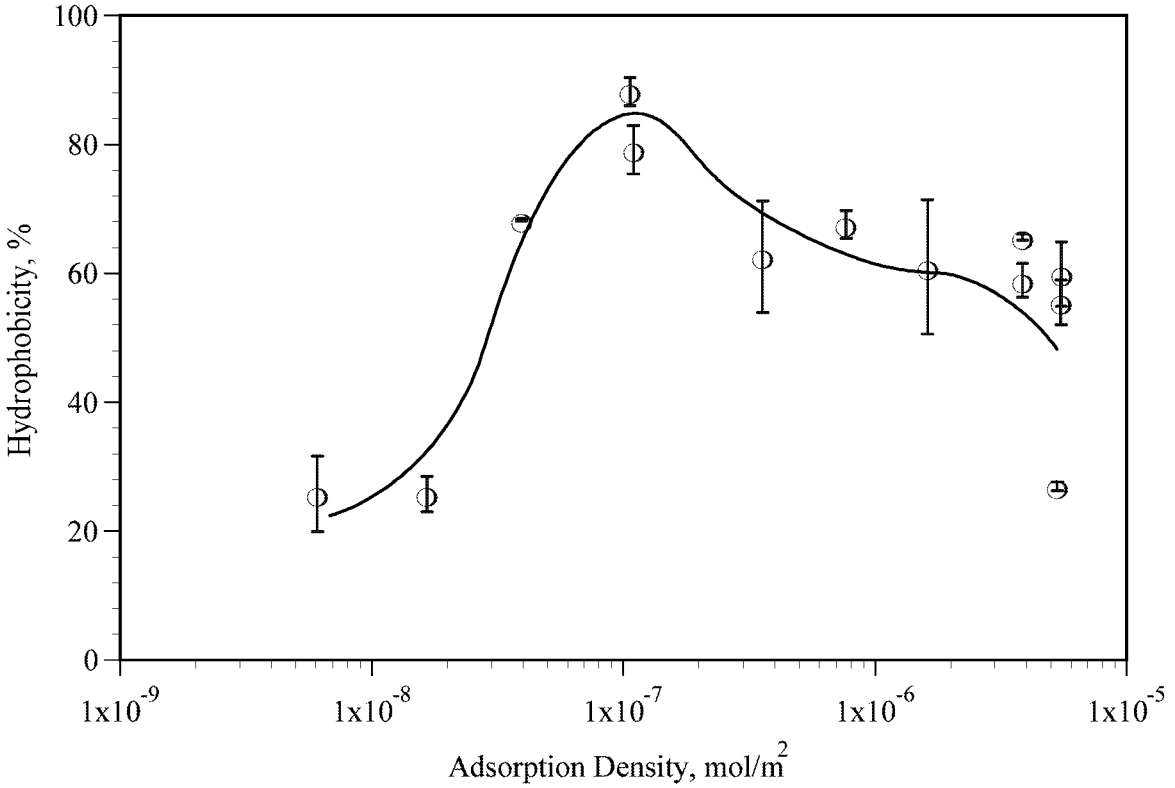


**Figure 32. Hydrophobicity of Alumina Particles after N-Dodecyl-β-D-Maltoside Adsorption**

## 4. ADSORPTION MECHANISM OF N-DODECYL-β-D-MALTOSIDE ON ALUMINA

As mentioned above, it was found that n-dodecyl-β-D-maltoside adsorbs on alumina, hematite and titania, but markedly less on silica. This behavior is opposite to that of the nonionic ethoxylated surfactants, which adsorb on silica but not on alumina and hematite. This unique behavior of sugar-based surfactants, plus the environmental advantage of these biodegradable substance, enable them to be utilized in various applications such as flocculation/dispersion, wetting and enhanced oil recover. Since adsorption on silica and silicates are relevant to EOR systems, it is important to explore the reasons for the different adsorption behavior of these surfactants for efficient usage of them.

It is known that polysaccharide polymers such as dextrin and starch also adsorb on alumina and hematite but not on silica. This behavior is similar to that of n-dodecyl-β-D-maltoside. Since n-dodecyl-β-D-maltoside, as well as alkyl polyglucosides, has oligo-saccharide headgroups, the interactions between their headgroups and oxides could be similar to those between polysaccharide polymers and oxides. Hydrogen bonding has been proposed as the driving force for the adsorption of polysaccharides. However, some experimental evidence has been obtained suggesting also chemical interactions between polysaccharides and oxides. In this section, adsorption mechanism of n-dodecyl-β-D-maltoside was investigated systematically by combining adsorption and electrokinetic observations and spectroscopic analysis with theoretical considerations.

*Adsorption/Desorption of n-dodecyl-β-D-maltoside on alumina*

Adsorption isotherm of n-dodecyl-β-D-maltoside on alumina is shown in Figure 33 along with the corresponding desorption isotherm. The isotherm shows a typical three stage adsorption with a very low adsorption at low concentrations, a sharp increase at concentrations close to the

critical micelle concentration of the surfactant, and a plateau region at concentrations higher than CMC. It is to be noted that the isotherm has a very small slope in the low concentration range, indicating weak driving force for adsorption, since stronger interactions such as electrostatic interactions would result in a slope of 1 at low concentrations under constant ionic strength conditions. The S shape of the adsorption isotherm indicates strong interactions between the adsorbate species, in this case hydrophobic chains, and comparatively weaker interactions between the adsorbate and the adsorbent. The corresponding desorption isotherm shows that the adsorption process is reversible with no hysteresis under the tested conditions. This also suggests a lack of strong specific interactions such as chemisorption between this surfactant and the solid.

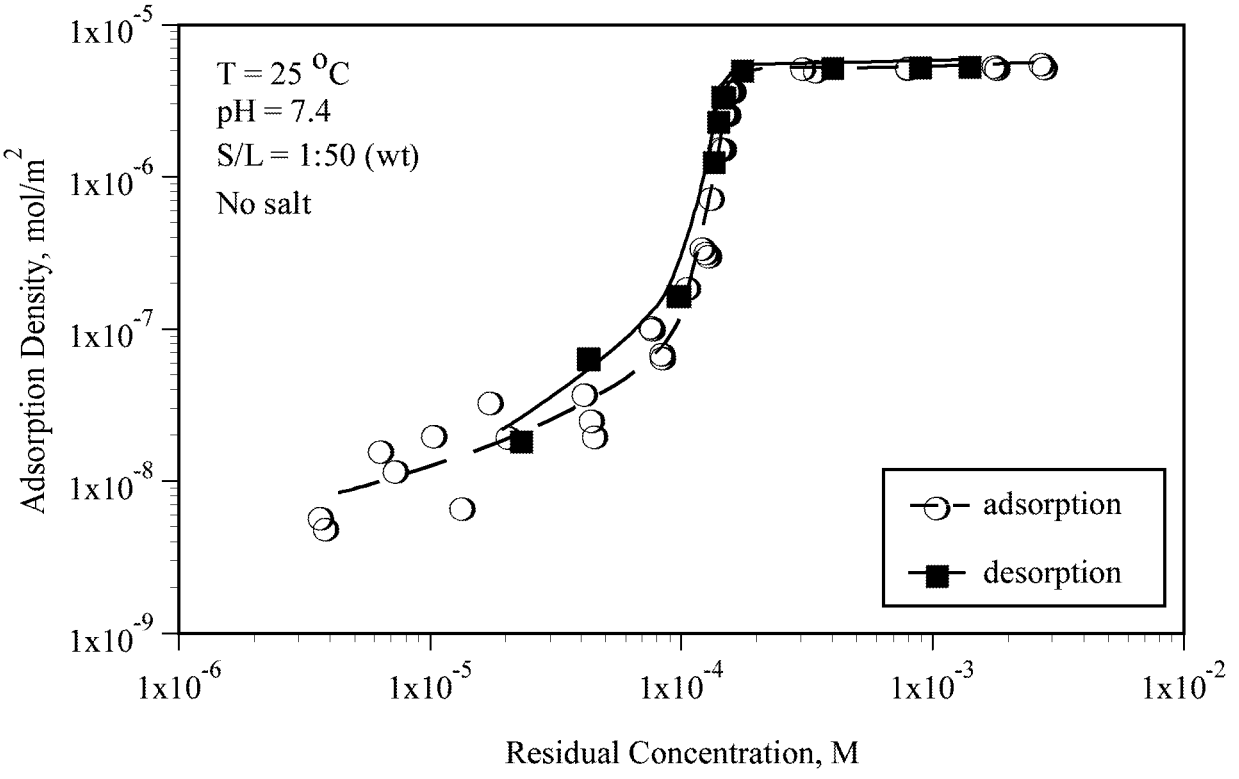


**Figure 33. Adsorption and Desorption Isotherms of n-Dodecyl-β-D-Maltoside on Alumina**

*Zeta-potential of alumina after n-dodecyl-β-D-maltoside adsorption*

The effect of pH on the adsorption of DM on alumina was shown in Figure 27. The result suggests that surface charge of alumina does not govern the adsorption of n-dodecyl-β-D-maltoside under the tested conditions.

In order to further examine the role of electrostatic interactions, electrokinetic measurements were made on alumina after n-dodecyl-β-D-maltoside adsorption and the results are shown in Figure 34. The zeta-potential of alumina changed only slightly by the adsorption of DM surfactant. This small decrease of zeta-potential in the case of alumina is proposed to be due to the masking of the solid surface by the adsorbed surfactant species. These results are in accord with the non-ionic nature of the n-dodecyl-β-D-maltoside and eliminate the possibility of any electrostatic interaction between the solid and the surfactant.

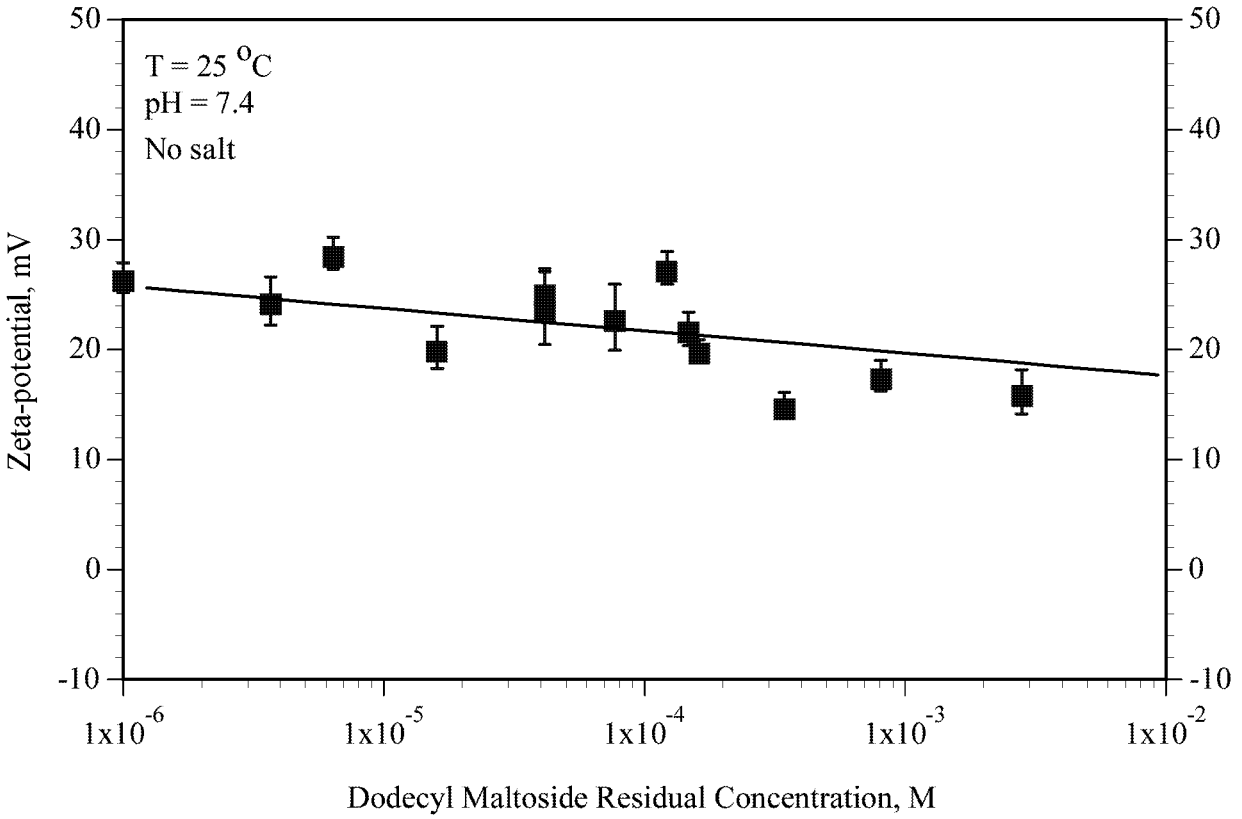


**Figure 34. Zeta-potential of Alumina after n-Dodecyl-β-D-Maltoside Adsorption at Neutral pH**

*Interaction between calcium ion and n-dodecyl-β-D-maltoside*

Multivalent metal cations such as calcium and aluminum ion are known to interfere with the performance of some surfactants by precipitation or complexation. No such interactions have been found for n-dodecyl-β-D-maltoside in solution by surface tension studies. To further explore the possibilities of such interactions, the concentration change of calcium ion has been measured in the presence of n-dodecyl-β-D-maltoside using conductivity technique.

Two DM concentrations were chosen such that one is with surfactant micelles in solution while the other is without. The results illustrated in Figure 35 show the calcium ion conductivities in water, 0.1 mM and 0.5 mM DM solutions to be identical. It can therefore be concluded that there is no interaction between calcium ion and n-dodecyl-β-D-maltoside. Implications of the absence of calcium sensitivity to EOR is very important.

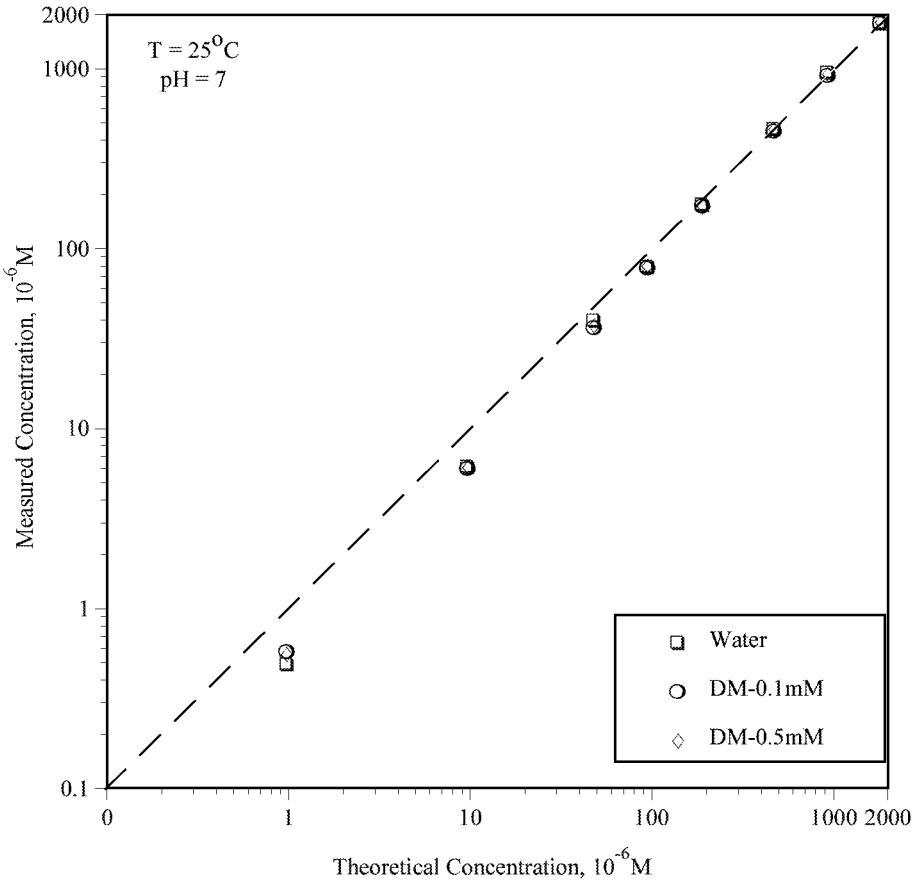


**Figure 35. Effect of n-Dodecyl-β-D-Maltoside on the Calcium Conductivity**

*Adsorption of maltose on alumina*

Since the adsorption of n-dodecyl-β-D-maltoside on alumina is considered to be first due to the interactions between surfactant maltose headgroup, and surface species of alumina, the adsorption of maltose on alumina was also investigated. The adsorption isotherm of maltose is shown in Figure 36 along with that for n-dodecyl-β-D-maltoside. There is only a small amount of maltose adsorbed on alumina and there is no sharp rise in adsorption, suggesting that there exists only weak interaction between maltose and alumina. The sharp rise in adsorption density in the case of dodecyl maltoside surfactant at higher concentrations is due to the hydrophobic interactions between the surfactant chains. This can be concluded by noting the different shapes of the adsorption isotherms for maltose and n-dodecyl-β-D-maltoside.

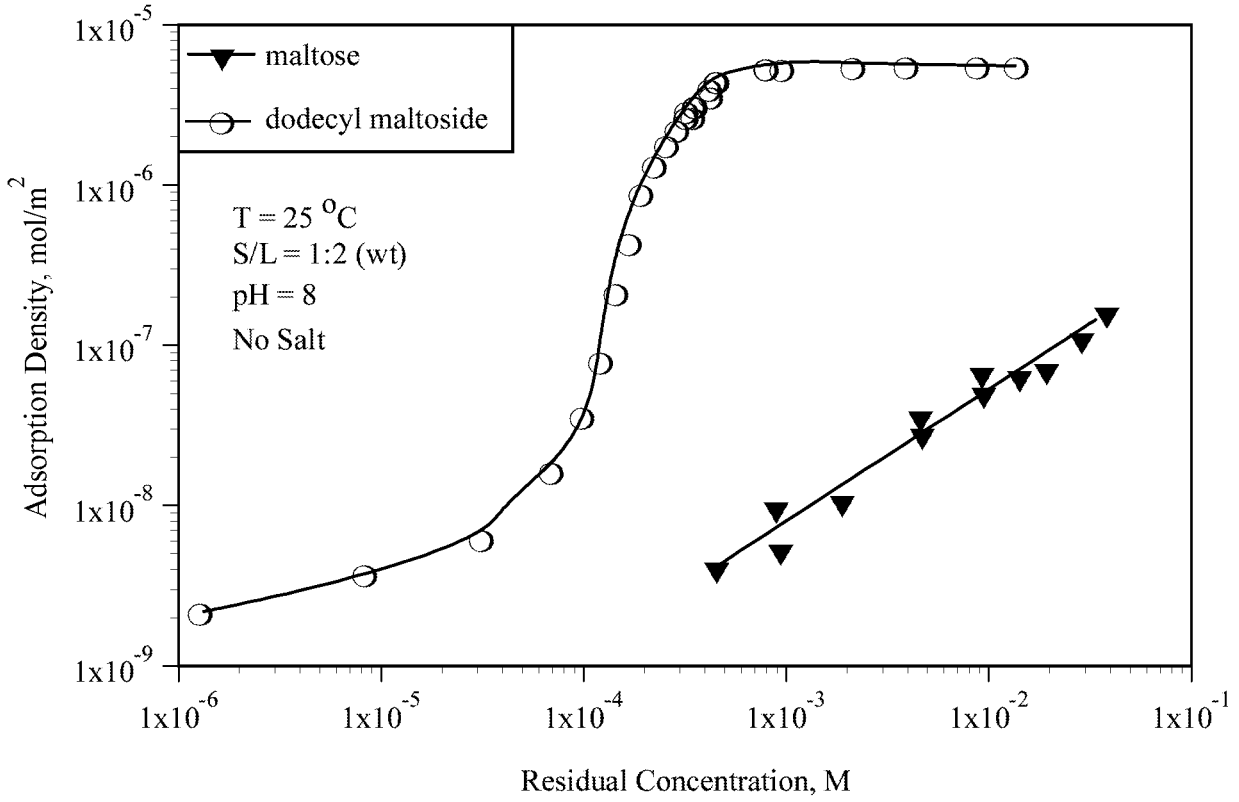


**Figure 36. Adsorption of Maltose on Alumina Compared with that of n-Dodecyl-β-D-Maltoside**

*Effect of temperature on adsorption of n-dodecyl-β-D-maltoside on alumina*

Adsorption of nonionic surfactants is usually sensitive to temperature. For ethoxylated surfactants, increase in temperature usually causes an increase in the adsorption density due to their dehydration at elevated temperatures. To investigate this aspect, the effect of temperature on the adsorption of n-dodecyl-β-D-maltoside on alumina is tested and results are shown in Figure 37. Temperature has almost no effect on the adsorption of n-dodecyl-β-D-maltoside. Also, the maximum adsorption density is not affected by the temperature change. The shift in inflection point (between the sharp-rising region and the plateau region) is mostly due to the increase in critical micelle concentration of the surfactant upon elevating the temperature. Since the chemical reaction rate is a function of temperature, the negligible dependence of adsorption on temperature in this case suggests that there is no chemical interaction between the surfactant and the solid.

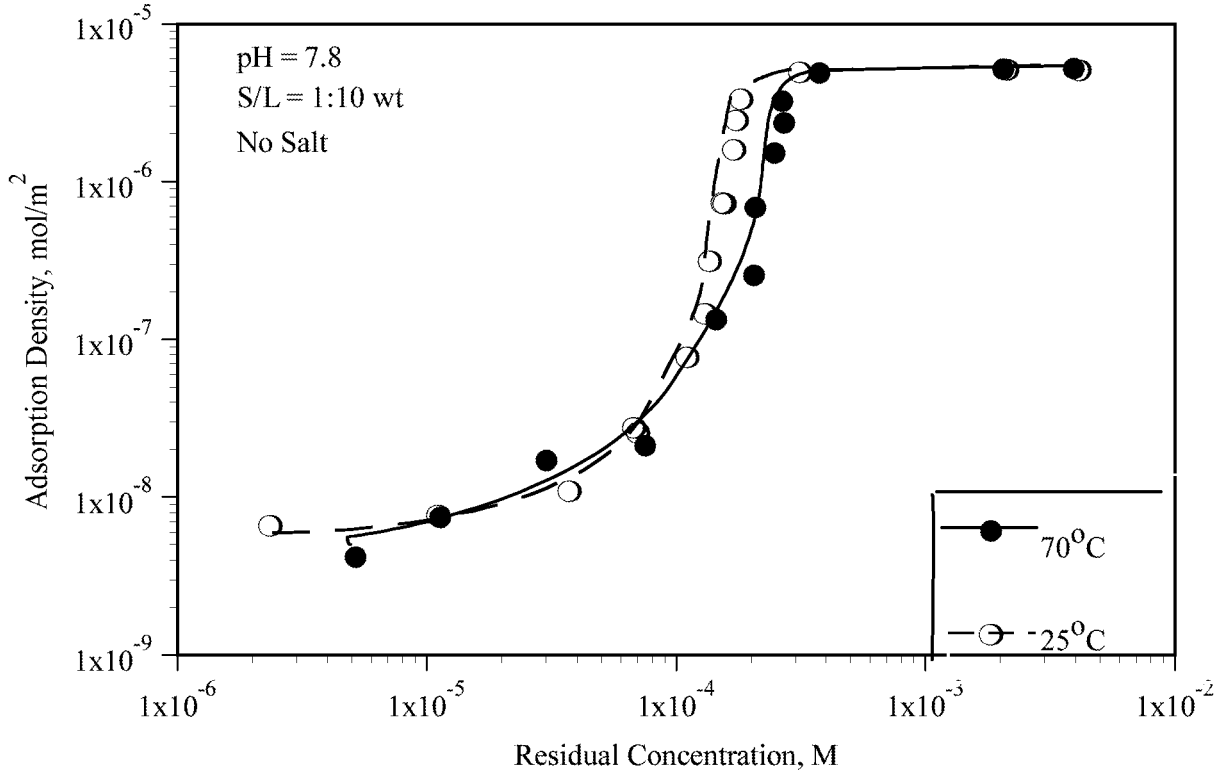


**Figure 37. Effect of Temperature on the Adsorption of n-Dodecyl-β-D-Maltoside on Alumina**

*Adsorption/desorption of n-dodecyl-β-D-maltoside on alumina in urea and DMSO solutions*

It is proposed that hydrogen bonding is the most possible driving force for the adsorption of n-dodecyl-β-D-maltoside on alumina. To test this hypothesis, adsorption in various solvents were carried out. Urea and dimethyl sulfoxide(DMSO) are strong hydrogen bonding acceptors. They can be expected to affect the hydrogen bonding between the solid substrate and the surfactant in solution by preferential formation of hydrogen bonds between themselves and with either the solid or the surfactant. The presence of urea or DMSO should affect the adsorption of n-dodecyl-β-D-maltoside on alumina, if hydrogen bonding is the driving force for the adsorption.

Adsorption and desorption isotherms of n-dodecyl-β-D-maltoside on alumina in urea and DMSO solutions are shown in Figures 38 and 39. The results show that adsorption density is affected markedly by both urea and DMSO. In urea solution, the maximum adsorption is lower and the inflection points of the isotherms are shifted to higher concentrations. Urea is known to affect the solvent properties. The DMSO not only decreased the adsorption density, but also yielded a very different isotherm shape. There is no clear inflection point on the isotherm in the 85% DMSO solution. These results suggest that hydrogen bonds between solid and surfactant are weakened in the presence of urea and DMSO. The different shapes of adsorption and desorption isotherms of DM on alumina in the 85% DMSO solution can be explained by the absence of DM aggregation at the solid/liquid interface. The sharp rise in the adsorption isotherm is obtained only when solloids (surface aggregates, hemimicelles) form.

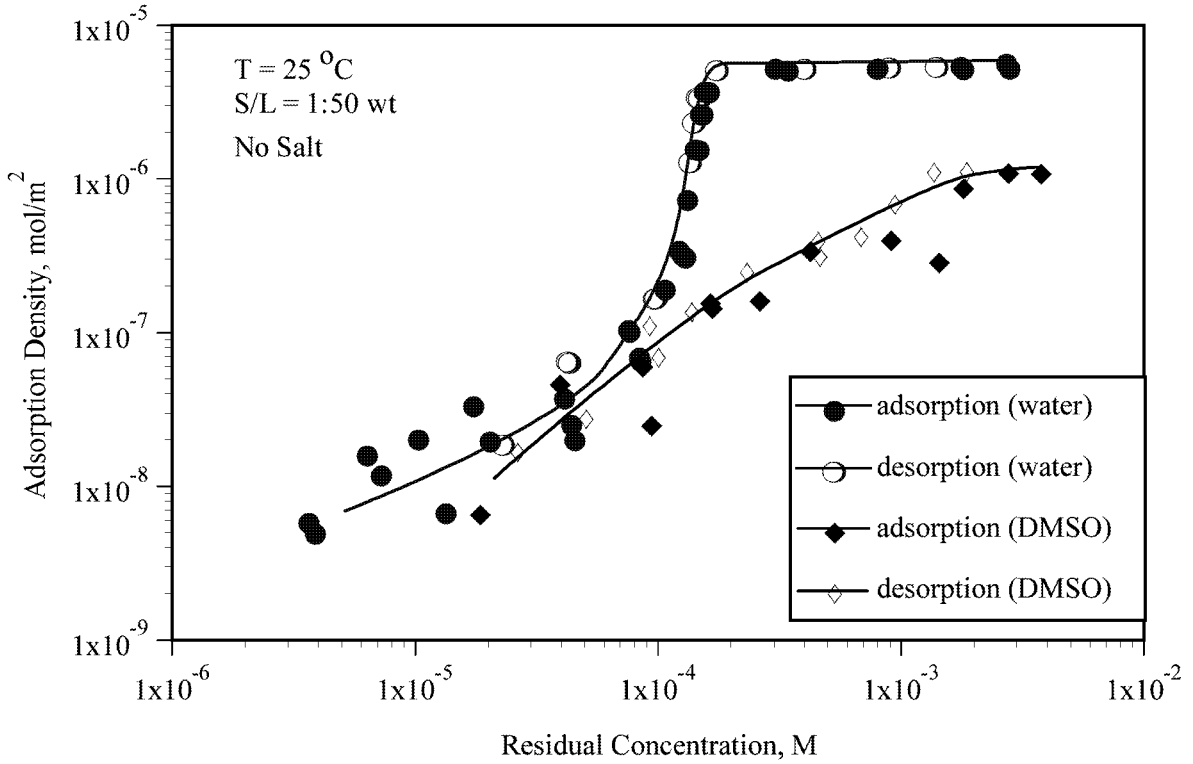


**Figure 38. Adsorption and Desorption of n-Dodecyl-β-D-Maltoside in the Presence of 5M Urea**

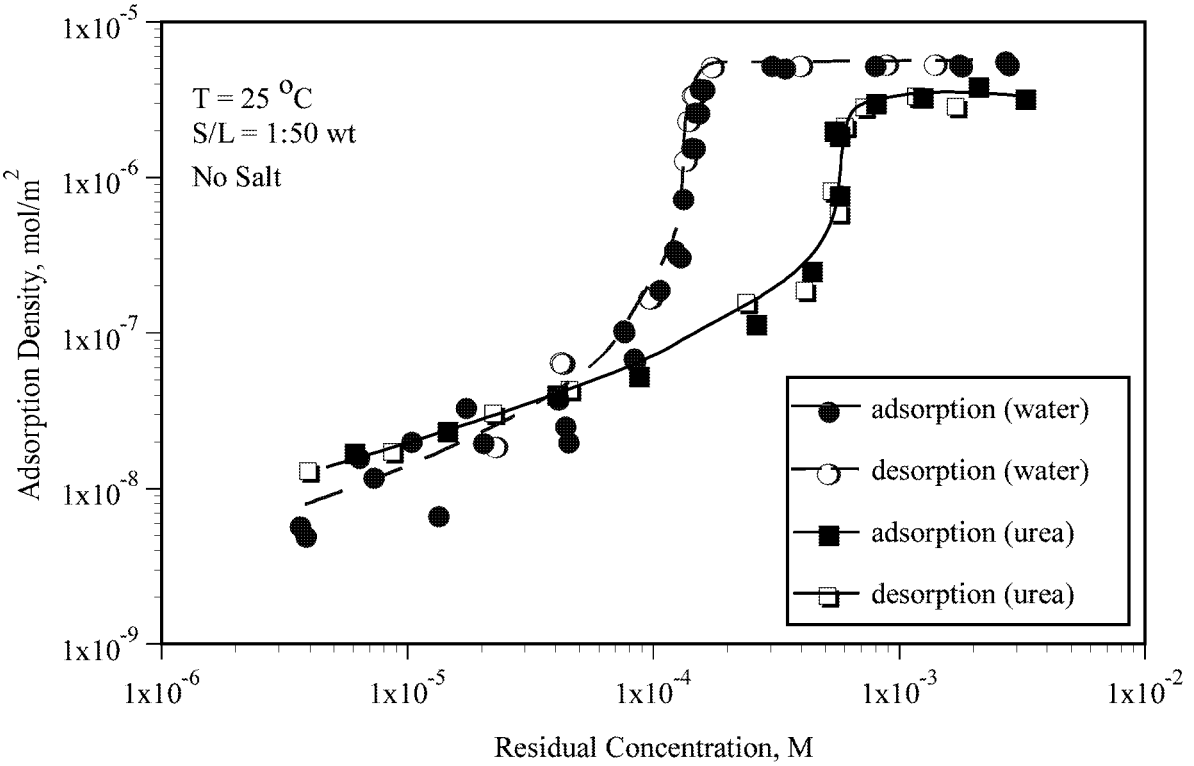


**Figure 39. Adsorption and Desorption of n-Dodecyl-β-D-Maltoside in the Presence of 85% DMSO**

*Characterization of N-Dodecyl-β-D-Maltoside/Alumina Interactions by FTIR Spectroscopy*

FTIR spectroscopy can give direct evidence for certain chemical interactions between surfactants and solids. Attenuated total reflectance (ATR) technique was used here to probe in-situ interactions of the surfactant with the solid. The ATR spectra of n-dodecyl-β-D-maltoside in solution and adsorbed on alumina in the region 4000-400 $cm^{-1}$ are shown in Figure 40. The spectrum of adsorbed n-dodecyl-β-D-maltoside on surfaces was obtained by subtracting the spectrum of alumina slurry from that of alumina/surfactant system. As water was used for the background scan, the strong peak around 1640 $cm^{-1}$ is attributed to the H-O-H bending of the water molecules. Strong absorption by water and the solid also occurs in the 4000-3000 $cm^{-1}$ and 800-400 $cm^{-1}$ regions.

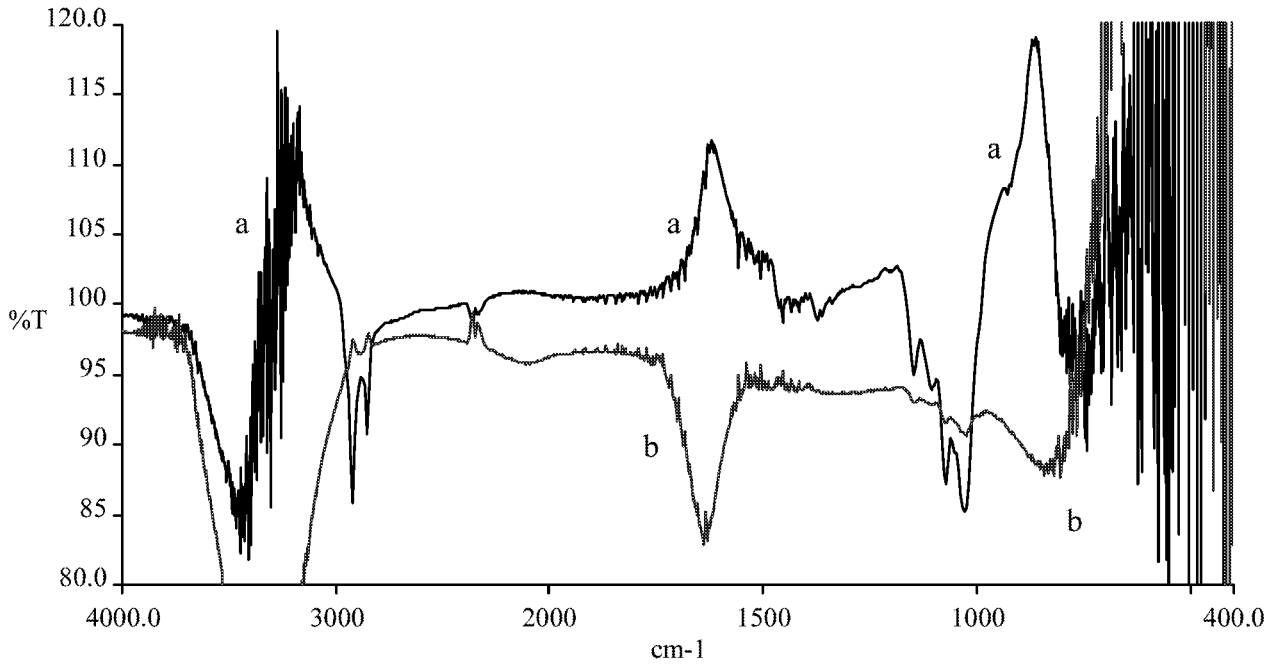


**Figure 40. 4000-400 $cm^{-1}$ ATR Spectrum of DM Adsorbed on Alumina with Alumina Subtracted(a), Compared to the Spectrum of DM in Solution (b) (T : Transmittance)**

The 1300-700 $cm^{-1}$ range is very infrared active for the polysaccharides. Spectra of the adsorbed surfactant and the surfactant in solution in the region 1200-800 $cm^{-1}$ are shown in Figure

41 (enlarged from Figure 40). In the spectrum of the adsorbed surfactant, the intense bands at 1149, 1075 and 1030 $cm^{-1}$ are characteristic of various -C-OH stretchings of the glucose and the peak at 859 $cm^{-1}$ is for the ring vibration. The spectrum of the surfactant in solution has no strong absorption bands. The bands at 1075, 1027, 836, 822, 819 and 807 $cm^{-1}$ shift very slightly upon adsorption of the surfactant, indicating no chemical interaction between the surfactant and alumina.

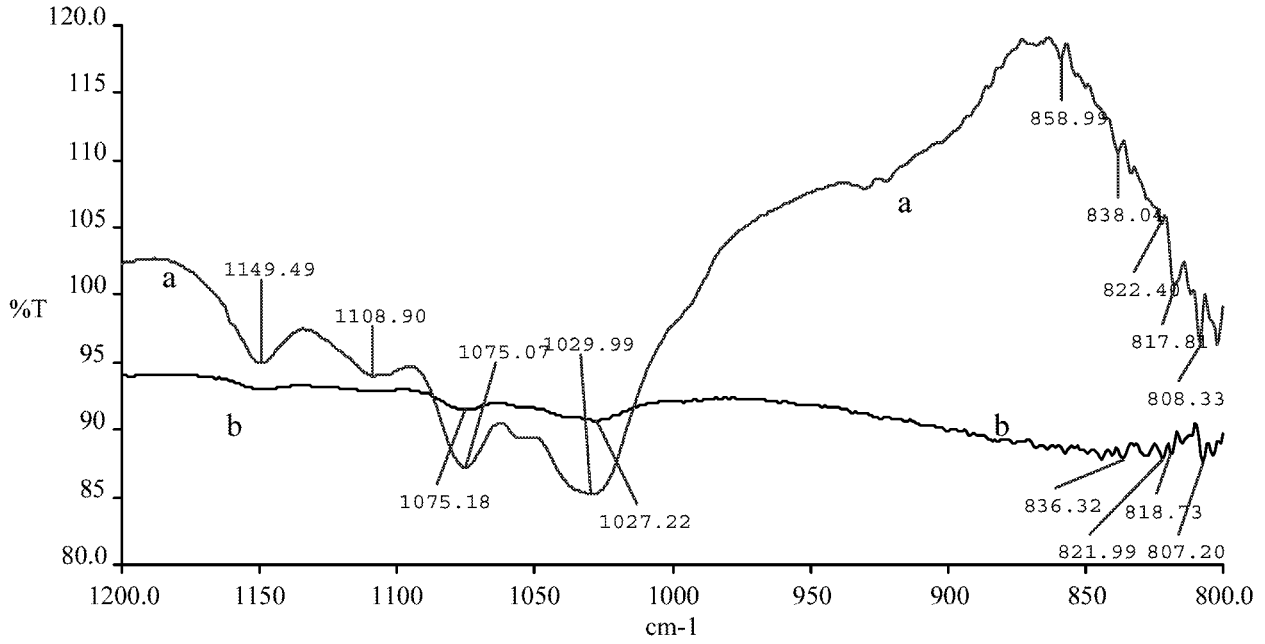


**Figure 41. 1200-800 $cm^{-1}$ ATR Spectrum of DM Adsorbed on Alumina with Alumina Subtracted(a), Compared to the Spectrum of DM in Solution (b)**

To further explore the adsorption of n-dodecyl-β-D-maltoside on alumina, the spectrum of maltose/alumina system was also studied since maltose is the functional group on the former. The ATR spectra obtained for maltose in solution and at solid/liquid interface show that the peaks of the maltose adsorbed on solid surfaces are similar to those of maltose itself, indicating that there is no chemical interaction between maltose and alumina as well (Figure 42).

The spectra of n-dodecyl-β-D-maltoside and maltose in solution and those at the solid/liquid interface show no significant band shift due to the adsorption over the region studied. These results

further suggest that the adsorption of n-dodecyl-β-D-maltoside on alumina is not due to specific interactions between the DM surfactant and the solid.

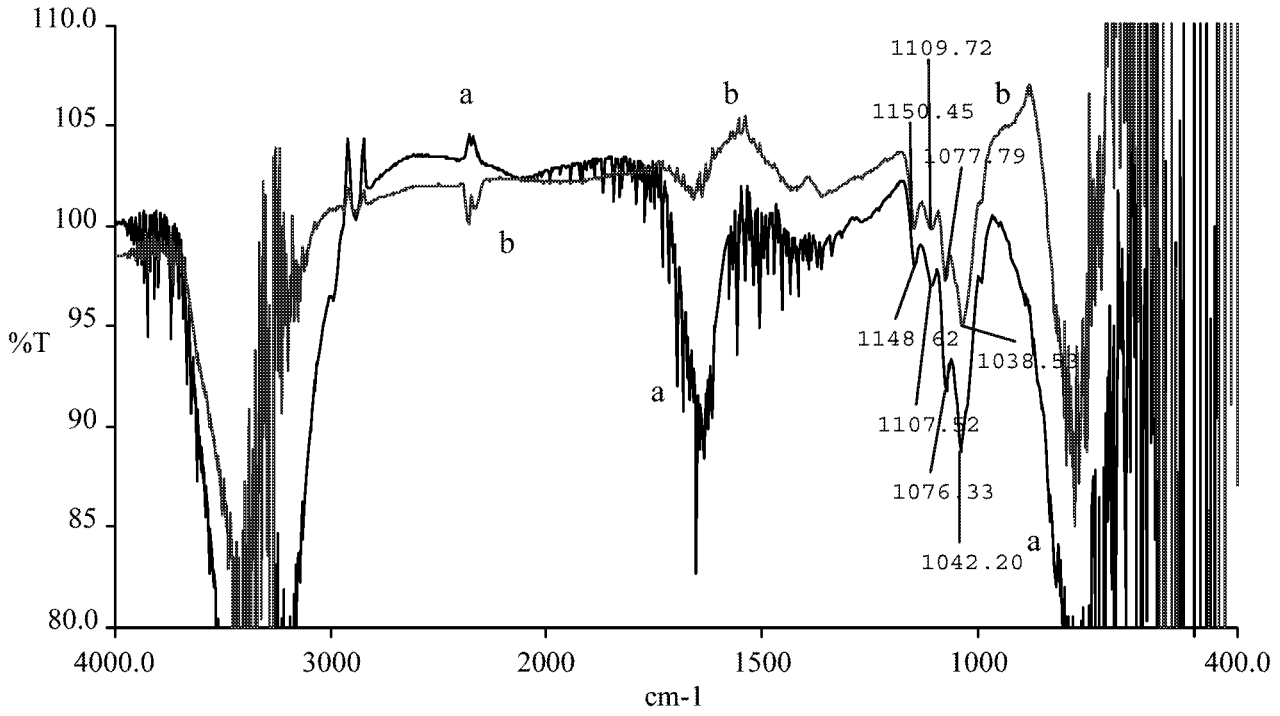


**Figure 42. ATR Spectrum of Maltose Adsorbed on Alumina with Alumina Subtracted(a), Compared to the Spectrum of Maltose in Solution (b)**

It is therefore proposed that hydrogen bonding between hydroxyl groups on the surfactant and alumina surface hydroxyl species is the driving force for the adsorption of n-dodecyl-β-D-maltoside on it. Experimental evidence for hydrogen bonds formed between surfactant hydroxyl groups and solid surface hydroxyl groups in aqueous solution is rather difficult to obtain, since water molecules are capable of hydrogen bonding extensively with each other and with hydroxyl groups of the solids and the surfactants. However, disruption of the adsorption by hydrogen bond breaker has been observed. By elimination of other possibilities such as electrostatic interactions and chemical interactions, hydrogen bonding is proposed to be the most possible driving force for the adsorption

of n-dodecyl-β-D-maltoside on alumina. These results suggest that the potential loss of sugar-based surfactants by adsorption on oil field rocks is likely to be minimal. This and the insensitivity to calcium may be two significant advantages for using sugar-based surfactants in enhanced oil recovery (EOR).

## 5. MIXTURES OF SUGAR-BASED SURFACTANTS WITH OTHER TYPES OF SURFACTANTS IN SOLUTION

To better understand the surfactant interactions at solid/liquid interface relevant to the enhanced oil recovery process, it is necessary to have also a knowledge of their solution behavior. It was also an aim to investigate the properties of surfactant mixtures in solution by studying their surface tension behavior.

The interactions of sugar-based dodecyl polyglucoside (C12-APG) and n-dodecyl-β-D-maltoside (DM) with anionic sodium dodecylsulfate (SDS), cationic dodecyl trimethylammonium bromide (DTAB), and nonionic pentaethyleneglycol monododecyl ether ($C_{12}EO_5$) were studied with and without a supporting electrolyte in the solution. As they all have the same hydrophobic chain length, any deviation from ideality can be ascribed to dissimilarity in the hydrophilic headgroups. The results are analyzed by regular solution theory.

*Regular solution theory and interaction parameter*

The description of the physicochemical behavior of binary surfactant mixtures depends upon both the value of the cmc and the distribution of surfactant components between micellar and aqueous phases. In a binary mixture, the excess free energy of mixing, $G^E$, can be expressed as:

$$G^E = RT \{x_1 \ln f_1 + (1 - x_1) \ln f_2\} \qquad (1)$$

where $x_1$ is the mole fraction of component 1, $f_1$ ,$f_2$ are the activity coefficients of components 1 and 2. By definition, such activity coefficients become equal to one for both ideal mixtures and pure components.

The regular solution approximation has been one of the most widely used for modeling mixed surfactant systems. This theory assumes that the entropy of mixing is zero and therefore the excess

heat of mixing, $H^E$, dominates the mixing process:

$$H^E = \beta x_1 (1 - x_1) RT \tag{2}$$

where $\beta$ is a dimensionless parameter which represents in terms of $RT$ the difference in the interaction energy between mixed and unmixed systems. Substitution of Equation 2 into 1 leads to the activity coefficients of binary mixtures:

$$f_1 = \exp \beta (1 - x_1)^2 \tag{3}$$

$$f_2 = \exp \beta x_1^2 \tag{4}$$

This theory provides a good physical description for a wide range of surfactant combinations with a single interaction parameter, $\beta$. This parameter, by definition, is a measure of the deviation of the behavior of the mixtures from ideality and is an indication of the molecular interactions of the surfactants in mixed micelles.

Among the experimental techniques routinely used for measuring mixed cmcs is surface tension measurement. The following equations permit solution for $\beta$ in terms of cmc of the each component and mixed systems.

$$\frac{x^2 \ln[\frac{C^* \alpha}{C_1 x}]}{(1 - x)^2 \ln[\frac{C^* (1 - \alpha)}{C_2 (1 - x)}]} = 1 \tag{5}$$

$$\beta = \frac{\ln(\frac{C^* \alpha}{C_1 x})}{(1 - x)^2} \tag{6}$$

where $C^*$ is the cmc of the mixed system, $C_1$, $C_2$ are cmcs of pure surfactants 1 and 2 respectively, $\alpha$ is the mole fraction of surfactant 1 in the total mixed solute, $x$ is the mole fraction of surfactant 1 in the total mixed micelle and $\beta$ is the interaction parameter. Equation 5 can be solved iteratively for

$x$. This, in turn, can then be used in equation 6 to calculate $\beta$.

*Mixtures of sugar-based surfactants with anionic surfactant*

Surface tension data for DM, SDS, and DM/SDS 3:1, 1:1, and 1:3 mixtures, with and without salt, are shown in Figures 43 and 44 as a function of the total concentration. The relevant data such as the critical micelles concentrations, the mole fraction of DM in the mixed micelles, and the interaction parameters of the mixtures are listed in Tables 3 and 4. The mole fractions and interaction parameters are calculated using the regular solution theory.

From Figures 43 and 44 as well as Tables 3 and 4, it can be concluded that in the surfactant mixture, dodecyl maltoside has the predominant role in mixed micellization at various mixture ratios. It is also the dominant component in the micellar phase. In surfactant mixtures, the component that has a lower cmc usually will be presented in a higher percentage in micelles and at the air-water interface because of its higher surface activity. These results are in accord with the fact that DM is much more surface active than sodium dodecylsulfate.

**Table 3 Results of Surface Tension Data Analysis for DM/SDS Mixtures Without Salt at 25°C**

| DM : SDS | 100 : 0 | 75: 25 | 50 : 50 | 25 : 75 | 0 : 100 |
|---|---|---|---|---|---|
| cmc (M) | 0.00018 | 0.000196 | 0.000255 | 0.000438 | 0.008 |
| DM mole fraction in micelle | | 0.867 | 0.801 | 0.731 | |
| interaction parameter $\beta$ | | -4.00 | -3.77 | -3.25 | |
| average $\beta$ | -3.67 | | | | |

**Table 4 Results of Surface Tension Data Analysis for DM/SDS Mixtures With Salt at 25°C**

| DM : SDS | 100 : 0 | 75: 25 | 50 : 50 | 25 : 75 | 0 : 100 |
|---|---|---|---|---|---|
| cmc (M) | 0.000169 | 0.000179 | 0.000227 | 0.000349 | 0.00267 |
| DM mole fraction in micelle | | 0.833 | 0.774 | 0.719 | |
| interaction parameter β | | -1.70 | -2.78 | -4.19 | |
| average β | -2.89 | | | | |

The average interaction parameter β is -3.67 for the system without salt and -2.89 for system with, indicating strong interaction between DM and SDS. This β value is typical of nonionic-ionic mixed surfactant systems. The synergy comes from two factors. First, the mixing of an ionic surfactant with a nonionic surfactant will cause a decrease in the surface charge density of the micelles, so that a mixed micelle of ionic and nonionic surfactants is more stable than a micelle containing only the ionic surfactant. Second, these different surfactant headgroups at the micellar surface can reduce any steric repulsion. Both factors favor micellization.

The presence of salt is found to reduce the synergy between the surfactants. In 0.03M NaCl the interaction parameter of DM/SDS is reduced from -3.67 to -2.89. This is mainly due to charge neutralization by the sodium counterions.

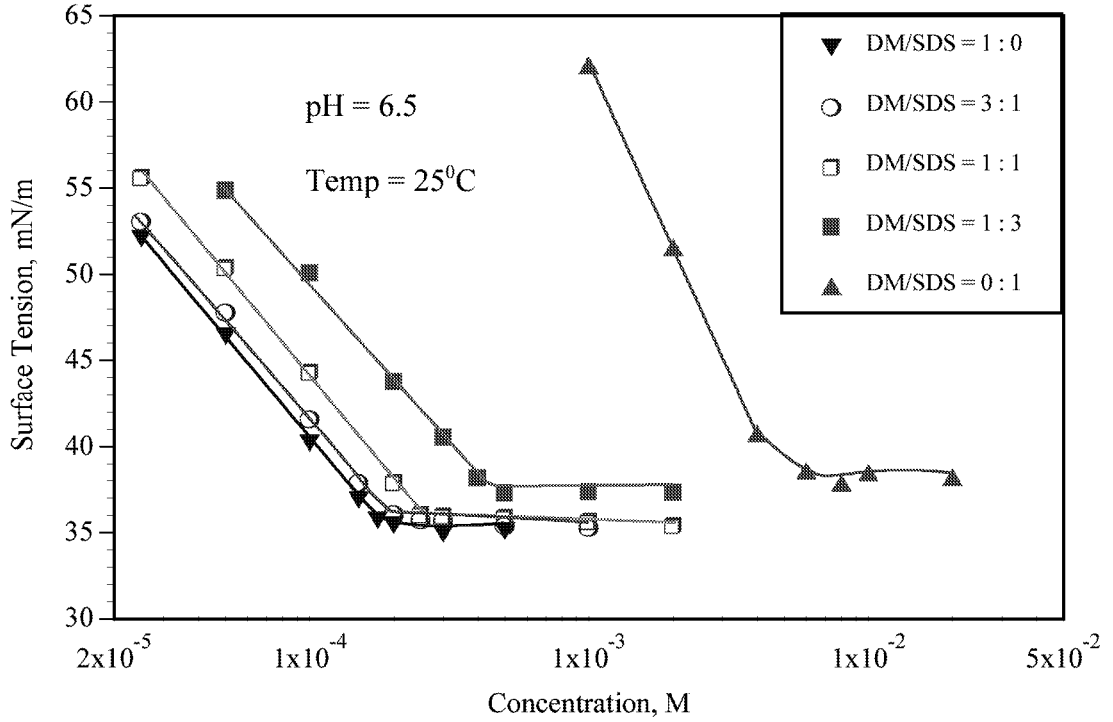


**Figure 43 Surface Tension vs. Concentration of DM/SDS Mixed Surfactant System Without Salt**

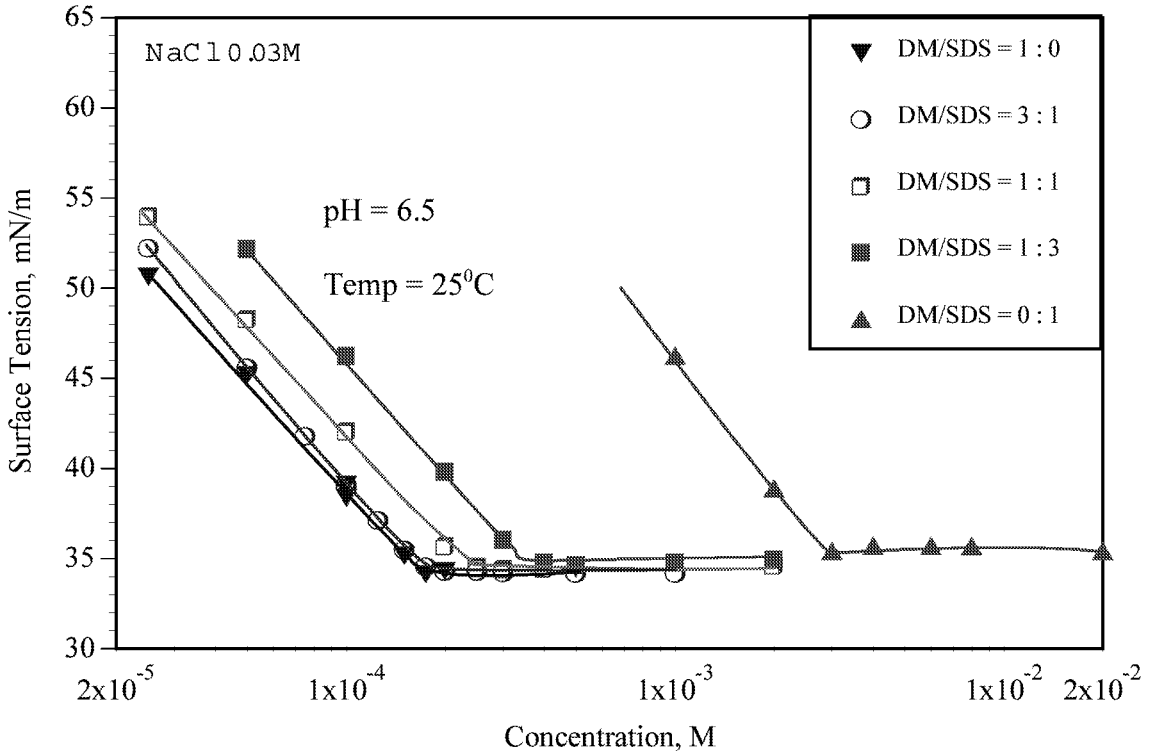


**Figure 44 Surface Tension vs. Concentration of DM/SDS Mixed Surfactant System With Salt**

To correlate the laboratory dodecyl maltoside sample with industrial alkyl polyglucoside samples, dodecyl polyglucoside ($C_{12}$-APG)/SDS system was studied next. Surface tension data obtained for the dodecyl polyglucoside mixture with the anionic SDS is plotted in Figure 45. Again, it is seen that APG is dominant in the APG/SDS mixtures. The interaction parameter for this system is -3.20, suggesting strong synergy. Similarity in interactions between DM/SDS and APG/SDS also implies that commercial polyglucosides are similar to pure laboratory samples with respect to synergistic interactions with the anionic surfactant, suggesting that the pure alkyl polyglucosides may be used for studying interactions of sugar-based surfactants in general

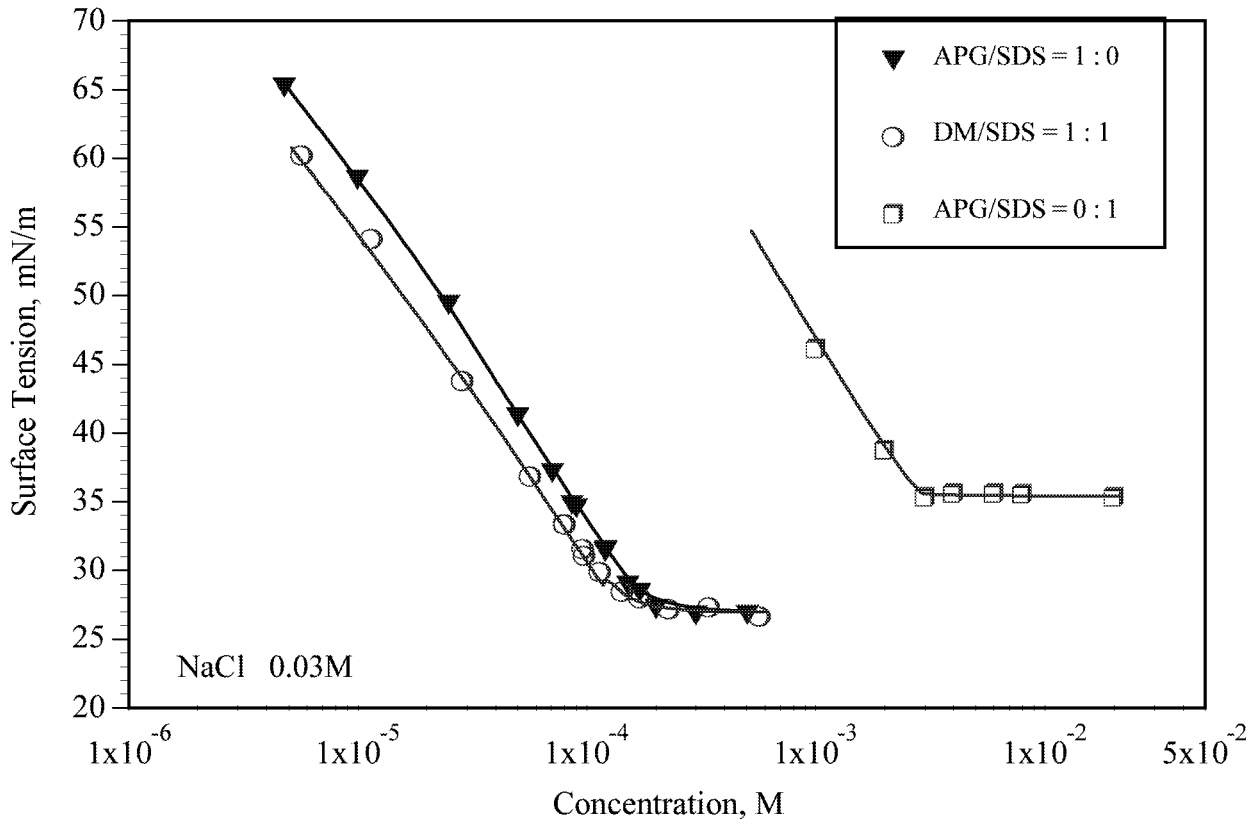


**Figure 45 The Surface Tension vs. Concentration of C12APG/SDS Mixed Surfactant System With Salt**

*Mixtures of sugar-based surfactants with cationic surfactant*

The interactions of sugar-based dodecyl polyglucoside (C12-APG) and n-dodecyl-β -D-maltoside(DM) with a typical cationic surfactant, dodecyltrimethylammonium bromide (DTAB), were studied under different conditions. The results obtained from surface tension measurements of DM, DTAB, and their mixtures, with and without salt, are shown in Figures 46 and 47, respectively, as a function of the total concentration.

From Figures 46 and 47, it can be seen that DM has the predominant role in mixed micellization. A small amount of DM can affect the surface tension of the mixture to a very large extent. The relevant data such as the critical micelles concentrations, the mole fraction of DM in the mixed micelles, and the interaction parameters of the mixtures are listed in Tables 5. The mole fractions and the interaction parameters are calculated based on the regular solution theory. DM is also the dominant component in the micellar phase. This is reasonable since the component with a lower cmc usually has a high percentage in micelles and at the air-water interface because of its higher surface activity.

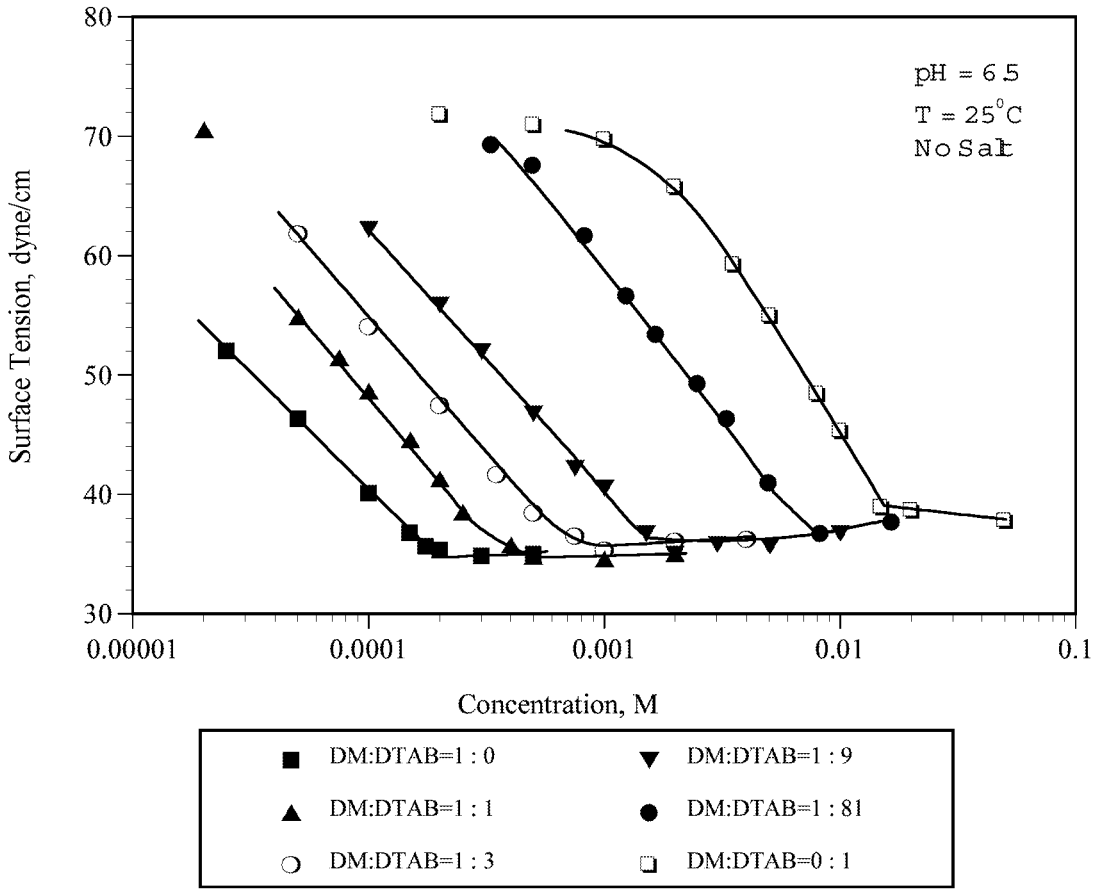


**Figure 46. Surface Tension vs. Concentration of DM/DTAB Mixed Surfactant Systems Without Salt**

**Table 5. Results of Surface Tension Data Analysis for DM/DTAB Mixtures Without Salt at 25°C**

| DM : DTAB | 1 : 0 | 1 : 1 | 1 : 3 | 1 : 9 | 1 : 81 | 0 : 1 |
|---|---|---|---|---|---|---|
| cmc (M) | 0.000182 | 0.000346 | 0.000642 | 0.00145 | 0.00672 | 0.015 |
| DM mole fraction in micelles | | 0.954 | 0.903 | 0.829 | 0.506 | |
| interaction parameter $\beta$ | -1.08 | | | | | |

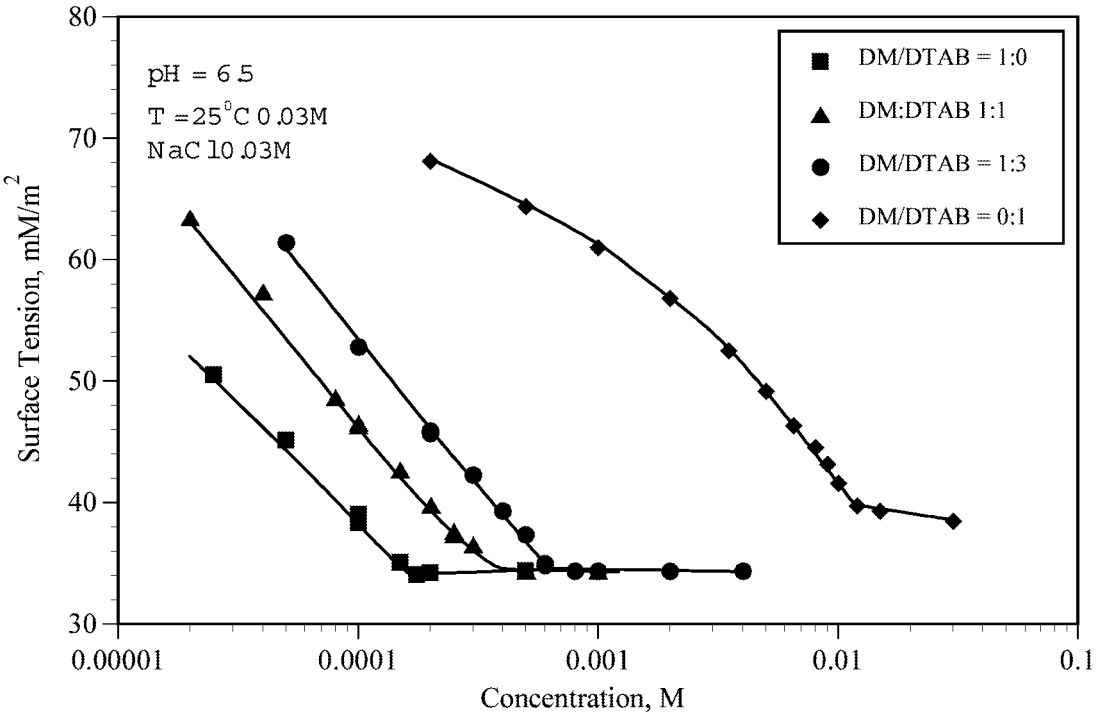


**Figure 47. Surface Tension vs. Concentration of DM/DTAB Mixed Surfactant Systems With Salt**

The interaction parameter β is -1.08 for the system without salt, indicating strong interaction between DM and DTAB. This interaction, however, is less than that between DM and sodium dodecylsulfate (SDS), which is -3.67.

The presence of salt is found to reduce the synergy between the surfactants though charge neutralization effect. In 0.03M NaCl the interaction parameter of DM/DTAB is reduced from -1.08 to -0.62. It is to be noted that the interaction parameter varies as a function of mixing ratios.

Industrial samples dodecyl polyglucoside ($C_{12}$-APG) was also studied in mixtures with DTAB. Surface tension data obtained for the dodecyl polyglucoside mixtures with DTAB is plotted in Figure 48. APG is dominant in the APG/DTAB mixtures also. The interaction parameter for this system is -0.41, which is lower than that obtained for the purer DM. Similarity in interactions between DM/DTAB and APG/DTAB implies that commercial polyglucosides also are similar to the

pure laboratory samples in synergistic interactions with the cationic surfactant.

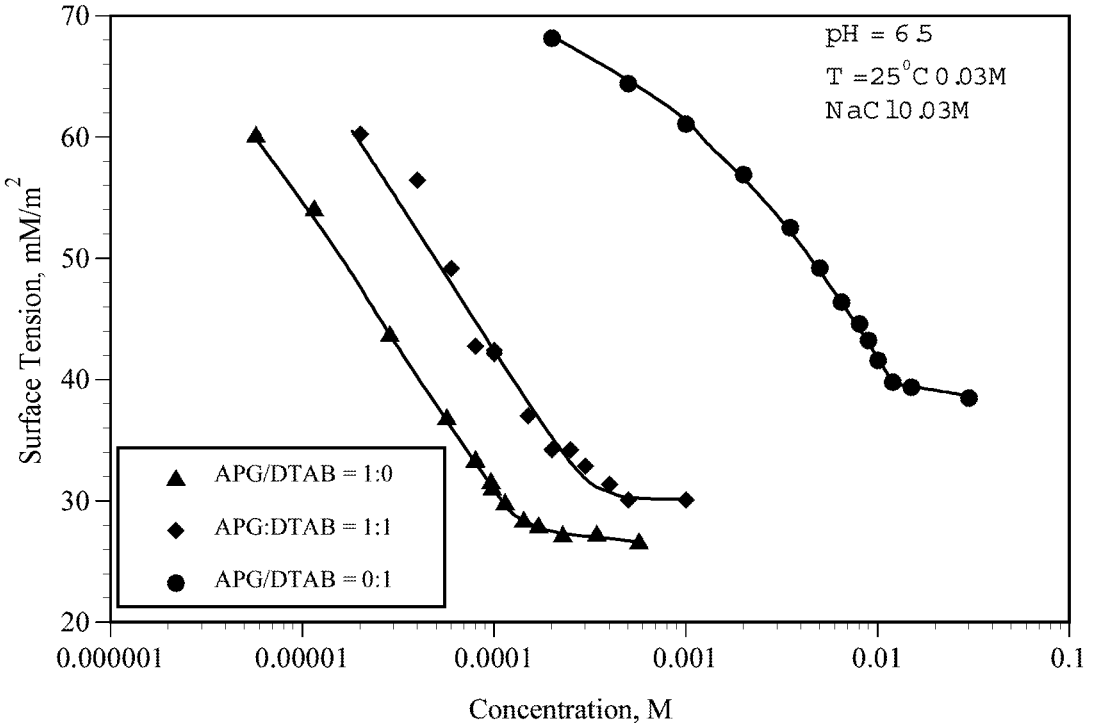


**Figure 48 The Surface Tension of C12APG/DTAB Mixed Surfactant Systems With Salt**

To obtain basic information on the structures of the micelles formed when mixed surfactants are used, the micellization was studied by fluorescence spectroscopy technique. In fluorescence spectroscopy the ratio of relative intensities of the $I_1$ (373nm) and $I_3$ (383nm) peaks ( $I_3/I_1$ ) on a pyrene emission spectrum shows the greatest solvent dependency. This ratio decreases as the polarity increases and can be used to estimate the solvent polarity of an unknown environment. The polarity parameter of pyrene is shown in Figure 49 as a function of concentration. At low concentrations, the value of $I_3/I_1$ ratio corresponds to that for water (0.5~0.6). At certain concentrations, there is a rapid increase in the value of $I_3/I_1$ ratio indicating the formation of micelles at this concentration. The cmc of the surfactant obtained from fluorescence tests are in good agreement with those obtained from surface tension measurements (Figure 46).

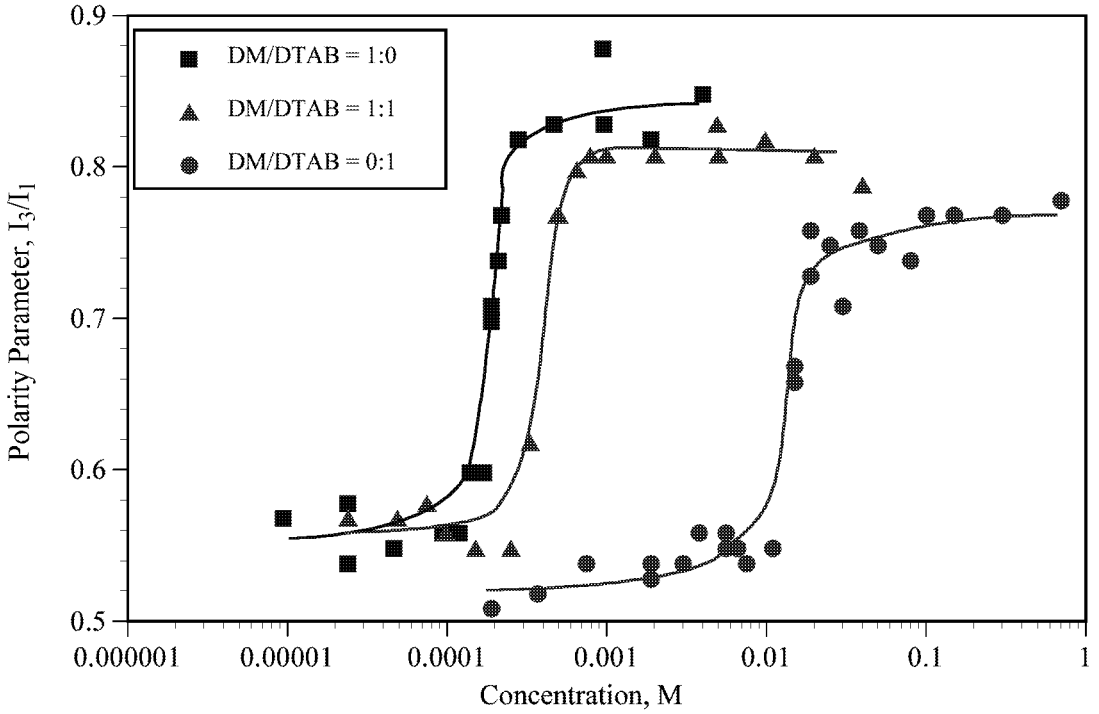


**Figure 49. Polarity parameters of DM/DTAB mixtures**

The polarity parameters of the pyrene at concentrations higher than cmc also give information on the hydrophobicity of the micelles. In DM/DTAB system, $I_3/I_1$ ratio for DM is higher than that for DTAB above cmc, suggesting that the core of DM micelles is more hydrophobic than that of DTAB micelles, but less hydrophobic than that of pure hydrocarbons.

*Mixtures of sugar-based surfactants with nonionic surfactant*

Sugar-based surfactants are nonionic, but their interfacial properties are quite different from the commonly used nonionic ethoxylated surfactants. For example, sugar-based surfactant adsorbs on alumina but very little on silica. The behavior of ethoxylated surfactants that are also nonionic is just the opposite. It is the aim to study their mixtures to reveal the reasons for this difference.

Surface tension of sugar-based dodecyl polyglucoside (C12-APG) and n-dodecyl-β-D-maltoside(DM) with pentaethyleneglycol monododecyl ether ($C_{12}EO_5$) was measured

and results are given in Figure 50 and 51.

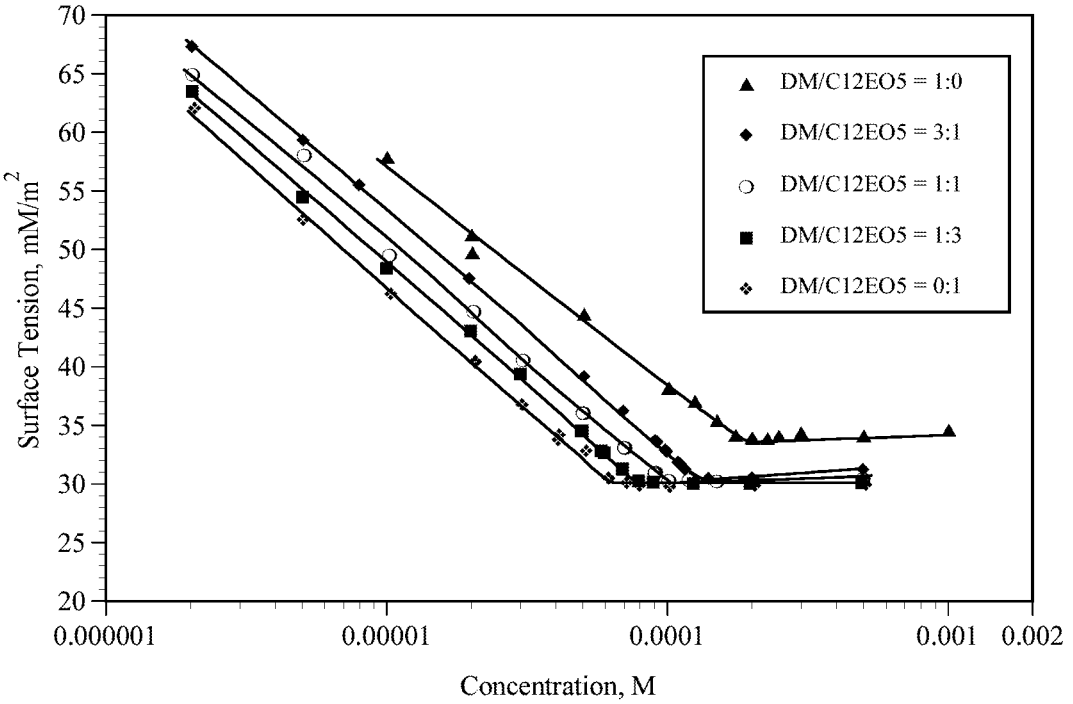


**Figure 50. The Surface Tension of DM/$C_{12}EO_5$ Mixed Surfactant Systems**

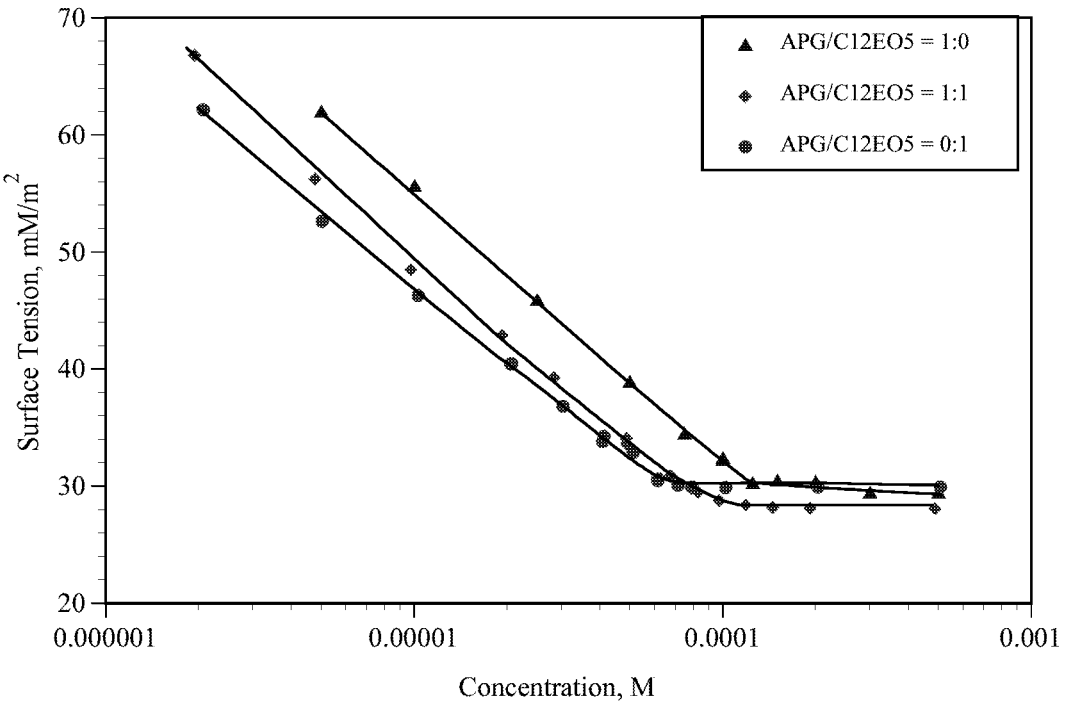


**Figure 51. The Surface Tension of C12APG/$C_{12}EO_5$ Mixed Surfactant Systems**

Interestingly, in these systems, $C_{12}EO_5$ is more surface active than the sugar-based surfactants, even though both have the same hydrocarbon chain. This suggests the higher hydrophilicity of the sugar molecules than that of ethoxyl groups. The interaction parameters are -0.18 for DM/$C_{12}EO_5$ and -0.04 for C12APG/$C_{12}EO_5$, respectively, indicating almost ideal mixing in solutions. These low values of interaction parameters are expected since both surfactants are nonionic and there is very little interaction between them in a solution.

The polarity parameter of pyrene in DM/$C_{12}EO_5$ system is studied by fluorescence spectroscopy and is illustrated in Figure 52 as a function of concentration. The rapid increase in the value of $I_3/I_1$ ratio occurs at the cmc of the surfactants. The $I_3/I_1$ for both DM and $C_{12}EO_5$ are similar at concentrations higher than cmc, suggesting that the core of micelles for both surfactants have similar hydrophobicity. Surprisingly, the maximum polarity in these mixed systems is similar to that obtained for the mixture of the sugar-based surfactants with the cationic surfactants suggesting again the predominant role of the sugar-based surfactants in determining the polarity of the micellar interior. This also suggests that pyrene is possibly locating itself in similar compatible part of the micelle core. It is to be noted that solubilization of the oil in micelles in EOR will depend very much on the hydrophobicity of the micellar interior.

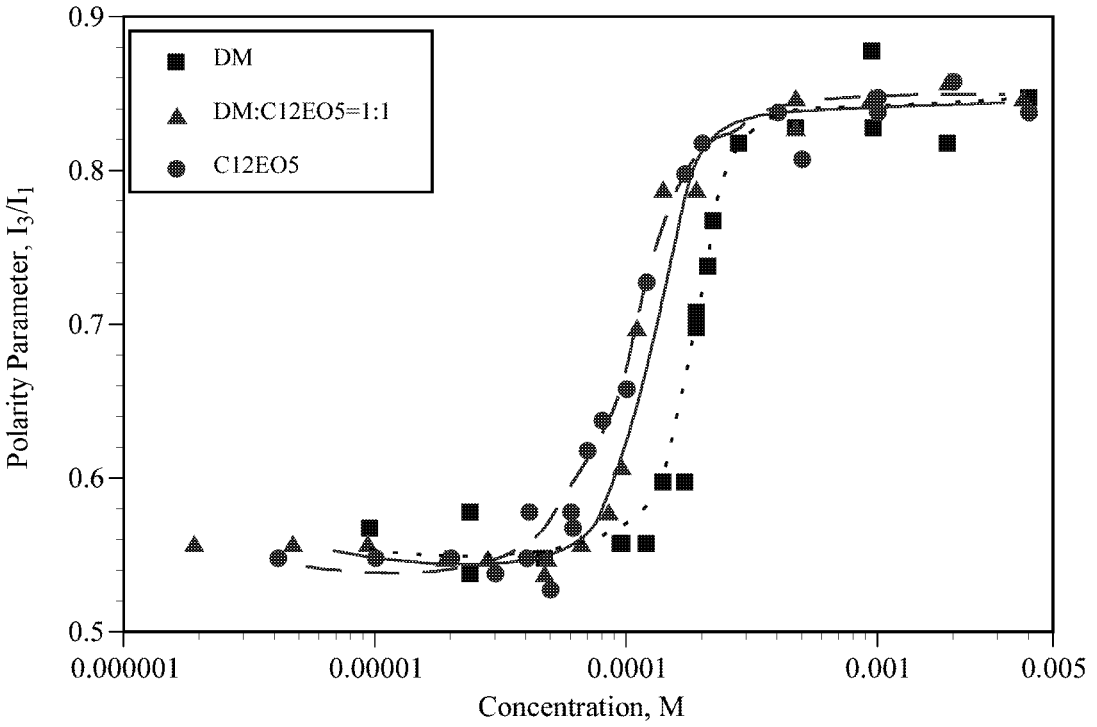


**Figure 52. Polarity parameters of DM/$C_{12}EO_5$ mixtures**

*Summary of mixtures of sugar-based surfactants with other surfactants*

Mixtures of sugar-based n-dodecyl-β-D-maltoside(DM) and dodecyl polyglucoside (C12-APG) with cationic dodecyltrimethyl ammonium bromide (DTAB), anionic sodium dodecylsulfate (SDS) and nonionic pentaethyleneglycol monododecyl ether ($C_{12}EO_5$)in solution, with and without supporting electrolyte, have been studied by surface tension measurement and fluorescence spectroscopy. The interaction parameters, as indicators of surfactant interactions, for these systems are summarized in Table 6.

**Table 6. Summary of Results for Sugar-based Surfactant in Mixtures**

| Mixtures | nonionic/anionic | | nonionic/cationic | | nonionic/nonionic | |
|---|---|---|---|---|---|---|
| | DM : SDS | APG : SDS | DM: DTAB | APG: DTAB | DM:$C_{12}EO_5$ | APG:$C_{12}EO_5$ |
| β (w/o salt) | -3.67 | | -1.08 | | -0.18 | -0.04 |
| β (w/salt) | -2.89 | -3.20 | -0.62 | -0.41 | | |

Since all the surfactants studied have the same hydrophobic chain, any deviation from ideality can be ascribed to dissimilarities in the hydrophilic headgroups. Sugar-based surfactants in mixing with cationic and anionic surfactants show strong synergy. This is because the mixing of an ionic surfactant with a nonionic surfactant will cause a decrease in the surface charge density of the micelles, and as a result a mixed micelle of ionic and nonionic surfactants should be more stable than a micelle containing only the ionic surfactant. This effect is further accompanied by a depression of the steric repulsion between the headgroups at the micellar surface. All these effects cause synergism, which dominates the cmc behavior over a large composition range. On the other hand, behavior of mixtures of nonionic surfactants is close to ideal mixing since there is no change in the electrostatic interactions in these micelles. Salt is found to reduce the synergy between surfactants. This is mainly due to charge neutralization effect of counter ions.

The magnitude of interactions between n-dodecyl-β-D-maltoside with other surfactants follows the order anionic/nonionic > cationic/nonionic > nonionic/nonionic. The weaker interaction in cationic/nonionic system is possibly due to the fact that DTAB has a bulky headgroup that can hinder the formation of compact micelles. This order is also in accord with the general trend of mixed surfactant systems.

Industrially prepared sugar-based surfactant dodecyl polyglucoside ($C_{12}$-APG) yields results

similar to that by dodecyl maltoside, implying that commercial polyglucosides are similar to pure laboratory samples in synergistic interactions with the other surfactants, and the pure alkyl maltosides may be used for studying interactions of sugar-based surfactants in general.

Polarity parameter, as studied by the fluorescence, shows the interior of all the above mixed micelles to be mildly hydrophobic (value of 0.82-0.84 in comparison to 0.78 obtained for ionic micelles and 0.85 for nonionics). Similarities in value for mixtures with cationic and the nonionic surfactants suggest the predominating effects of the nonionic surfactants.

# 6. ADSORPTION OF MIXTURES OF NONIONIC SUGAR-BASED SURFACTANT WITH ANIONIC SURFACTANT

To explore the role of structure in determining the interfacial behavior of mixed surfactant systems containing sugar-based surfactants for possible applications in EOR, the adsorption of sugar-based surfactants in mixtures with other surfactants was studied. Adsorption of nonionic-anionic mixtures of dodecyl polyglucosides (C12-APG)/sodium dodecyl sulfate (SDS), as well as n-dodecyl-β-D-maltoside (DM)/ sodium dodecyl sulfate (SDS), on alumina at pH 6 and 11 was studied first. This is also as part of our effort to understand the effect of pH change in these mixtures. Sugar-based surfactant adsorbs on alumina at both pH, whereas SDS adsorbs on alumina only at pH 6. The study of the adsorption behavior under different pH conditions offers an opportunity to observe possible synergism or antagonism between the two surfactants, and to compare the commercial sugar-based surfactants with laboratory counterparts.

*Adsorption of dodecyl polyglucoside/sodium dodecylsulfate and n-dodecyl-β-D-maltoside/sodium dodecylsulfate 1:1 mixtures at pH 6*

The adsorption isotherms of dodecyl polyglucoside/sodium dodecyl sulfate 1:1 mixture and n-dodecyl-β-D-maltoside/sodium dodecyl sulfate 1:1 mixture on alumina at pH 6 are shown in Figures 53 and 54, together with those of dodecyl polyglucoside, dodecyl-β-D-maltoside and sodium dodecyl sulfate alone. The adsorption of the mixtures is higher than either of the components in the sharp rising part of the isotherm, showing strong synergy between the sugar-based surfactants and sodium dodecyl sulfate. This is the region where hydrophobic chain-chain interaction dominates the adsorption process, with the surface not yet saturated with the surfactant. At lower concentrations, SDS adsorbs more than APG or DM. In this region, adsorption takes place mainly due to

electrostatic attraction between the negatively charged surfactant and positively charged alumina. Some adsorption of the sugar-based surfactant is evidently due to hydrogen bonding. At higher concentrations, the adsorbed SDS forms mixed aggregates with APG/DM through hydrophobic chain-chain interactions and promotes the APG/DM adsorption. The low critical micellar concentration of APG/DM causes the aggregates to form at lower concentrations and this promotes total adsorption as well. In the plateau region, the adsorption density of the mixture is slightly less than that of SDS. As the surface is usually saturated with surfactants under these conditions, this can be attributed to the larger head group of the sugar-based surfactant.

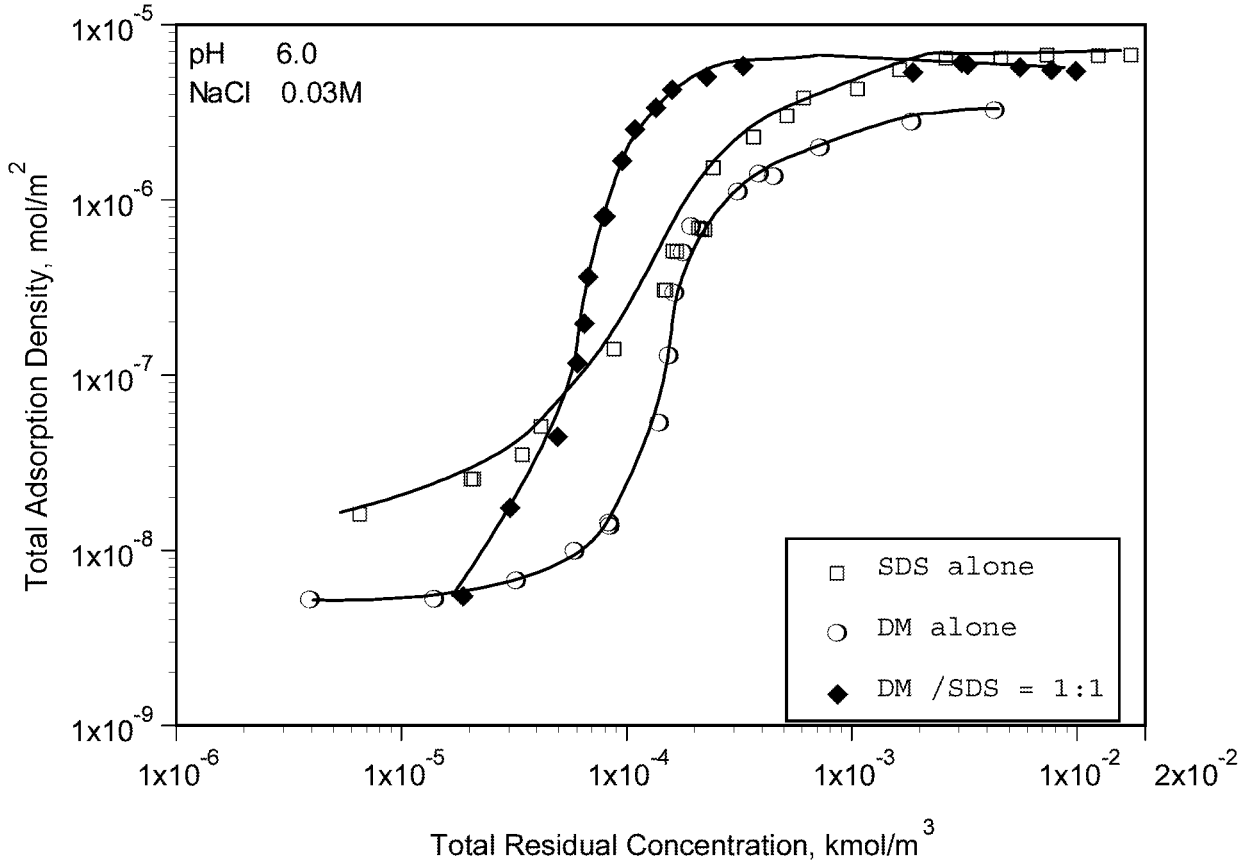


**Figure 53. Adsorption of DM, SDS and DM/SDS 1:1 Mixture on Alumina**

Adsorption behavior of dodecyl polyglucoside/sodium dodecyl sulfate is comparable to that

of n-dodecyl-β-D-maltoside/sodium dodecyl sulfate but with much less synergy. The head group of the dodecyl polyglucoside in this study has an average DP (degree of polymerization) of 1.8. This is very close to that of dodecyl maltoside (DP = 2).

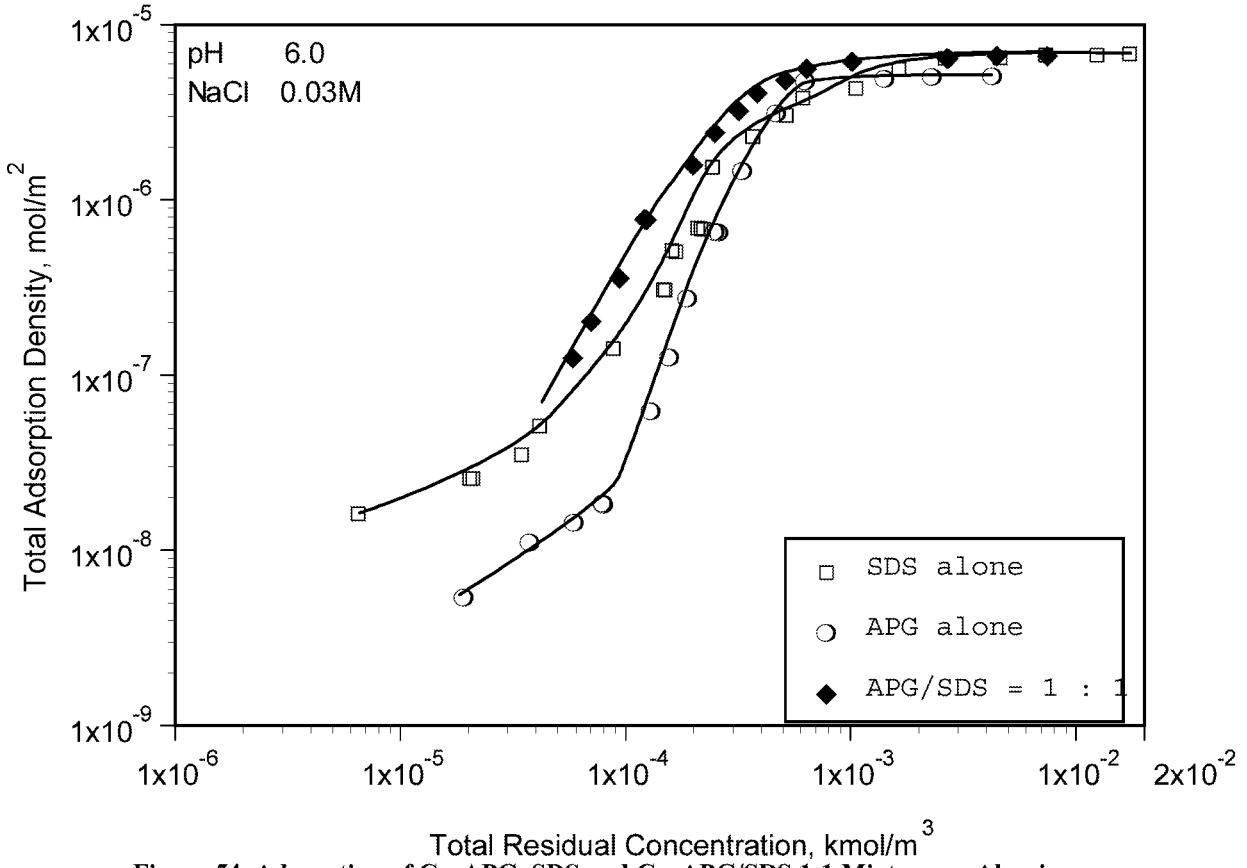


**Figure 54. Adsorption of $C_{12}$-APG, SDS and $C_{12}$-APG/SDS 1:1 Mixture on Alumina**

*Adsorption of n-dodecyl-β-D-maltoside/sodium dodecylsulfate 3:1 and 1:3 mixtures at pH 11*

Experiments were also done for other mixing ratios of DM/SDS. The adsorption of DM, SDS and their 3:1, 1:1 and 1:3 mixtures are illustrated in Figure 55. All mixtures show synergistic effects in the rising part of the isotherms. It is interesting that DM/SDS 1:1 mixture shows the strongest synergy, suggesting that the synergistic action is stoichiometric due to possible 1:1 complex

formation or better packing.

The adsorption densities of sodium dodecyl sulfate alone and from the DM/SDS mixtures on alumina are plotted in Figure 56 as a function of residual SDS concentration. Clearly the adsorption of SDS from the mixtures is higher than that of SDS from its single component solutions

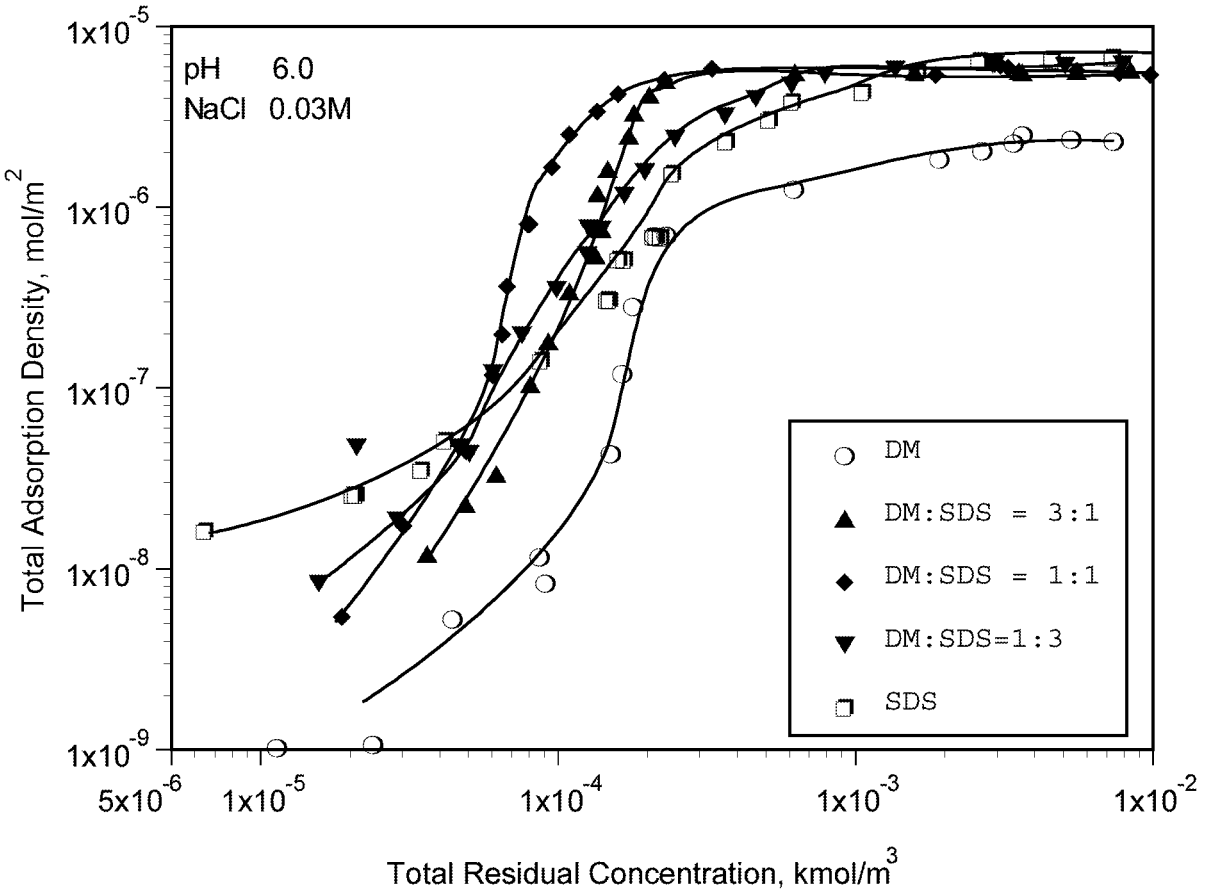


**Figure 55. Adsorption of DM, SDS and their 3:1, 1:1 and 1:3 Mixtures on Alumina**

in the sharp rising part of the isotherm. The more DM in the system (the higher the DM/SDS ratio), higher is the adsorption density at give concentrations, suggesting that the presence of DM promotes SDS adsorption. As mentioned above, in the plateau region, the surface is saturated with the surfactant, and under these conditions the adsorption of SDS is lower than that when it is present alone due to competition from DM in the system. The higher the DM in the mixing ratio, the lower

the adsorption of SDS, suggesting that more SDS is replaced by DM at the solid/liquid interface.

Similar data for DM adsorption alone from the DM/SDS mixtures and that from DM is given in Figure 57. It can be seen that the adsorption of DM is enhanced by the SDS in this case in the entire concentration range. Interestingly, more the SDS in the system, higher is the adsorption of DM in the rising part.

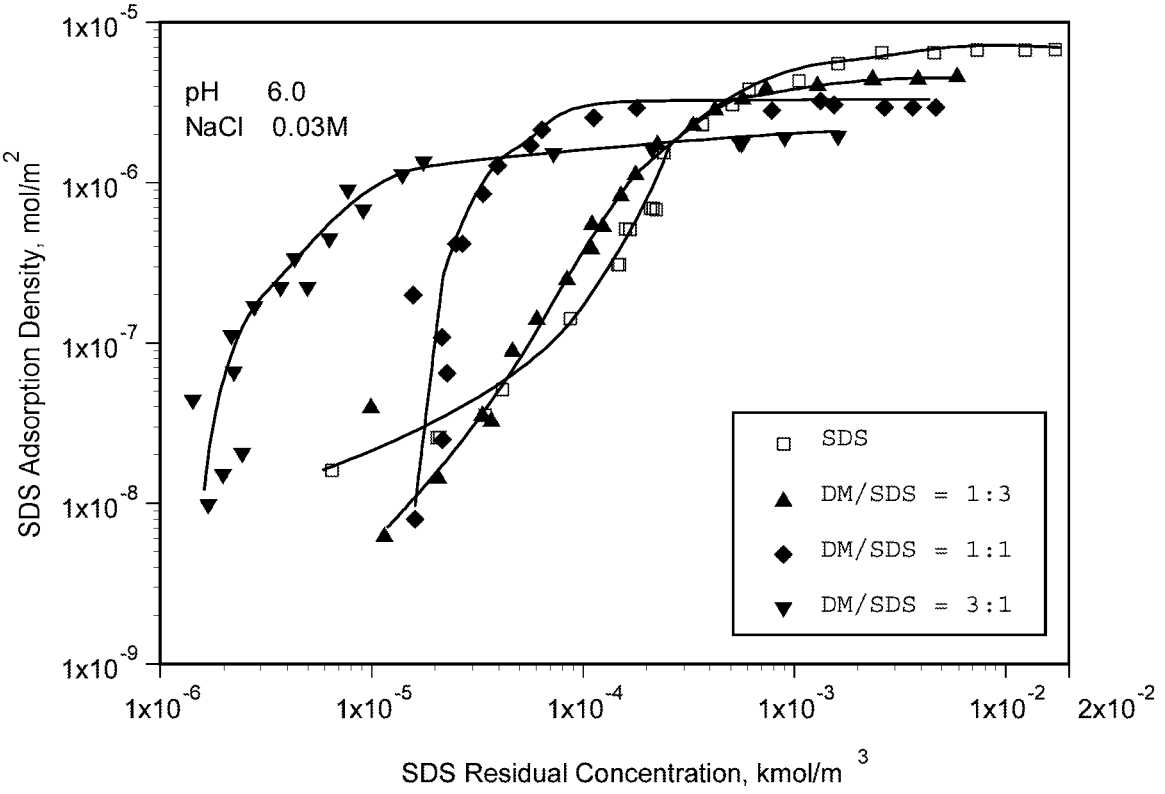


**Figure 56. Adsorption of SDS on Alumina: Adsorption for SDS alone and from DM/SDS 3:1, 1:1 and 1:3 Mixtures**

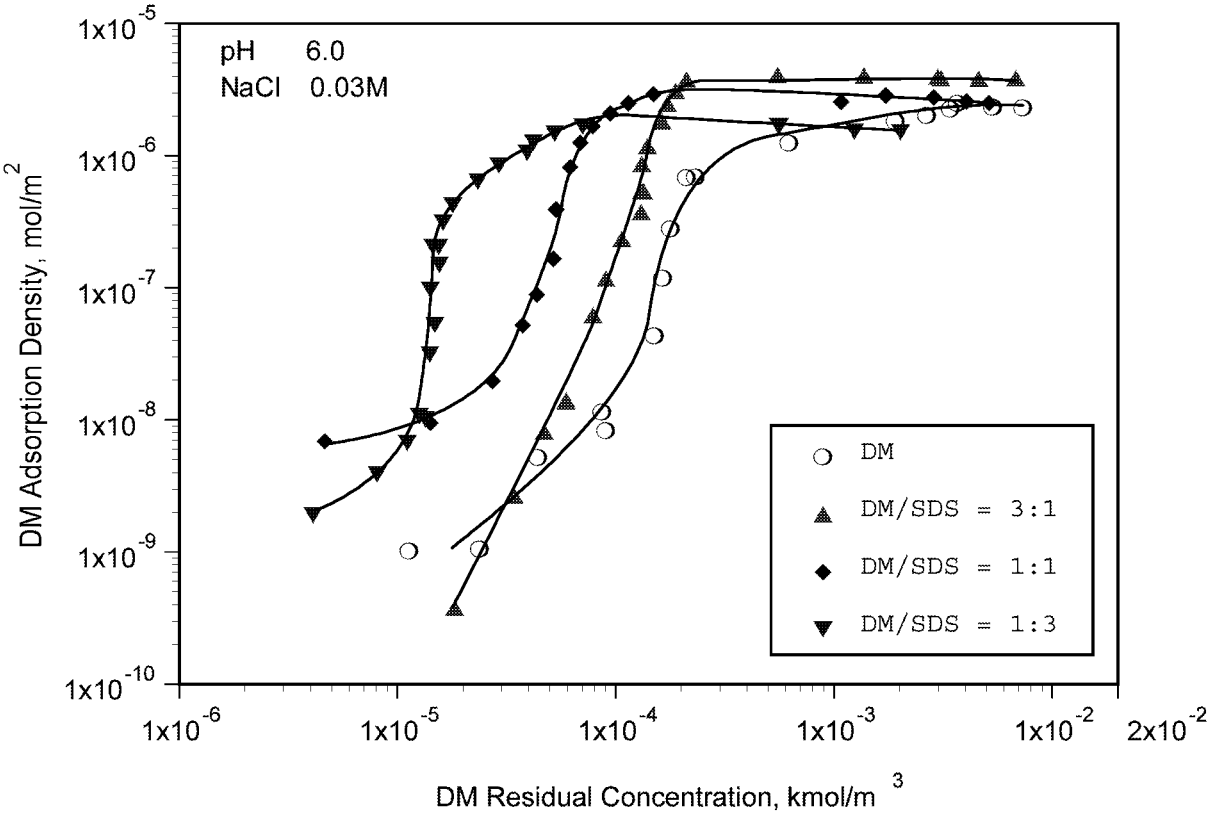


**Figure 57. Adsorption of DM on Alumina: Adsorption for DM alone and from DM/SDS 3:1, 1:1, 1:3 Mixtures**

Composition of the adsorbed layer will determine to a larger extent the interfacial behavior of the particles and hence it is plotted in Figure 58 as a function of the residual concentration of the surfactant in the mixture. In the case of DM/SDS 1:1 and 1:3 mixtures, the ratio at the S/L interface is very close to the bulk mixing ratio. However, for the 3:1 mixture, the DM/SDS ratio is small at low concentrations and reaches a maximum at the on-set of the adsorption plateau and then decreases again. In the entire concentration range tested, the DM/SDS ratio is smaller than 3, the total mixing ratio. This phenomenon is attributed to the stronger interaction between the SDS and the solid, as the electrostatic interaction between SDS and alumina is stronger than that of the hydrogen bonding between DM and alumina. Clearly this effect is more pronounced for mixtures that have smaller amounts of SDS.

A)

B)

C)

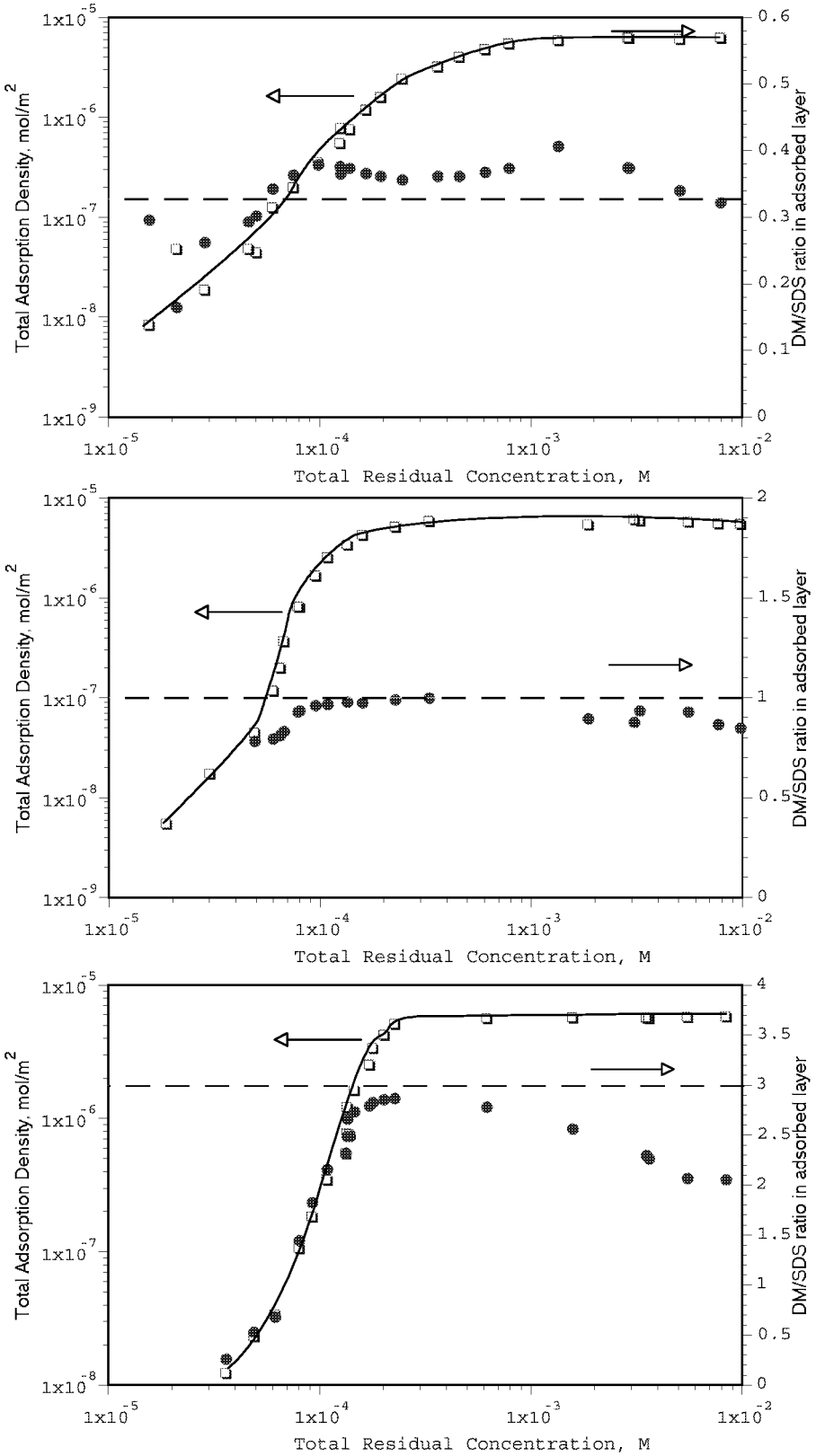


**Figure 58. Adsorption of DM/SDS Mixtures and the DM/SDS ratios in the Adsorption Layer**
**A) 1:3; B) 1:1; C) 3:1**

The synergism for APG/SDS system can also be seen by comparing the adsorption of APG in the APG/SDS mixture with the adsorption of APG from its solution when present alone (Figure 59). The adsorption of APG from the mixture is markedly higher than that of APG from its single component solutions. At high concentrations, the adsorption of APG is lower because the surface is saturated.

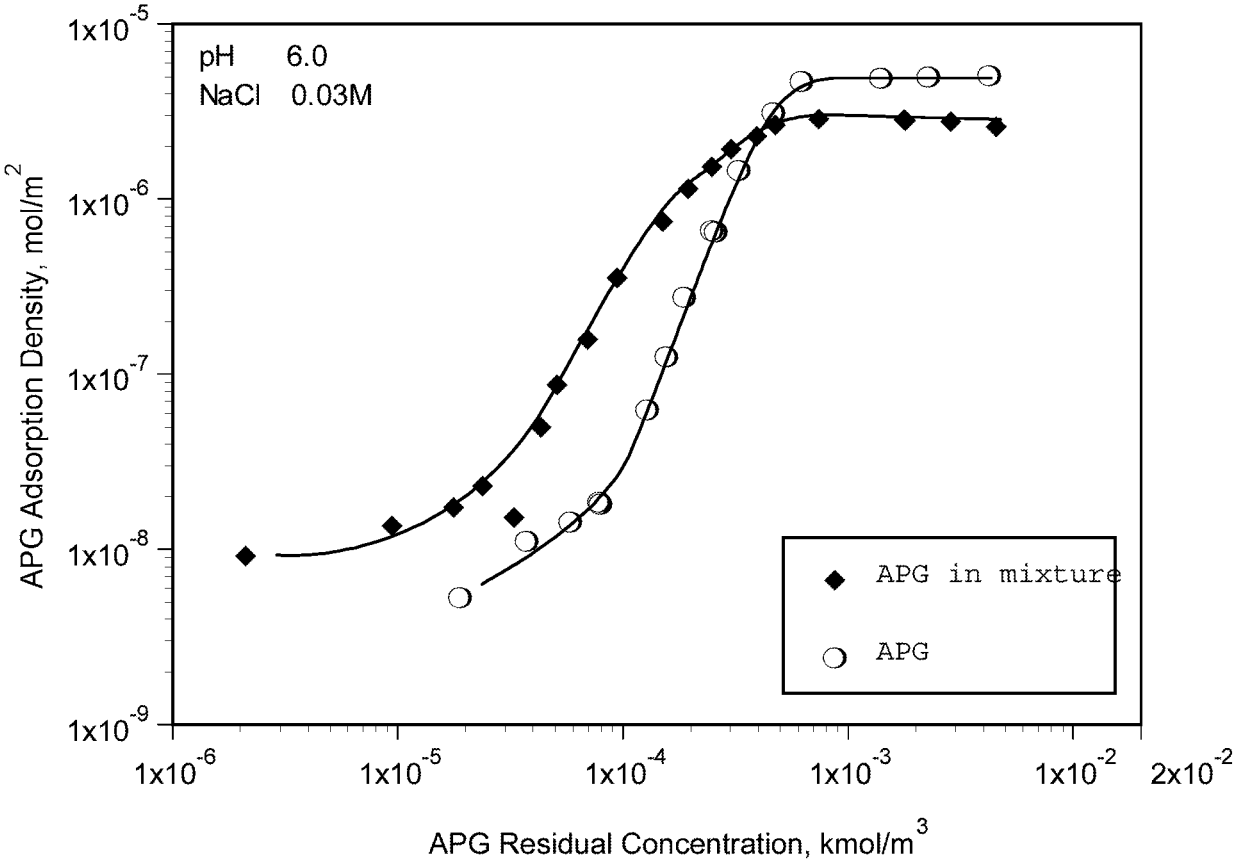


**Figure 59. Adsorption of APG alone and from APG/SDS 1:1 Mixture on Alumina**

Similarly, the synergy for SDS can be observed by comparing the adsorption of SDS from the APG/SDS mixture with that from SDS alone in single component system (Figure 60). The adsorption of SDS from the mixture is much higher than when SDS alone due to the aggregation

enhanced by the nonionic co-adsorbate, APG. In the plateau region, the adsorption density of SDS in the mixture is lower due to the competitive adsorption with APG.

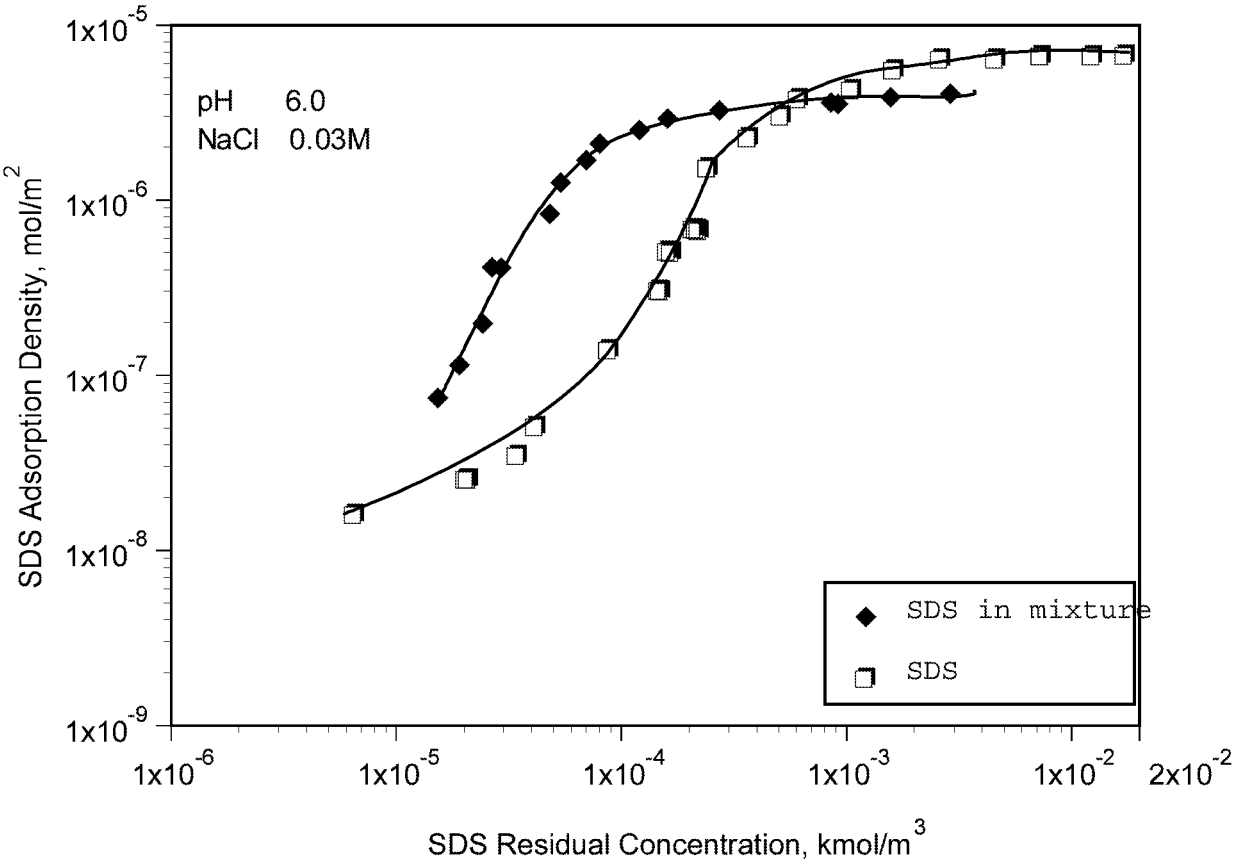


**Figure 60. Adsorption of SDS alone and from APG/SDS 1:1 Mixture on Alumina**

*Adsorption of dodecyl polyglucoside/sodium dodecylsulfate and n-dodecyl-β-D-maltoside/sodium dodecylsulfate mixtures at pH 11*

Co-adsorption is examined under basic pH condition (pH 11) when the negatively charged sulfate adsorbs very little on alumina. The results obtained for the dodecyl polyglucoside/sodium dodecyl sulfate 1:1 mixture and n-dodecyl-β-D-maltoside/sodium dodecyl sulfate 1:1 mixture on alumina at pH 11 are illustrated in Figures 61 and 62. It is to be noted that at this pH, adsorption of negatively charged SDS on the similarly charged alumina is very low. The adsorption of the mixtures under these conditions is between that of DM/$C_{12}$-APG and SDS, even when the surface is not fully covered by the surfactant. The presence of SDS in the system reduces the adsorption of the sugar-based surfactants under these conditions.

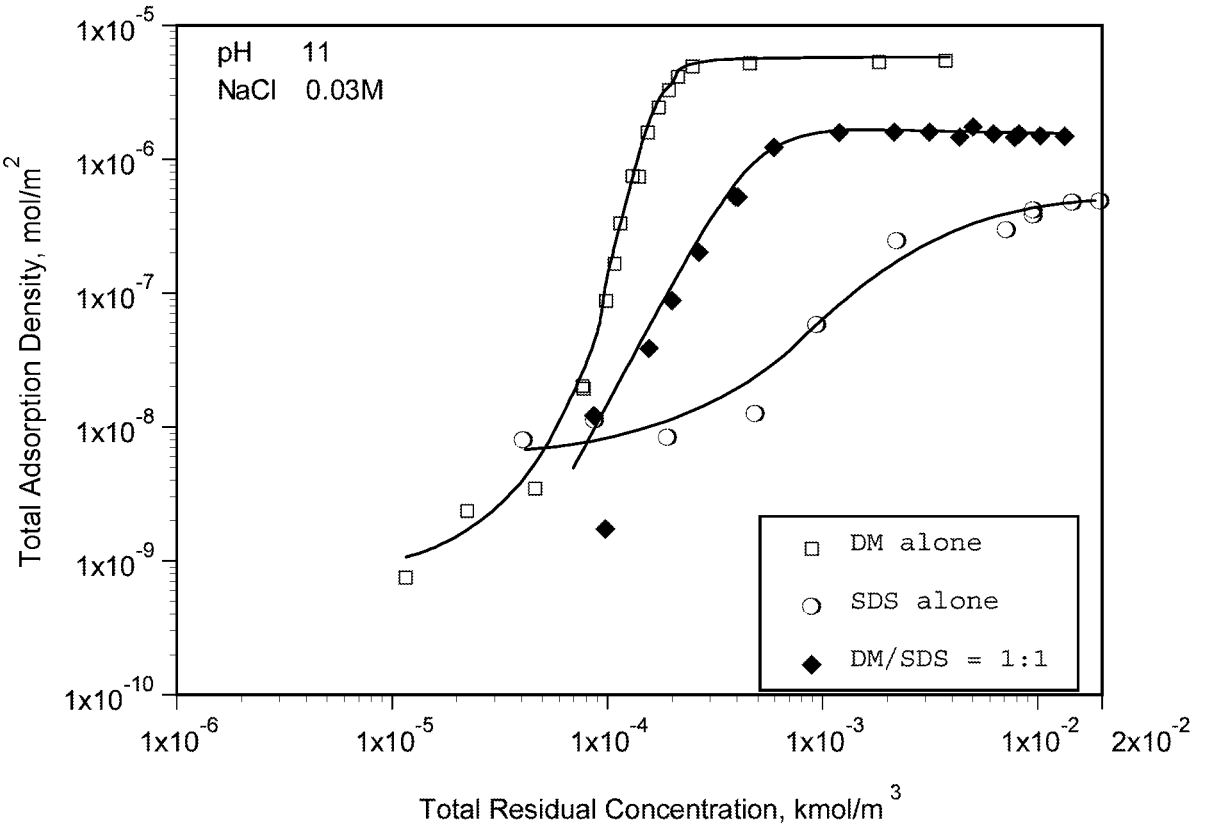


**Figure 61. Adsorption of n-dodecyl-β-D-maltoside(DM), sodium dodecyl sulfate (SDS) and $C_{12}$-APG/SDS 1:1 Mixtures on Alumina at pH 11**

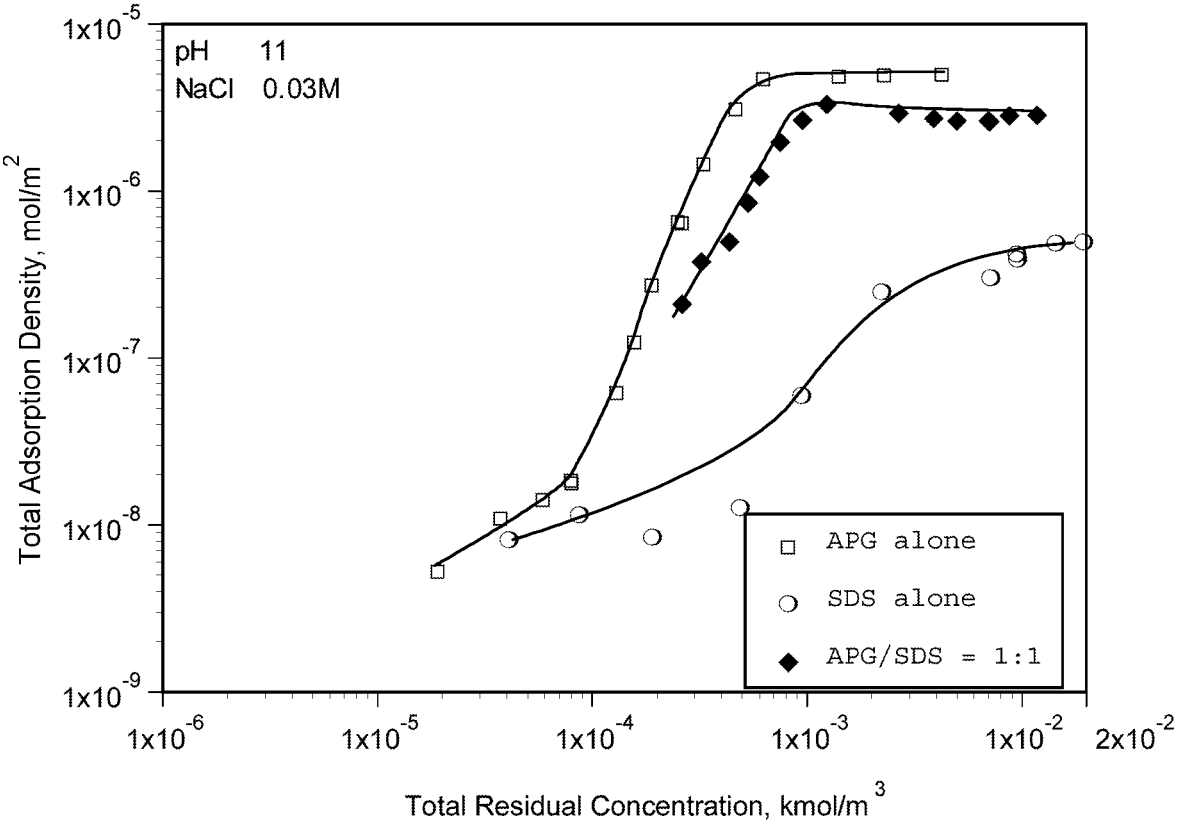


**Figure 62. Adsorption of dodecyl polyglucosides(C12-APG), sodium dodecyl sulfate (SDS) and $C_{12}$-APG/SDS 1:1 Mixtures on Alumina at pH 11**

The effect of n-dodecyl-β-D-maltoside (DM) and sodium dodecyl sulfate (SDS) mixing ratios on the adsorption of DM, SDS and their mixtures is illustrated in Figure 63 for 3:1, 1:1 and 1:3 ratios. The results show that more the SDS in the system, lower is the total adsorption density of the surface mixtures. Interestingly, there are antagonistic or competitive effects between SDS and DM under these conditions.

The adsorption of sodium dodecyl sulfate from SDS solution and from the DM/SDS mixtures on alumina is plotted in Figure 64 as a function of the residual SDS concentration. Adsorption of SDS from the mixtures is enhanced by the presence of DM except in the very high concentration regions. This is proposed to be due to the adsorbed DM functioning as anchor molecules for the SDS through hydrophobic chain-chain interactions. Thus at least for SDS, there are some synergistic effects in the surfactant mixtures with DM.

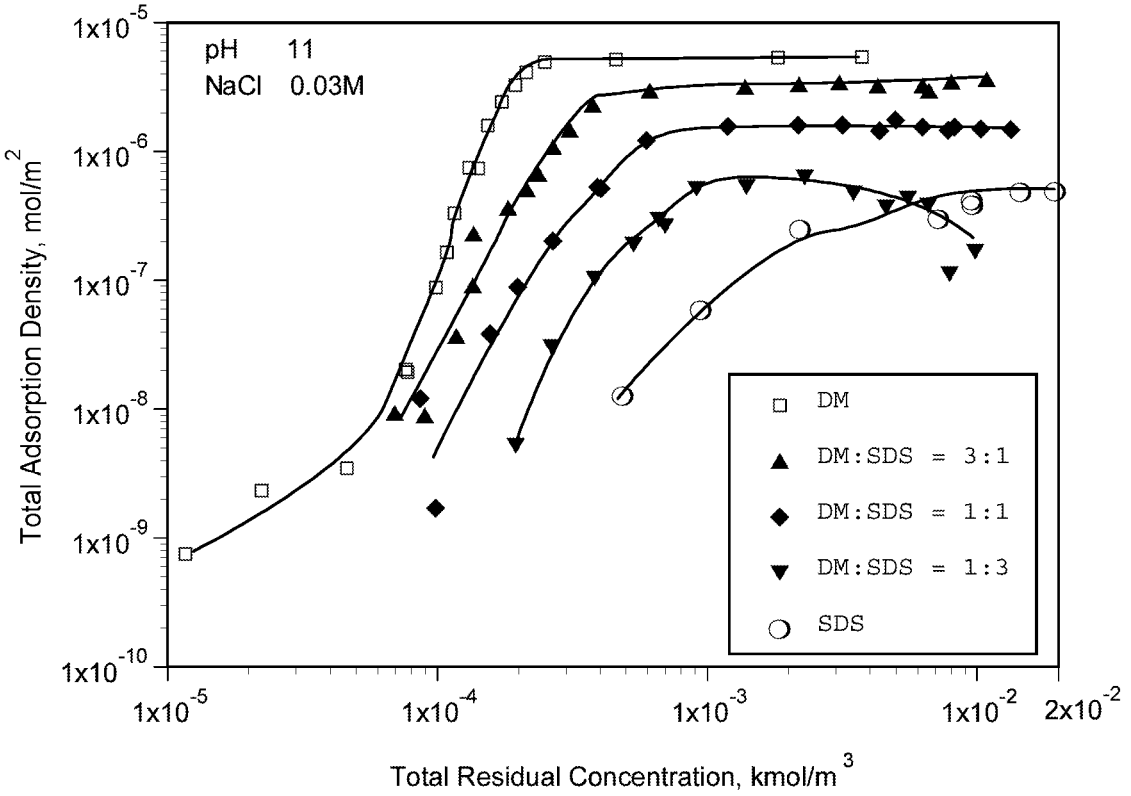


**Figure 63. Adsorption of DM, SDS and their 3:1, 1:1 and 1:3 Mixtures on Alumina at pH 11**

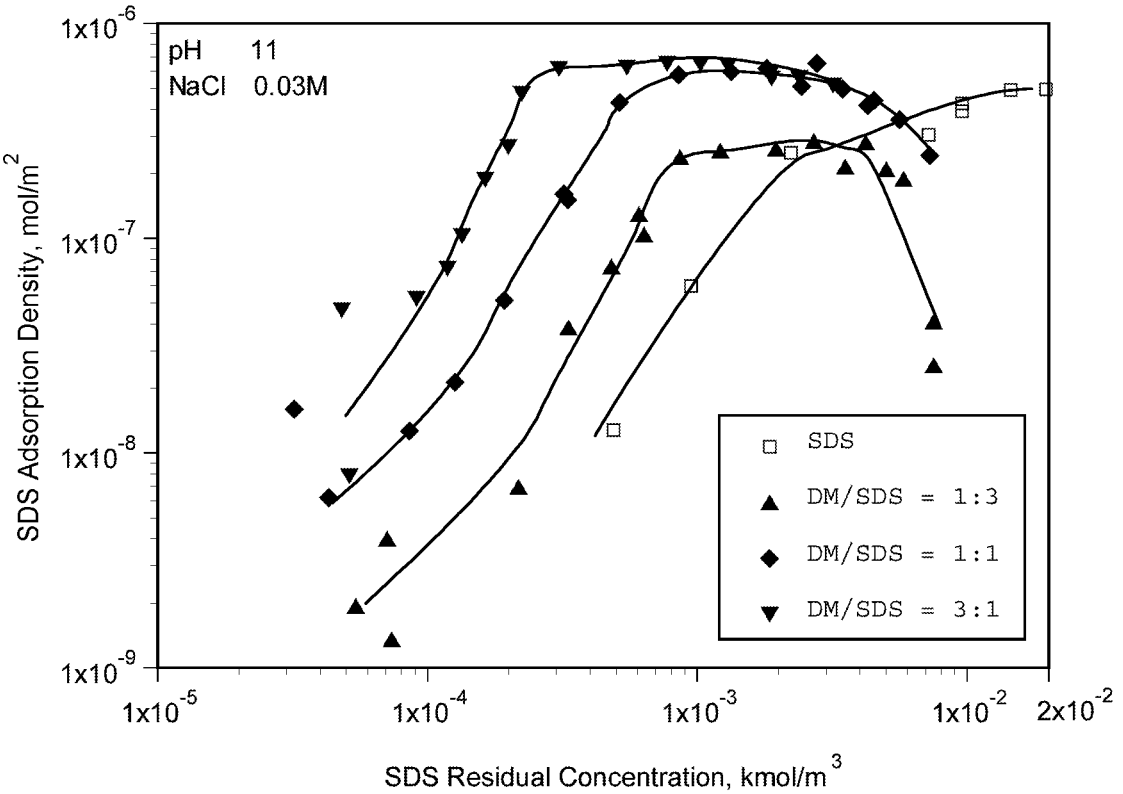


**Figure 64. Adsorption of SDS on Alumina at pH 11: Adsorption for SDS alone and from DM/SDS 3:1, 1:1 and 1:3 Mixtures**

In contrast to the above, it can be seen from Figure 65 that the DM adsorption is enhanced by SDS in the rising part but depressed in the plateau region. It can be seen from Figure 63 that the total adsorption of DM + SDS is decreased as SDS in the mixture increased. It can be concluded that in this system at pH 11, as a whole there are mainly antagonist effects between DM and SDS.

The same antagonism can be seen for the APG/SDS mixed system at pH 11 by comparing the adsorption of APG alone vs. that from the mixture (Figure 66), and adsorption of SDS alone vs. that from the mixture (Figure 67).

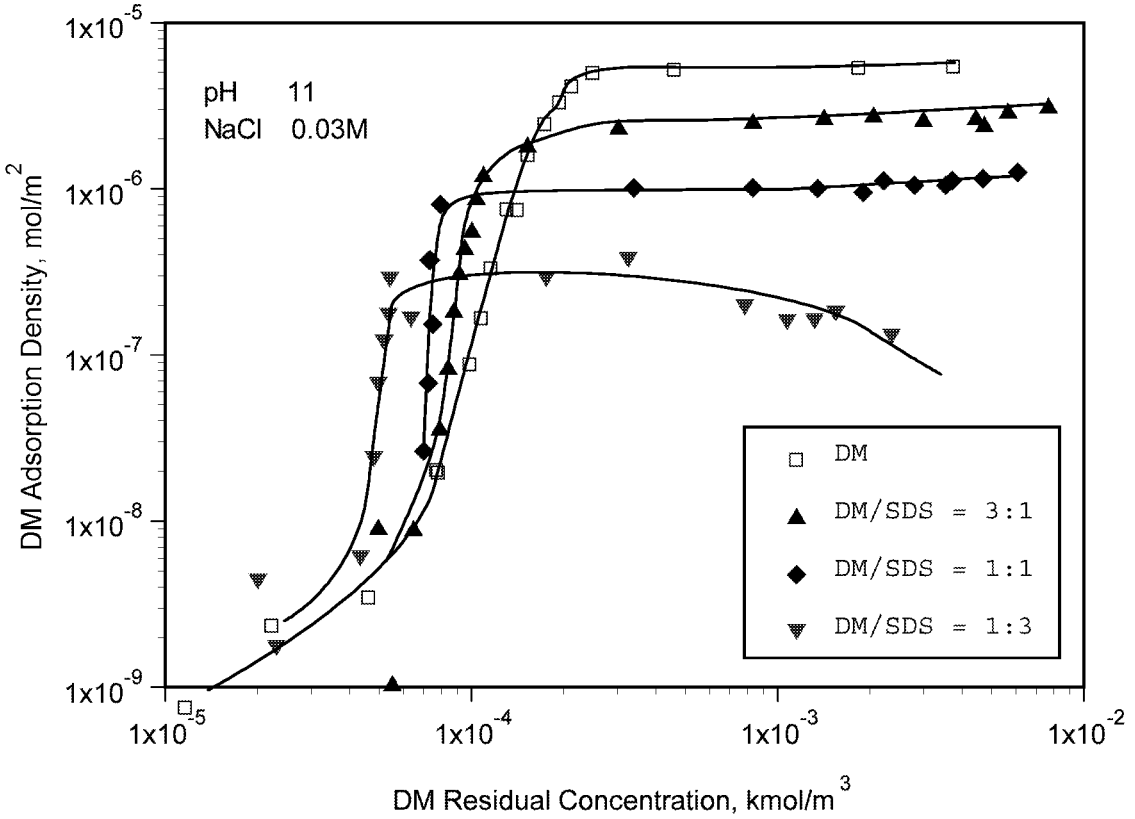


**Figure 65. Adsorption of DM on Alumina at pH 11:**
**Adsorption for DM alone and from DM/SDS 3:1, 1:1 and 1:3 Mixtures**

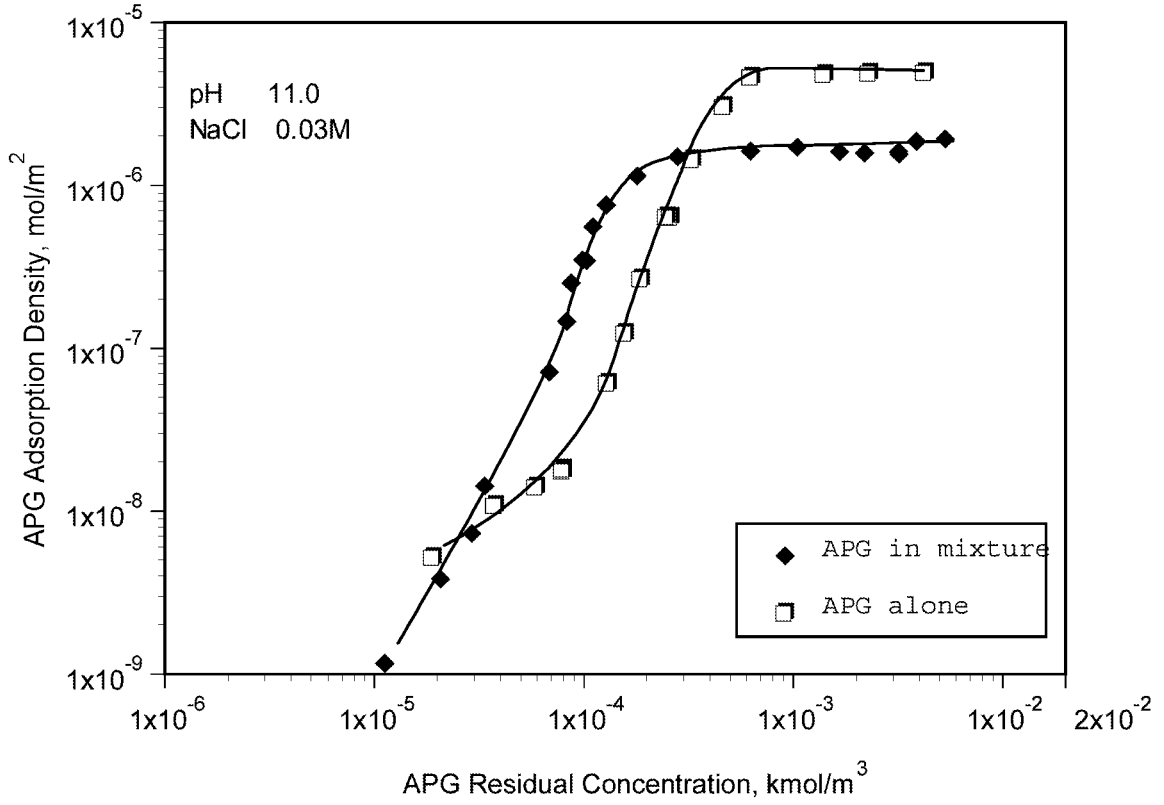


**Figure 66. Adsorption of APG alone and in APG/SDS 1:1 mixture on alumina at pH 11**

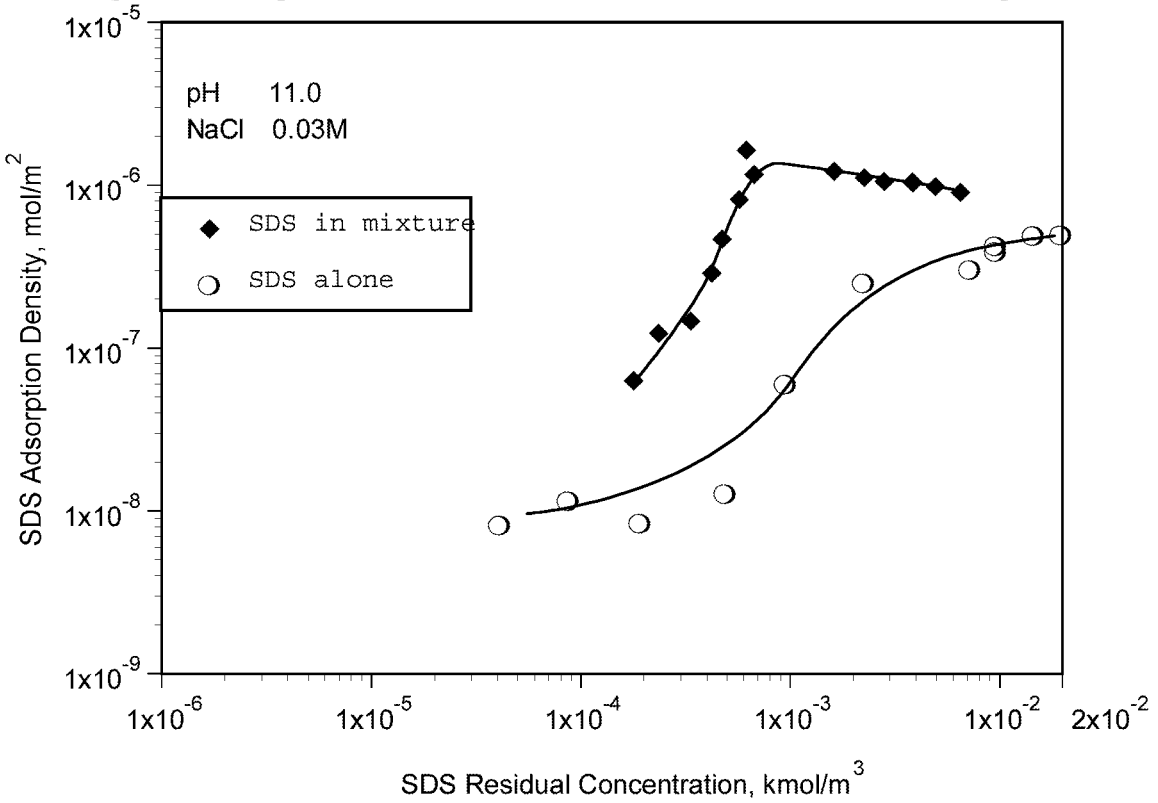


**Figure 67. Adsorption of SDS alone and in APG/SDS 1:1 mixture on alumina at pH 11**

*Summary of sugar-based surfactant/SDS mixtures adsorption on alumina*

In summary, the co-adsorption of n-dodecyl-β-D-maltoside(DM) and dodecyl polyglucoside with sodium dodecyl sulfate(SDS) on alumina was studied at pH 6 and 11. At pH 6, where alumina is positively charged, marked synergistic effects between DM/APG and SDS were observed, especially in the region where hydrophobic chain-chain interaction dominates the adsorption process as long as the surface is not saturated. In the plateau region, clearly there is competition for adsorption sites. At this pH, SDS and DM/APG promote the adsorption of each other and there exists mainly synergism. The strongest synergism was found when the DM:SDS was 1:1.

At pH 11 where it is negatively charged, the adsorption of APG/SDS, or DM/SDS mixture is less than those of APG or DM alone. The presence of SDS in the systems reduces the sugar-based surfactant adsorption except in the rising part of the isotherm, although the SDS adsorption is increased due to hydrophobic interaction with sugar-based surfactants. In general there is mainly antagonistic effects between n-dodecyl-β-D-maltoside (DM) and dodecyl polyglucosides (C12-APG) with sodium dodecyl sulfate (SDS) at this pH.

## 7. ADSORPTION OF MIXTURES OF NONIONIC SUGAR-BASED SURFACTANT WITH CATIONIC SURFACTANT ON SILICA

To further explore the interfacial behavior of mixed surfactant systems containing sugar-based surfactants for possible applications in EOR, the adsorption of nonionic-cationic mixtures (DM/DTAB) on silica was studied next. N-dodecyl-β-D-maltoside does not adsorb on silica at the tested pH, whereas cationic DTAB adsorbs strongly on silica under the same conditions. Study of such adsorption behavior offers an opportunity to observe possible synergism or antagonism between these surfactants.

The adsorption isotherms of 3:1, 1:1 and 1:3 n-dodecyl-β-D-maltoside(DM) and dodecyltrimethylammonium bromide (DTAB) mixtures on silica at pH 9 is shown in Figure 68, together with those of for single surfactant DM and DTAB. The adsorption of DM alone on silica is very low; this is in accord with our previously reported finding that DM adsorbs strongly on alumina but very weakly on silica. DTAB, on the other hand, exhibits strong adsorption on the negatively charged silica due to electrostatic interactions.

The adsorption of the mixtures is lower than that of DTAB at low concentrations because at these concentrations DM does not adsorb on silica. The isotherms show a sharp increase at 0.1-0.2 mM, indicating the onset of the region where hydrophobic chain-chain interaction dominates the adsorption process. In this region, the adsorption of the mixtures is higher than that of DM or DTAB alone. Two factors contribute to this increase. Firstly, the highly surface active DM reduces the critical micelle concentration of the surfactant mixture and for the same reason the hemimicelle concentration. Secondly, DM can adsorb on silica due to hydrophobic chain-chain interactions with adsorbed DTAB. These results show that there exists strong synergistic effect between dodecylmaltoside and dodecyltrimethyl ammonium bromide, especially in the sharp rising part of the isotherms.

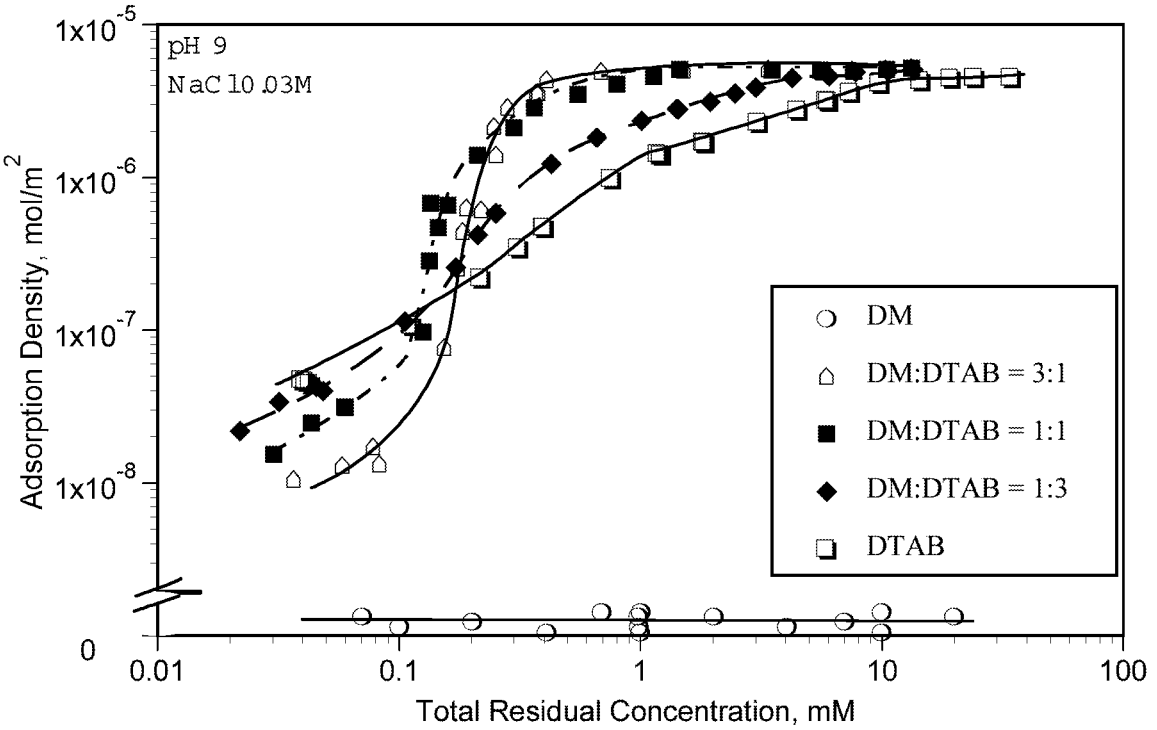


**Figure 68. Adsorption of DM, DTAB and Their Mixtures on Silica**

To elucidate the behavior of each surfactant component in the mixture, the adsorption densities of dodecyltrimethylammonium bromide alone and from the DM/DTAB mixtures on silica are plotted in Figure 69 as a function of residual DTAB concentration. Clearly the presence of DM promotes DTAB adsorption and the adsorption of DTAB from the mixtures is higher than that of DTAB from its single component solutions. More the percentage of DM in the mixture, higher is the adsorption of DTAB in regions below the plateau. In the plateau region, the surface is saturated with surfactants and under these conditions the adsorption of dodecyltrimethyl ammonium bromide (DTAB) is less than that when it is present alone due to the competition from dodecyl maltoside (DM) for adsorption sites on the solid.

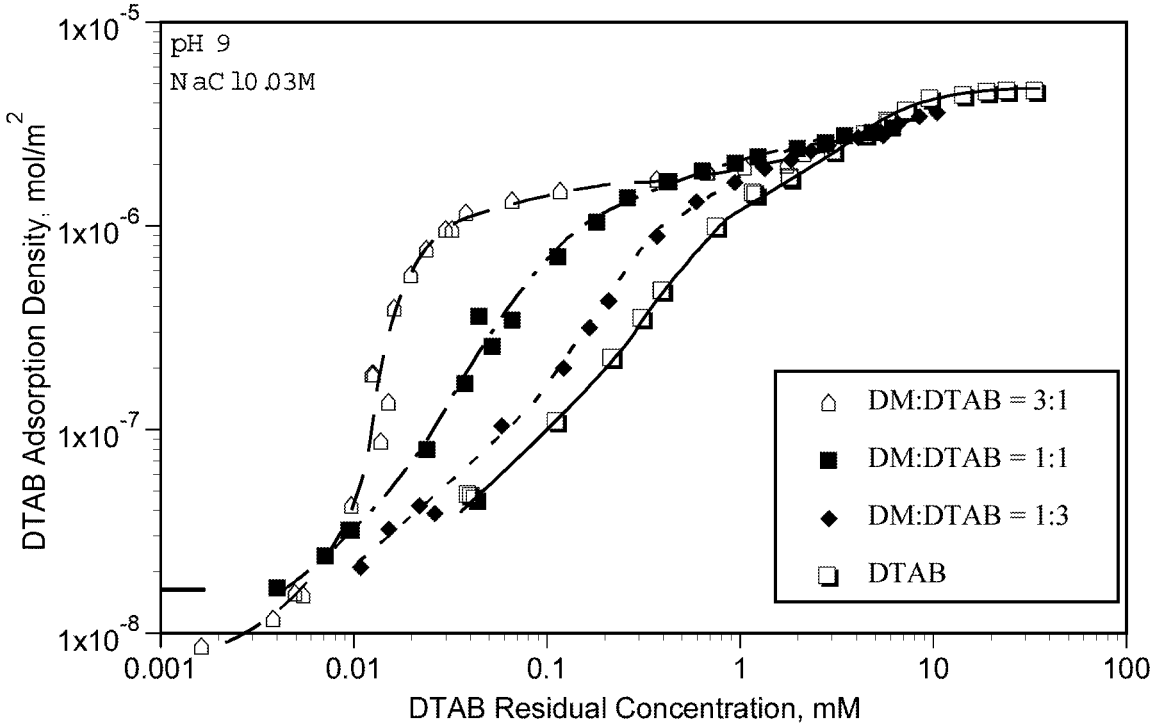


**Figure 69. Adsorption of DTAB on Silica: Adsorption alone and from DM/DTAB Mixtures**

Similarly, to identify the behavior of dodecyl maltoside in the mixture, adsorption of DM from the DM/DTAB mixtures is given in Figure 70 along with that from DM alone. It can be seen that while DM does not adsorb at all on silica by itself, its adsorption is enhanced greatly by the presence of DTAB. The adsorption in mixtures is due to the hydrophobic chain-chain interactions with DTAB. The DTAB in the hemimicelles that form at the solid/liquid interface acts as anchor for the DM molecules.

Thus, it can be concluded that sugar-based dodecylmaltoside, which does not adsorb on silica by itself, can adsorb in the presence of DTAB. In the mixed system, DTAB also adsorbs more from the mixture than it does alone, due to the reduction of critical micelle concentration by DM and hence the increase in the monomer activity.

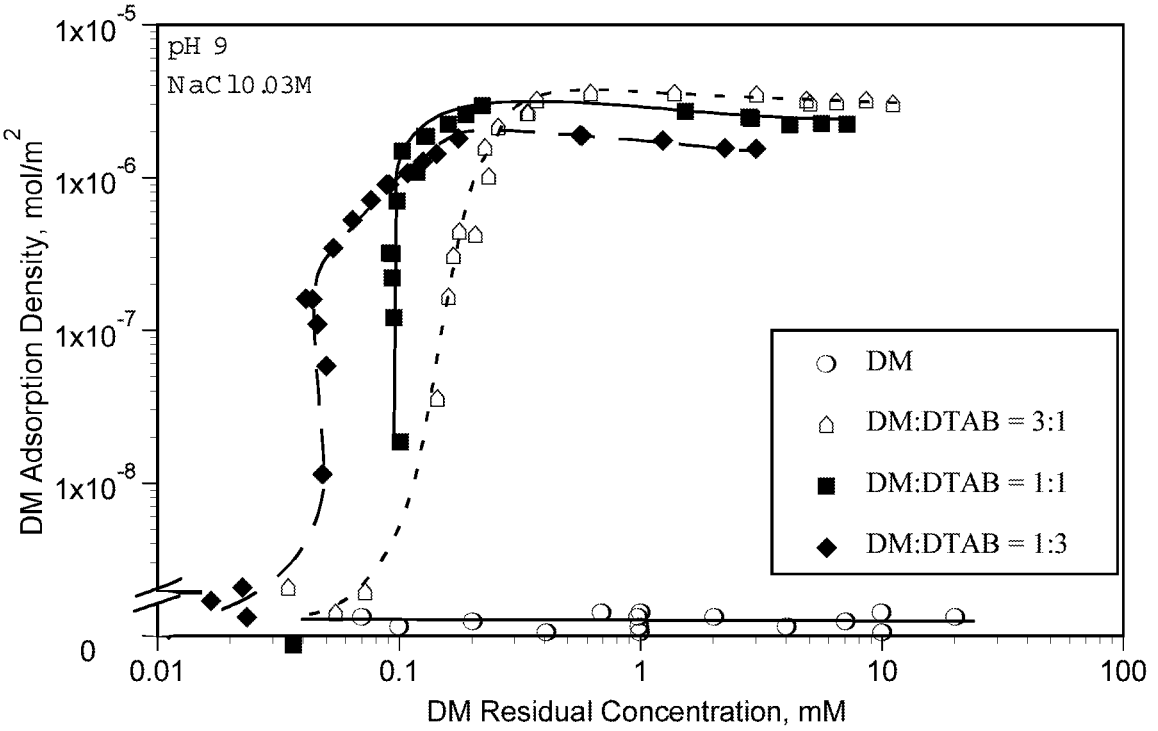


**Figure 70. Adsorption of DM on Silica: Adsorption alone and from DM/DTAB Mixtures**

The interaction between the two surfactants is clearly seen by plotting the adsorption of the mixtures together with DM:DTAB ratios in the adsorbed layer. The DM/DTAB ratio for 1:1 mixture is shown in Figure 71. At low concentrations (< 0.15 mM), DM shows a low ratio due to lack of specific interactions between it and the solid. Adsorption is mostly due to the adsorption of DTAB through electrostatic interactions. At about 0.15 mM residual concentration, the adsorption of the mixture rises sharply due to hydrophobic chain-chain interactions. The DM/DTAB ratio also increases rapidly at this concentration, suggesting strong hydrophobic chain-chain interactions to cause more DM to co-adsorb on the surface. In a certain concentration range, the DM/DTAB ratio is more than 1, suggesting that DM adsorbs more than DTAB, although it adsorbs through DTAB. The DM/DTAB ratio reaches a maximum and then decreases. The decrease is attributed to the competition between the micelles in solution and the hemimicelles at the solid/liquid interface for the more surface active DM. Interestingly, the maximum ratio corresponds to the onset of the plateau

region. All these suggest interactions between the surfactants in solutions and at solid/liquid interfaces dominated by different forces in different regions.

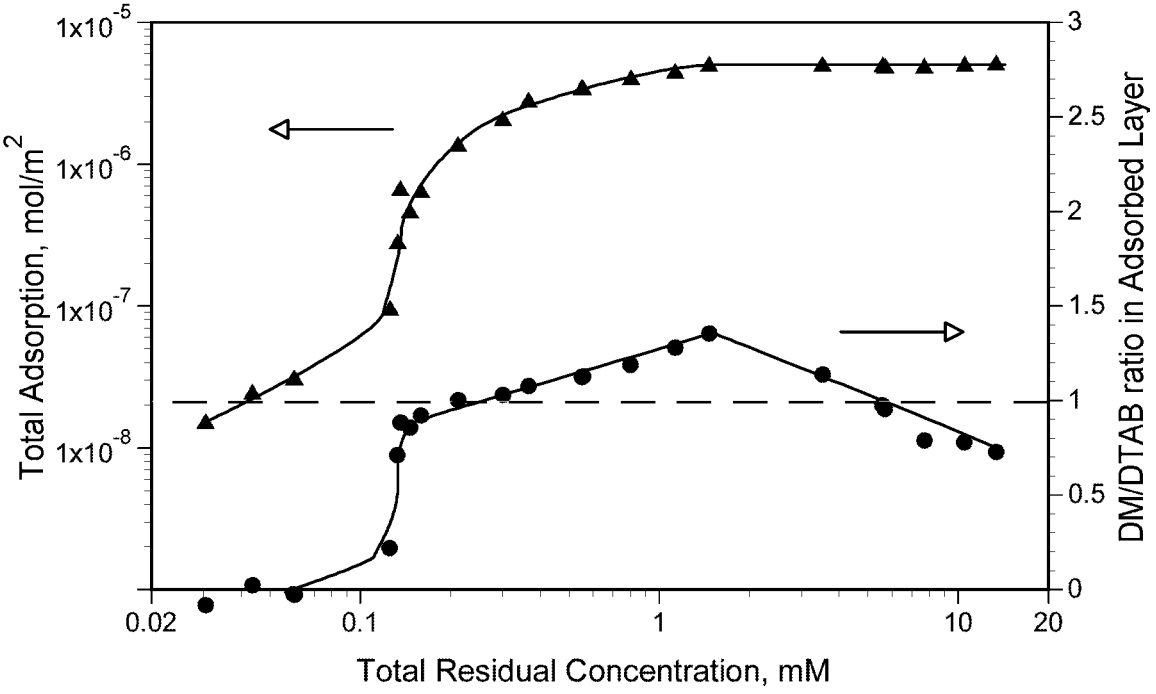


**Figure 71. Adsorption of DM/DTAB 1:1 Mixtures and the DM/DTAB ratios on Silica**

Similar trends are found for the DM/DTAB ratios in 3:1 and 1:3 mixtures (Figures 72 and 73). For both mixtures, the DM/DTAB ratio is low at low concentrations, increases rapidly at the concentration where hydrophobic chain-chain interaction dominates the adsorption process, reaches a maximum at the onset of the plateau region, and then decreases. Since composition of the adsorbed layer will determine to a large extent the interfacial behavior of the particles such as wettability and dispersion, the practical application of the above finding is to be noted.

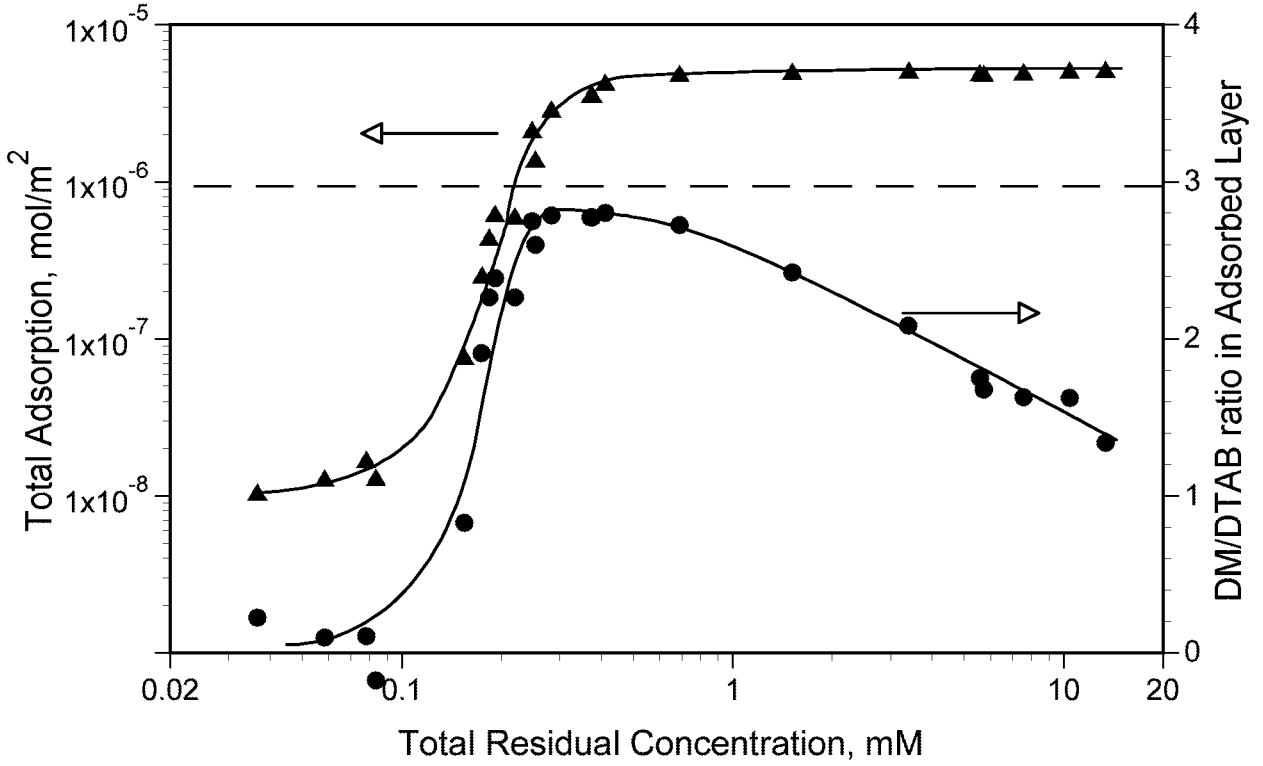


**Figure 72. Adsorption of DM/DTAB 3:1 Mixtures and the DM/DTAB ratios on Silica**

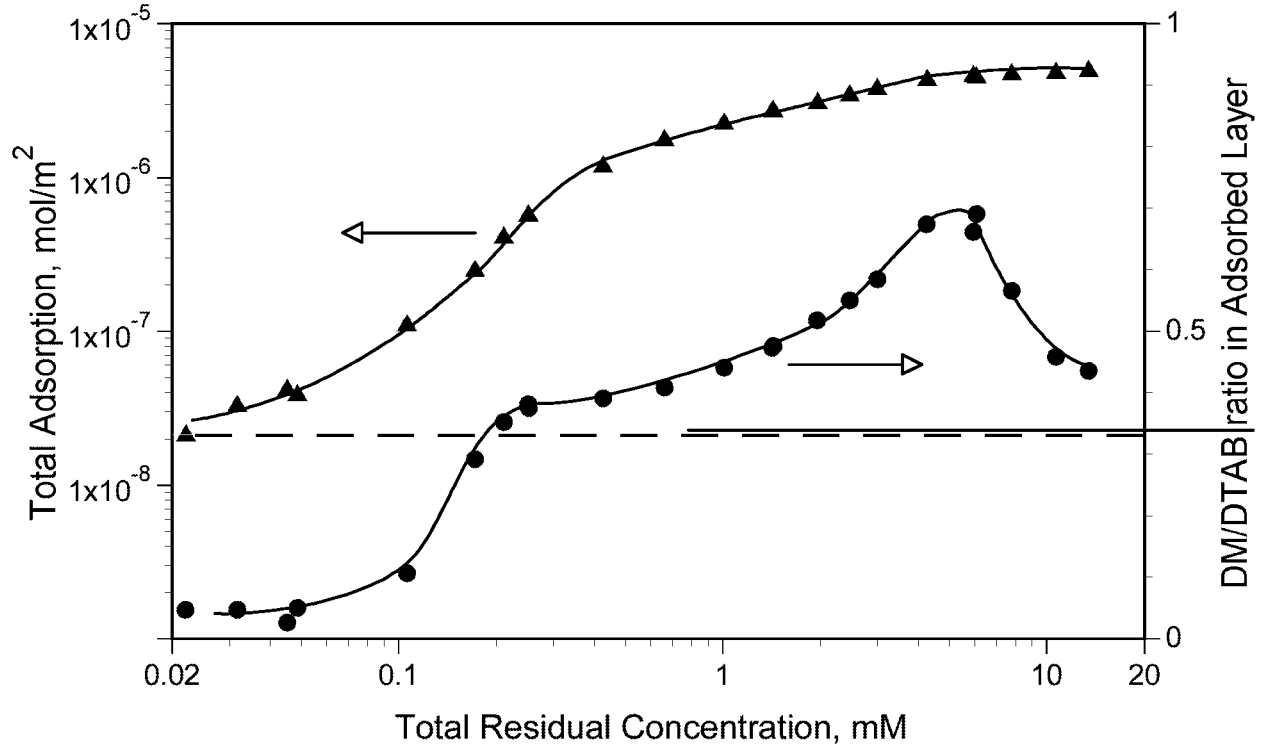


**Figure 73. Adsorption of DM/DTAB 1:3 Mixtures and the DM/DTAB ratios on Silica**

In general, the adsorption of the nonionic-cationic mixtures of n-dodecyl-β-D-maltoside(DM) and dodecyltrimethyl ammonium bromide (DTAB) on silica has been studied at various mixing ratios. DM does not adsorb on the silica by itself. However, in the mixtures, DM adsorbs on silica through hydrophobic chain-chain interactions with the adsorbed DTAB species. The DM adsorption is characterized by a sharp increase indensity at a given concentration.

In mixed systems, DTAB acts as anchor for DM. Its adsorption is markedly affected by the presence of DM. As long as the surface is not saturated, DTAB adsorbs more because of the presence of DM. When the surface is saturated, DTAB adsorption is reduced due to competition from DM for adsorption sites. The ratios of DM/DTAB in the adsorbed layer are found to be a function of the adsorption density. The ratios start low at low concentrations, increase rapidly in regions where chain-chain interactions dominate, reach a maximum at the onset of plateau region, and then decrease. These results have implications for designing surfactant combinations for controlled adsorption for optimum wettability and dispersion.

## 8. ADSORPTION OF MIXTURES OF NONIONIC SUGAR-BASED SURFACTANT WITH NONIONIC ETHOXYLATED SURFACTANT ON SILICA

The adsorption of n-dodecyl-β-D-maltoside(DM) and nonyl phenol ethoxylated decyl ether (NP-10) mixtures on silica were investigated next. Interestingly, although both surfactants are nonionic and their liquid/air interfacial behaviors are similar, they behave quite differently at solid/liquid interfaces. Sugar-based surfactants adsorb on alumina but not on silica, whereas ethoxylated nonionic surfactants demonstrate the opposite behavior. It is an interesting question as to how the mixture of the two would behave at solid/liquid interfaces.

The adsorption isotherms of n-dodecyl-β-D-maltoside(DM), nonyl phenol ethoxylated decyl ether (NP-10), and their mixtures on silica are shown in Figure 74. NP-10 adsorbs on silica strongly due to hydrogen bonding, while DM does not. Their mixtures adsorb less than that of NP-10 alone at low concentrations and approximately the same as that of NP-10 alone at higher concentrations.

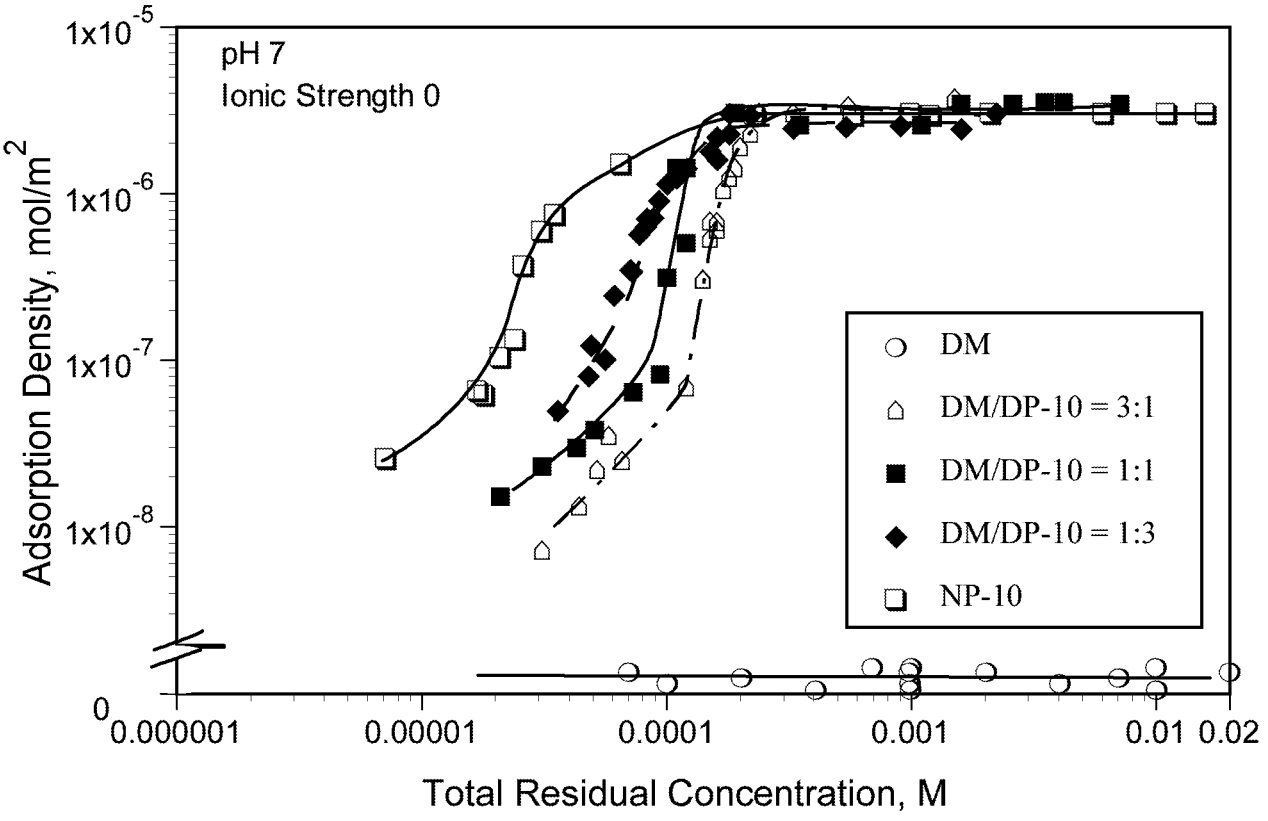


**Figure 74. Adsorption of DM, NP-10 and Their Mixtures on Silica**

This is different from that of DM/DTAB mixtures, where the adsorption densities of the mixture are higher than those of either DM or DTAB in the region where hydrophobic interactions dominate the adsorption process. This can be explained by the fact that NP-10 is more surface active than DM, and DM plays a smaller role in the mixtures.

By plotting the adsorption of NP-10 from the mixtures and that from NP-10 alone (Figure 75), it can be seen that DM increases the adsorption of NP-10 at low concentrations, similar to that in the case of DM/DTAB mixtures where DM promotes DTAB adsorption in the mixture. At higher concentrations, the adsorption of NP-10 in the mixture is lower than that of NP-10 alone due to competition from DM for adsorption sites.

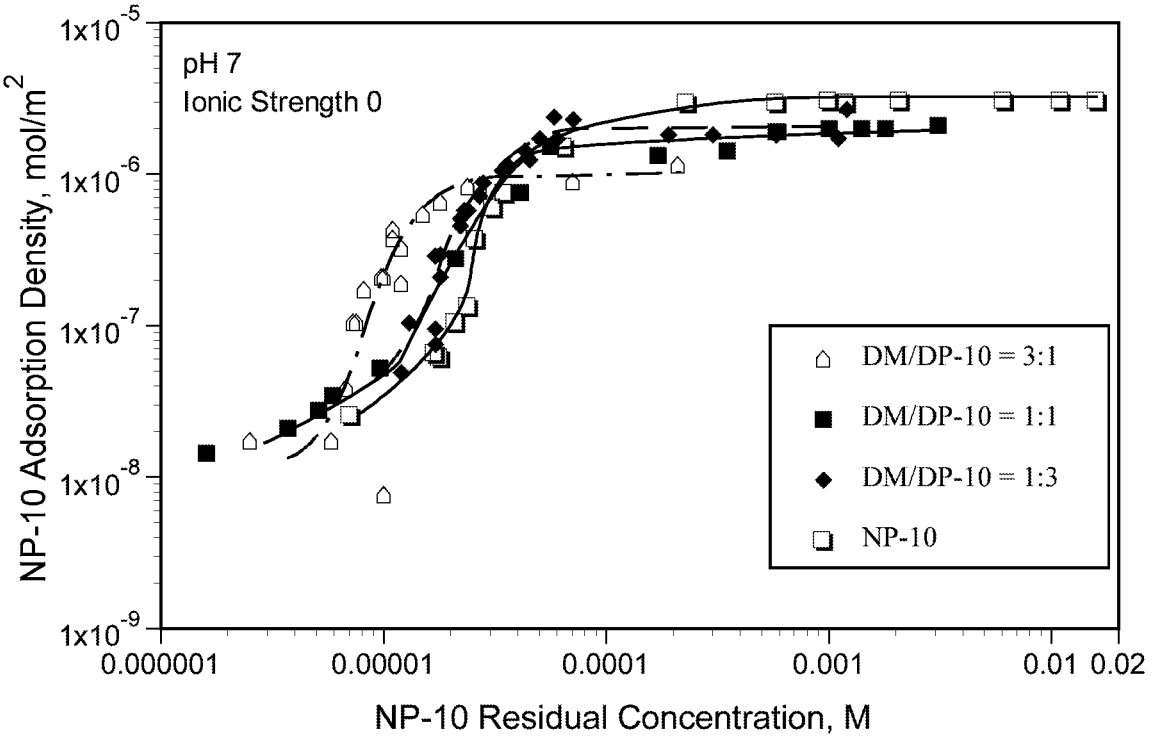


**Figure 75. Adsorption of NP-10 on Silica: Adsorption alone and from Mixtures**

The dodecyl maltoside in the DM/NP-10 mixture, on the other hand, adsorbs much more on the surface than DM alone (Figure 76). Again, the hydrophobic chain-chain interactions are proposed to promote the DM adsorption from the mixture. This phenomenon is very similar to that in the case

of DM adsorption in DM/DTAB mixtures.

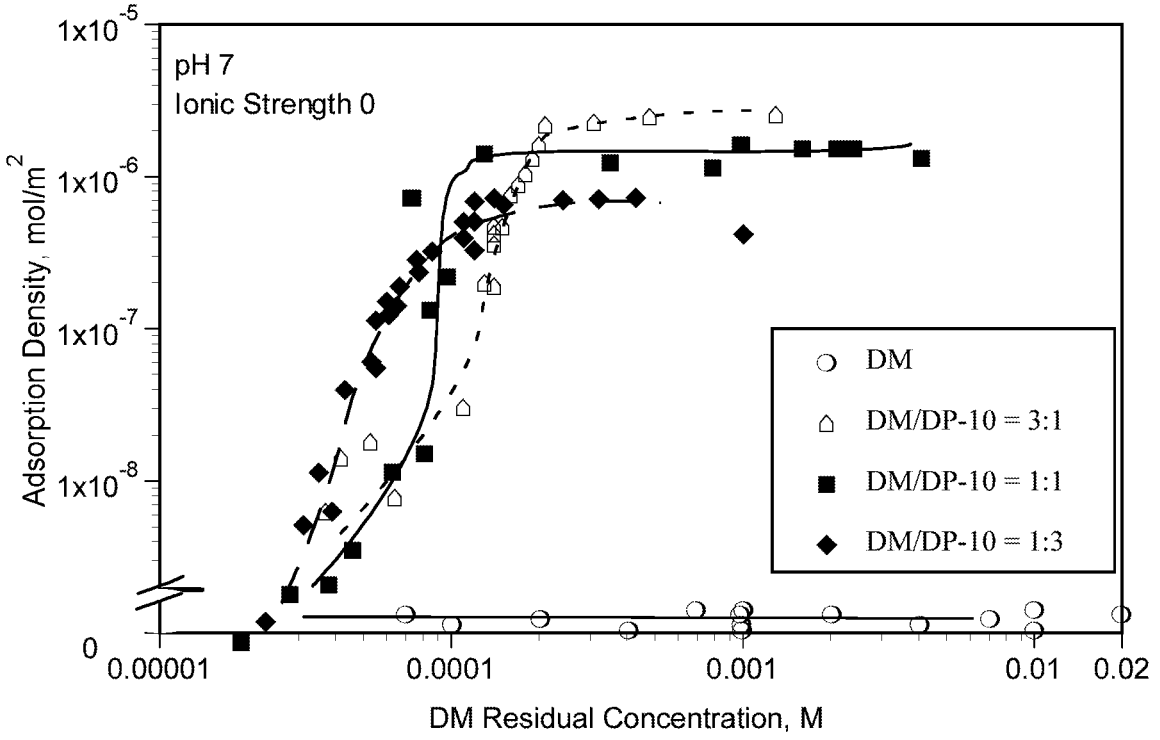


**Figure 76. Adsorption of DM on Silica: Adsorption alone and from Mixtures**

In order to illustrate the role of each surfactant in the mixture, the adsorption of DM/NP-10 mixtures is plotted together with the DM/NP-10 ratio in the adsorbed layer (Figure 77). For all mixtures, the DM/NP-10 ratios vary markedly as a function of concentration. The DM exhibits a low ratio at low concentrations since it does not adsorb on silica directly and there is no hydrophobic interactions at these concentrations. The DM percentage increases rapidly where the adsorption also increases rapidly, suggesting hydrophobic chain-chain interaction to be active in this concentration range. The DM/NP-10 ratios reach a maximum value and then decrease. This behavior is very similar to those of DM/DTAB mixtures.

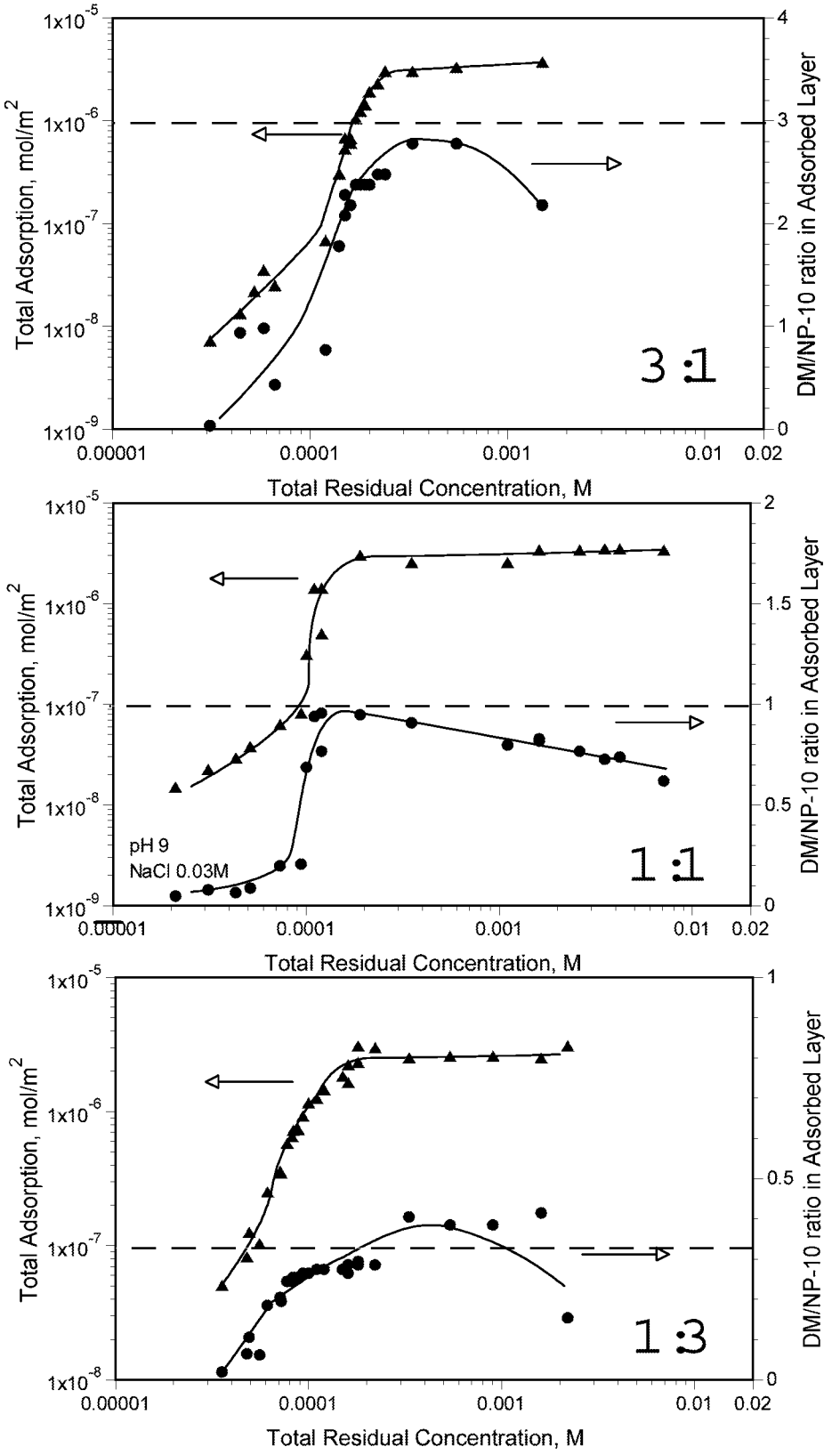


**Figure 77. Adsorption of DM/NP-10 Mixtures and the DM/NP-10 ratios on Silica**

The adsorption of nonionic-nonionic mixtures of n-dodecyl-β-D-maltoside(DM) and nonyl phenol ethoxylated decyl ether (NP-10) on silica is very similar to that of DM/DTAB system: DM adsorbs on silica through hydrophobic chain-chain interactions with the adsorbed NP-10 which acts as an anchor for DM. While NP-10 adsorption is influenced by the presence of DM. The ratios of DM/NP-10 in the adsorbed layer are also similar to those of DM/DTAB systems, suggesting that similar interactions are responsible for the adsorption of sugar-based DM on silica.

In summary, the adsorption of n-dodecyl-β-D-maltoside (DM) in mixtures with the nonionic nonylphenol ethoxylated decyl ether (NP-10), on silica has been studied at various mixing ratios. In these systems, DM does not adsorb on the silica by itself. However, in the mixtures, DM adsorbs on silica through hydrophobic chain-chain interactions with the adsorbed NP-10. The DM adsorption is characterized by a sharp increase of DM adsorption density at a given concentration. Again, NP-10 acts as anchors for DM, like in the case of DTAB/DM mixtures.

In mixed systems, NP-10 adsorptions are affected markedly by the presence of DM. As long as the surface is not saturated, NP-10 adsorbs more than when alone in the presence of DM. When the surface is saturated, NP-10 adsorption is reduced due to the competition from DM for adsorption sites. The ratios of DM/NP-10 in the adsorbed layer are found to be a function of the adsorption density. The ratios start low at low concentrations, increase rapidly in regions where chain-chain interactions dominate, reach a maximum at the onset of plateau region, and then decrease.

## 9. ADSORPTION/DESORPTION BEHAVIOR OF SURFACTANTS IN PACKED COLUMNS

Adsorption/desorption behavior of surfactants and their mixtures has been investigated by studying equilibrium adsorption/desorption process. Since the chemical flooding process in EOR is a dynamic and continuous operation, it is important to understand the kinetics of surfactant adsorption/desorption in the presence of packed reservoir materials. To relate results of equilibrium tests to field operations and design more relevant tests, some selected tests were done with packing columns. The surfactant used for these tests was a nonionic surfactant, pentadecylethoxylated nonyl phenol (NP-15).

It is known from our previous work that NP-15 will not adsorb on the alumina surface by itself. Hence a 5 x $10^{-4}$ M NP-15 solution was pumped through the alumina column continuously and the results shown in Figure 78(a) were used as a baseline for our analysis. In all our experiments, the pump was run from "0 minute" and the surfactant solutions were pumped in at "10 minutes". It took about 3 minutes for the surfactant to begin to elute out of the column, and about 6 minutes for the concentration to reach its original level. This is indicated by the higher level plateau in figure 78(a). Curve 78(b) shows the plot obtained for the elution of NP-15 pumped through the silica column at a concentration of 5x $10^{-4}$ M. It can be seen that there is no signal on the detector during the test period. This suggests that all the injected surfactant has been completely adsorbed on the silica, and it will take additional time before a steady state is attained. By subtracting curve (b) from curve (a), adsorption of NP-15 on silica is obtained as a function of time(curve c)

Adsorption behavior of the nonionic NP-15 at a higher concentration level (1.0 x$10^{-2}$ M) is illustrated in Figure 79. Again, curve (a) is the baseline obtained for 1.0 x$10^{-2}$ M NP-15 injected through the alumina column. Curve (b) is the signal recorded for the surfactant injected through the silica gel column. By subtracting curve (b) from curve (a), we obtain adsorption of NP-15 on silica as a function of time (curve c). These results show that it will take about 8 minutes for the surfactant NP-15 to reach equilibrium adsorption at the concentration of 1.0 x$10^{-2}$ M for the silica column used

in this study. Clearly, the time needed to reach equilibrium adsorption in the packing column is affected by the type of column, packing density, and flow rate of the mobile phase. These factors warrant further investigation.

During the chemical flooding process, surfactants and their mixtures are used along with other components such as polymers to lower the surface tension of water/oil interface and to displace oil from the rock surface. It can be useful to make the surfactants adsorb on the rock surface in such as way as to make it water wetted and thus displace oil efficiently. On the other hand, it will be useful to easily have the surfactant desorb by subsequent washes so that it is regenerated. To understand the desorption behavior of surfactants during chemical flooding process, packing column tests were conducted with wash solutions after the adsorption of the nonionic surfactant NP-15.

As mentioned earlier, it takes about 8 minutes for the nonionic NP-15 to reach equilibrium adsorption on the silica surface at a concentration of $1.0 \times 10^{-2}$ M. After the adsorption process is complete, the injection of the surfactant solution was discontinued and the mobile phase was switched to water. Desorption of NP-15 from this column was monitored and the results obtained are shown in Figure 80. In the current tests, the injection of the surfactant solution was stopped after 26 minutes. It appears that it takes a little longer for all the surfactant to desorb from the silica packed column than that from alumina column (curve a). The results obtained can be accounted for by the fact that NP-15 adsorbs on the silica surface but does not adsorb on the alumina surface. It is to be noted that once the desorption starts, the rate of desorption of NP-15 is faster than that indicated by the baseline (curve a). Thus, the curve c reaches a maximum rate at about 31 minutes. The enhanced desorption of NP-15 at this stage is attributed to the deaggregation of NP-15 solloids (hemimicelles) at the silica surface. This can indeed be useful since the net surfactant loss is thus minimized. It should be noted that there is always a small amount of NP-15 which does not desorb from the surface.

To understand the synergism between the surfactants in mixtures, packing column tests were done with mixtures of nonionic pentadecylethoxylated nonyl phenol (NP-15) and anionic sodium

dodecyl sulfate (SDS). It has been reported earlier by us that NP-15 does not adsorb on the alumina surface by itself. It can co-adsorb with anionic sodium dodecyl sulfate (SDS). In this case the dodecyl sulfate species can function as anchors to make the adsorption of NP-15 on alumina possible. The results obtained for packing column tests with the mixtures of nonionic NP-15 and the anionic SDS are shown in Figure 81. When $5.0 \times 10^{-4}$ M NP-15 solution was pumped through the alumina column, curve a was obtained and this serves as reference since there is no adsorption of NP-15 on alumina. The results obtained for the mixture of $5.0 \times 10^{-4}$ M NP-15 and $5.0 \times 10^{-3}$ M SDS pumped through alumina column are illustrated in Figure 81 (b). By subtracting curve b from curve a, results for adsorption of NP-15 on alumina (curve c) are obtained. A small adsorption peak of NP-15 is evident on curve c due to the synergism between the adsorbed SDS and NP-15. Clearly, the adsorbed SDS molecules facilitate co-adsorption of NP-15. It is noted that the adsorption peak of NP-15 occurred within a short time after the injection was started, and the NP-15 concentration level on curve b is always lower than that on curve a. This suggests that a small amount of NP-15 is being continuously adsorbed on alumina in the presence of SDS.

In summary, adsorption of NP-15 on silica gel reaches equilibrium within a few minutes and the kinetics of this adsorption merits further investigation. It is seen that the deaggregation of NP-15 hemimicelles from silica surface can enhance the desorption of NP-15 and this phenomenon might be utilized in designing efficient chemical flooding schemes. The adsorption of nonionic NP-15 on alumina is facilitated by the co-adsorbing anionic dodecyl sulfate and this co-adsorption can be a prolonged process. All such co-adsorption as well as desorption can have marked effects on surface properties such as wettability.

**Figure 78. Elution of 5 × $10^{-4}$ M NP-15 through alumina (a) and silica (b) column, and adsorption of NP-15 on silica (c)**

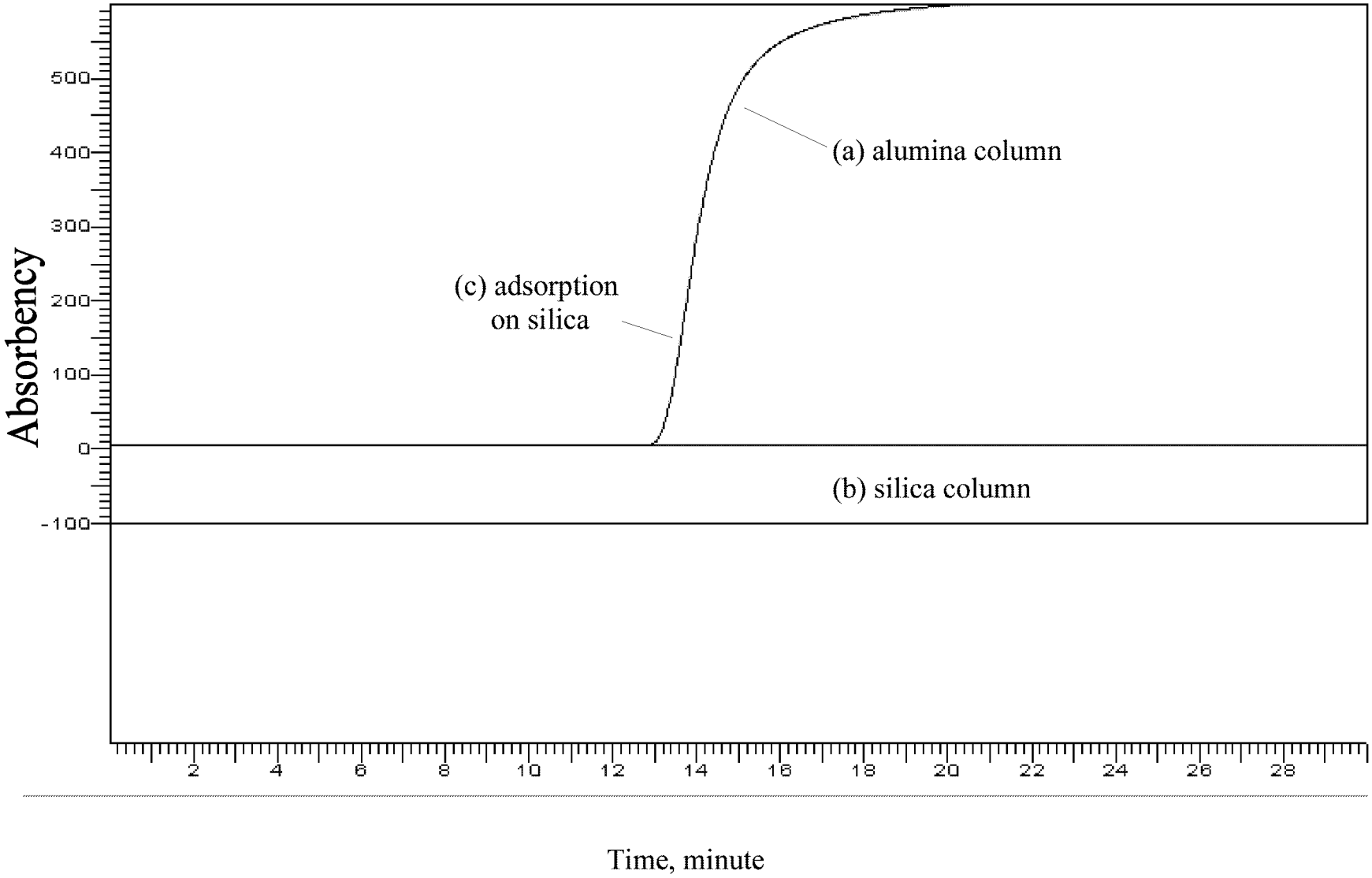

**Figure 79. Elution of 1 × $10^{-2}$ M NP-15 through alumina (a) and silica (b) column, and adsorption of NP-15 on silica (c)**

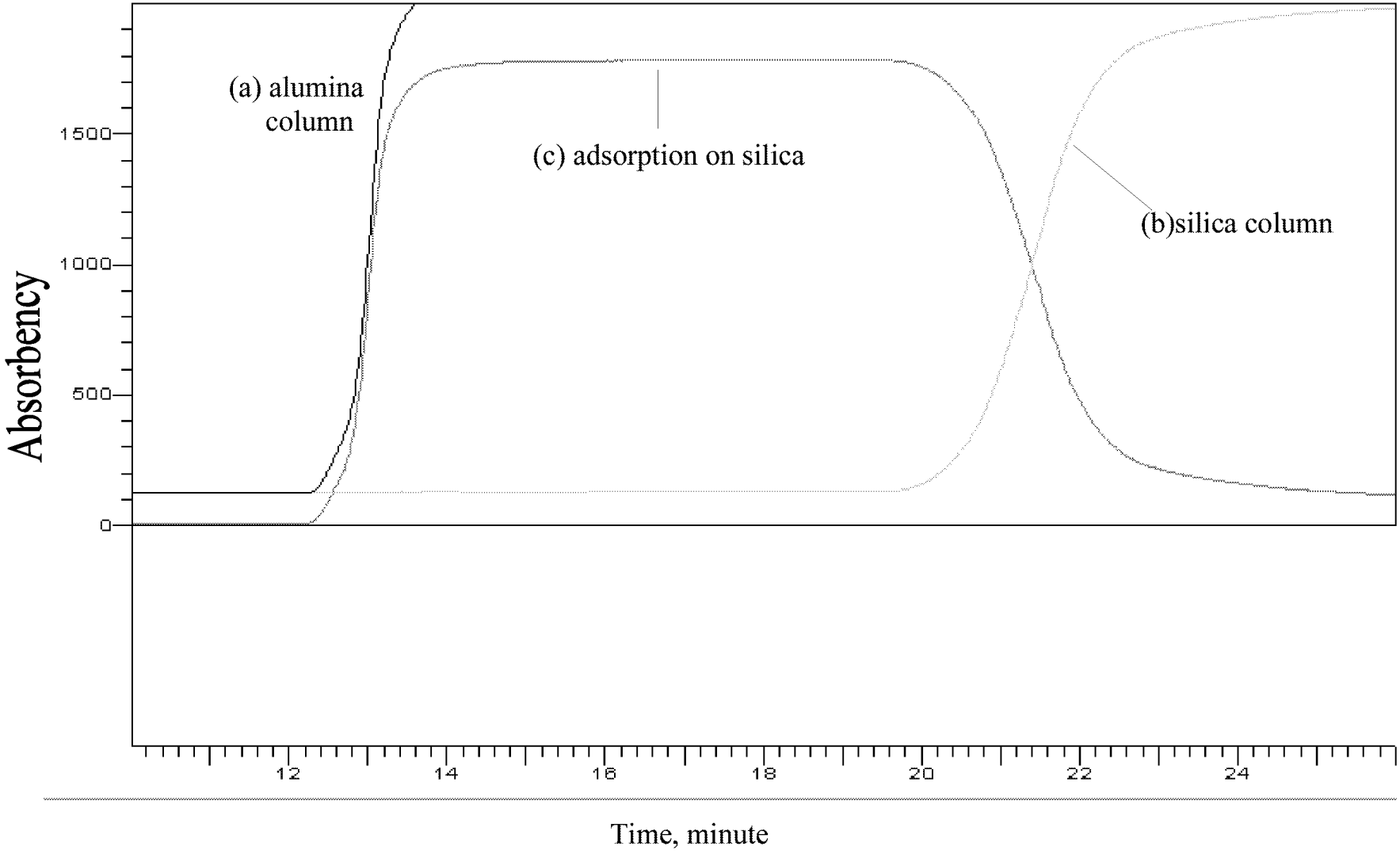

**Figure 80. Diagram illustrating desorption of 1 × $10^{-2}$ M NP-15 from alumina a) and silica b)columns, and net desorption of NP-15 from silica c)**

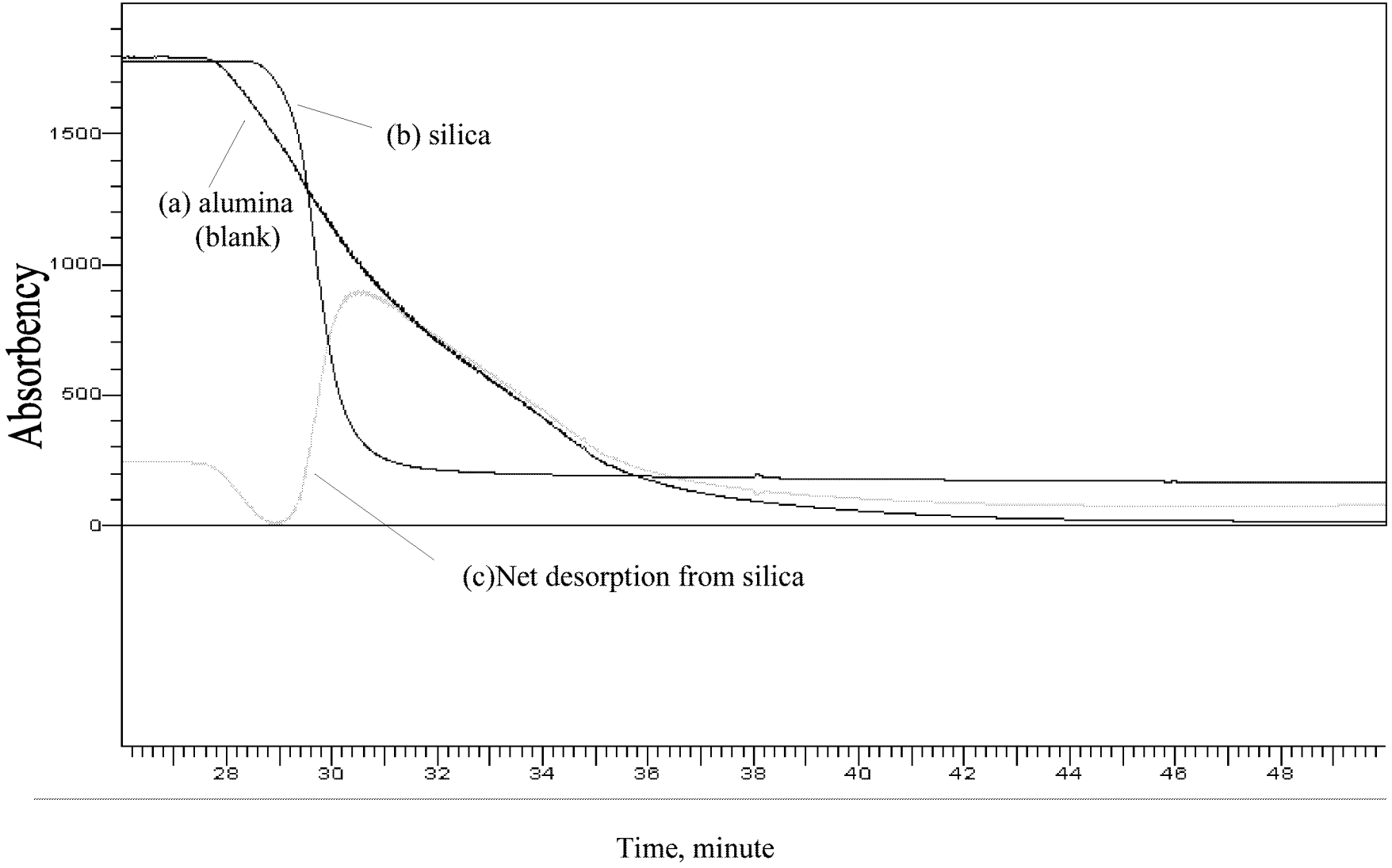

**Figure 81 Adsorption of nonionic NP-15 on alumina. a) NP-15 alone b) NP-15/SDS mixtures c) net adsorption of NP-15 from NP-15/SDS mixture**

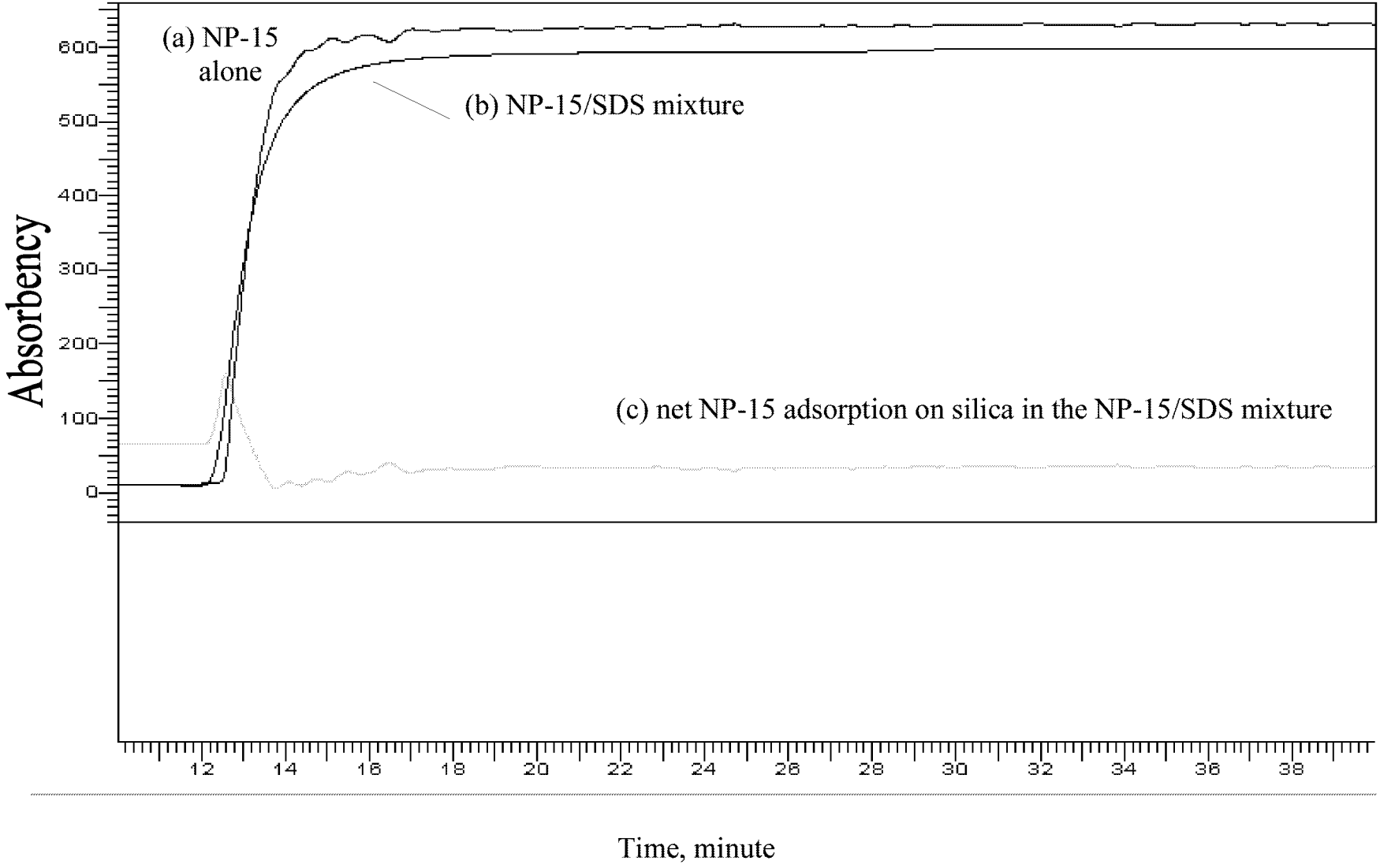

# 10. THEORETICAL AND EXPERIMENTAL STUDIES OF THE ADSORPTION OF SURFACTANT AT INTERFACES

*Description of The Model*

When a clean interface is created in a surfactant solution, surfactant monomer adsorbs onto the surface from the sublayer of liquid immediately adjacent to the surface as a function of time. The adsorption reduces the monomer concentration in the subsurface region causing breakdown and diffusion of micelles from regions far away from the surface towards the surface. We examine the case in which the rate of micelle breakdown is much faster than the rate of its bulk diffusion towards the surface. This will be the case as long as the micelle concentration is not too large. In this case, micelles act as reservoir to maintain a monomer concentration equal to the CMC. Two regimes of surfactant transport are studied.

In the first, the initial kinetic rate of monomer adsorption is assumed to be very fast compared to the rate at which micelles diffuse from the bulk to the surface. Micellar diffusion cannot supply surfactant fast enough to the subsurface region to maintain concentration of the monomer at CMC, and as a result micelles disappear in the vicinity of the interface creating a micelle-free zone the front of which moves outward from the surface. At the front, micelles break down to supply surfactant monomers to the zone. Within the micelle free zone, monomer diffuses to the surface from the front where its value is equal to the CMC and where the sublayer concentration is controlled by the kinetic quasi-equilibrium and is below the CMC. From the front of the micelle free zone to the region of the solution far from the interface, the monomer concentration is uniform. In this region, micelles diffuse from the far field (where the micelle concentration is prescribed) to the front (where the micelle concentration is zero) to replenish micelles breaking down at the front. As adsorption onto the surface proceeds, the monomer subsurface concentration increases towards the CMC, the

concentration gradient of monomer across the micelle-free zone is reduced and the front begins to move back towards the interface. The micelle diffusion gradient also relaxes as the monomer flux in the micelle free zone decreases. At equilibrium, the front arrives back at the interface and the bulk solution is once again a uniform micellar solution.

In the second regime, the initial rate of adsorption is assumed to be of the same order as the rate of micellar diffusion. Micellar diffusion can now supply enough micelles to the surface vicinity so that the micellar breakdown maintains a value of the monomer concentration equal to the CMC for an extended period. During this time the micelle concentration in the subsurface layer decreases so that diffusion of micelles can continue to match the kinetics of adsorption of surfactant onto the surface. Eventually, the micelle concentration at the sublayer falls to zero, and diffusion of micelles can no longer match the kinetics of adsorption. A micelle free zone once again forms as before, and the front of the zone moves outward and eventually returns to the surface at equilibrium. Numerical solutions of the dynamic surface concentration are obtained for both cases in terms of kinetic coefficients and monomer and micelle diffusion coefficients. By using an equation of state, the surface tension reduction accompanying the adsorption is calculated. Micelle diffusion coefficients and the number of monomers per micelle are known from light scattering experiments, and monomer diffusion coefficients and adsorption kinetics parameters are known from measurements of dynamic tension reduction for solutions below the CMC. As a result this micelle transport model can predict the adsorption (and tension reduction via the equation of state) with no adjustable parameters.

*Mathematical Formulation*

At t=0, a fresh interface is created and monomers begin to adsorb at the fresh interface. The Columbia model is for a flat interface that extends infinitely in the x-y direction and is located at z=0. The bulk fluid is assumed to extend infinitely in the z direction. The adsorption of the monomers is balanced by the breakup of the micelles that diffuse from the bulk. Let $c_m$ and c be the concentration of micelles and monomers respectively. The diffusion of both species is governed by the diffusion

equation:

$$\frac{\partial c}{\partial t} = D\frac{\partial^2 c}{\partial z^2}$$

$$\frac{\partial c_m}{\partial t} = D_m\frac{\partial^2 c_m}{\partial z^2}$$

The initial conditions are :

$c(z, 0) = CMC$

$c_m(z,0) = c_b$

The boundary conditions are:

at $z = 0$

$$D\frac{\partial c(0,t)}{\partial z} = \beta(\Gamma_\infty - \Gamma)C_s - a\Gamma$$

$$\frac{\partial \Gamma}{\partial t} = \beta(\Gamma_\infty - \Gamma)C_s - a\Gamma$$

at $z = \delta(t)$

$$D\frac{\partial c(d(t),t)}{\partial z} = ND_m\frac{\partial c_m(d(t),t)}{\partial z}$$

$C_M(\delta(t), t) = 0$

$C(\delta(t), t) = cmc$

at $z = \infty$

$C_M(\infty, t) = c_b$

*Experiments*

The surface tension experiments were done using a sessile bubble apparatus at room temperature of 25°C. Figures 82 through 86 show the surface tension of a $C_{14}E_6$ solution as a function of time; The critical micelle concentration of $C_{14}E_6$ is $9.19 \times 10^{-6}$ M. In Figure 82, the surfactant concentration is $5.965 \times 10^{-6}$ M which is slightly below the CMC; this concentration was used for the purpose of comparing with data previously obtained by other researchers and for checking our apparatus and solution. As shown in the plot, the surface tension starts at 72 mN/m which is the surface tension of a clean air-water interface and reduces to an equilibrium tension of 32 mN/m in about 400 seconds. In Figure 83, the bulk concentration of $C_{14}E_6$ is $1.927 \times 10^{-5}$ M which is approximately twice the CMC; at this concentration, the tension drops to 31 mN/m in 140 seconds. Since the bulk concentration at the beginning of the experiment is higher than the CMC and the depletion in the bulk concentration due to adsorption is negligible, the bulk concentration stays above the CMC even after the equilibrium has been reached. In our model, since there is no micelle adsorption on the interface, at equilibrium the adsorption of monomers is balanced by desorption, i.e., $\Gamma = \Gamma_\infty \frac{\beta\,CMC}{\beta\,CMC + \alpha}$. Thus, a further increase in the bulk concentration should not affect the equilibrium surface concentration and surface tension. However, the time needed to reduce the tension from that of a clean interface to the equilibrium value will decrease. The model predictions are supported by the experimental data in figures 84 through 86. The bulk concentration in Figure 84 is $3.911 \times 10^{-5}$ M which is about 4 times the CMC. As shown in the plot, the equilibrium tension is still 31 mN/m; however, the time needed to reach the equilibrium is about 60 seconds. At a concentration of $7.719 \times 10^{-5}$ M, approximately eight times the CMC, it takes 20 seconds to reach the

equilibrium and at a concentration of $9.666x10^{-5}$, approximately ten times the CMC, it takes 14 seconds to attain the equilibrium. These results are summarized in the following table:

**Table 7. Summary of Figures 82 - 86**

| Concentration [M] | Equilibrium Surface Tension [mN/m] | Time [seconds] |
|---|---|---|
| $5.965x10^{-6}$ (below CMC) | 32 | 400 |
| $1.927x10^{-5}$ | 31 | 140 |
| $3.911x10^{-5}$ | 31 | 60 |
| $7.719x10^{-5}$ | 31 | 20 |
| $9.666x10^{-5}$ | 31 | 14 |

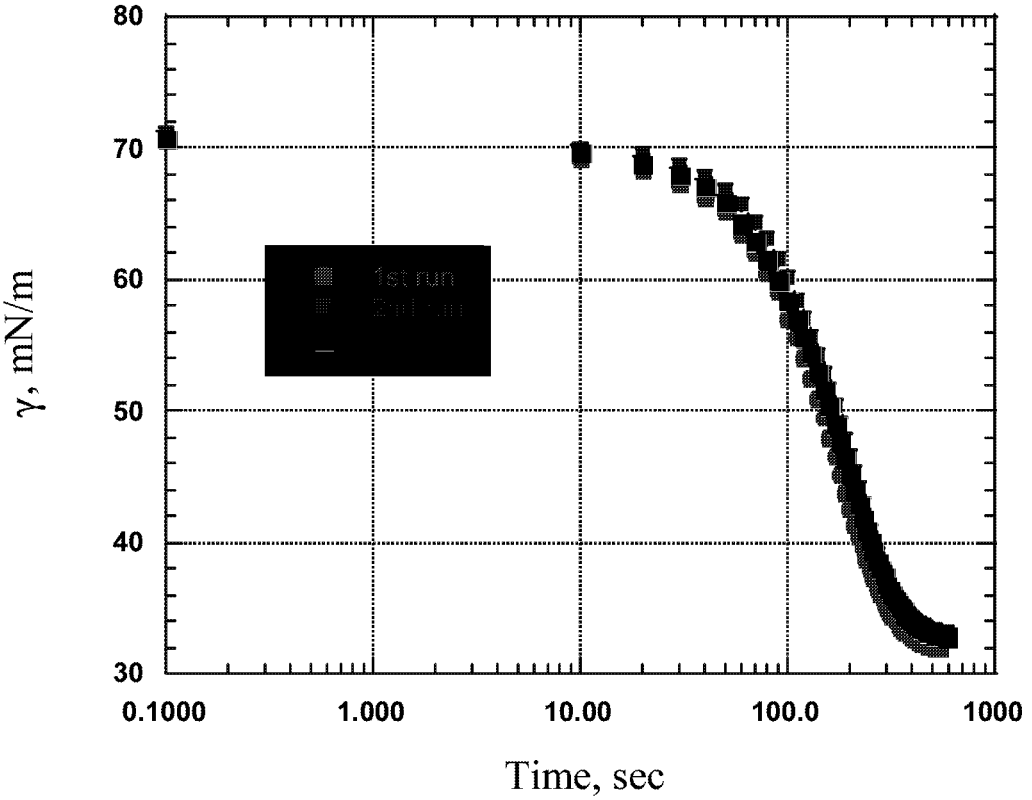


**Figure 82 Surface tension of $C_{14}E_6$ solution ($5.965 * 10^{-6}$M) as a function of time**

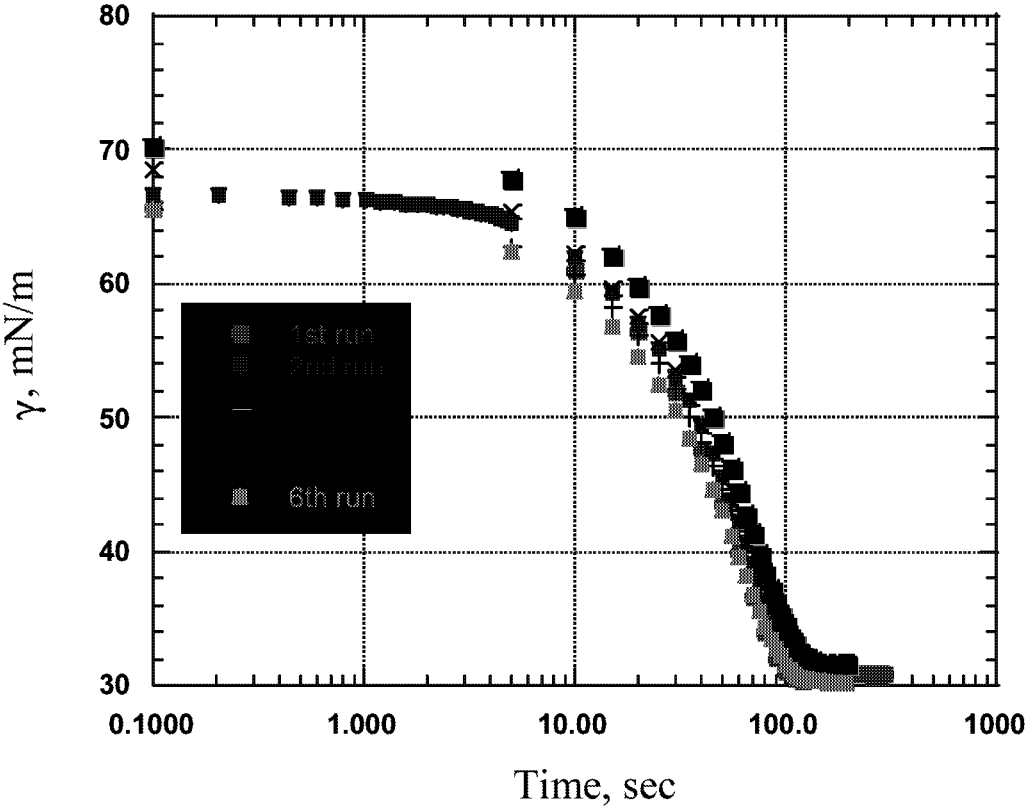


**Figure 83 Surface tension of $C_{14}E_6$ solution ($1.927 * 10^{-5}$M) as a function of time**

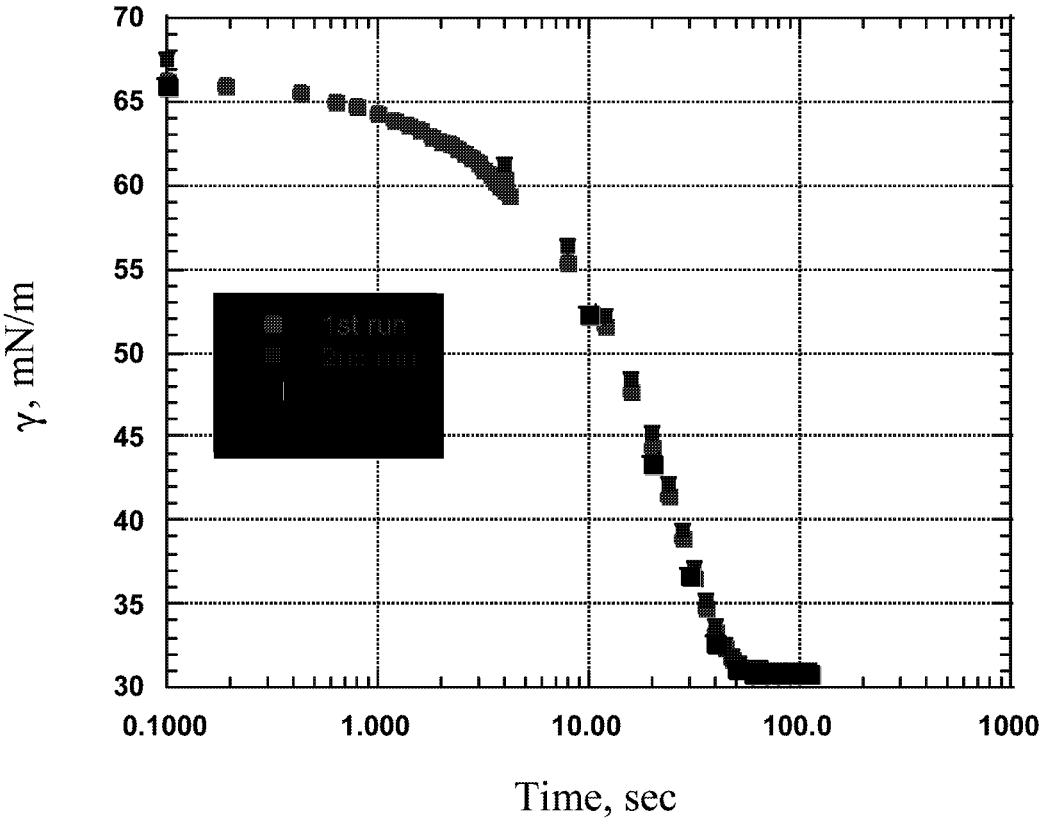


**Figure 84 Surface tension of $C_{14}E_6$ solution ($3.911 * 10^{-5}$M) as a function of time**

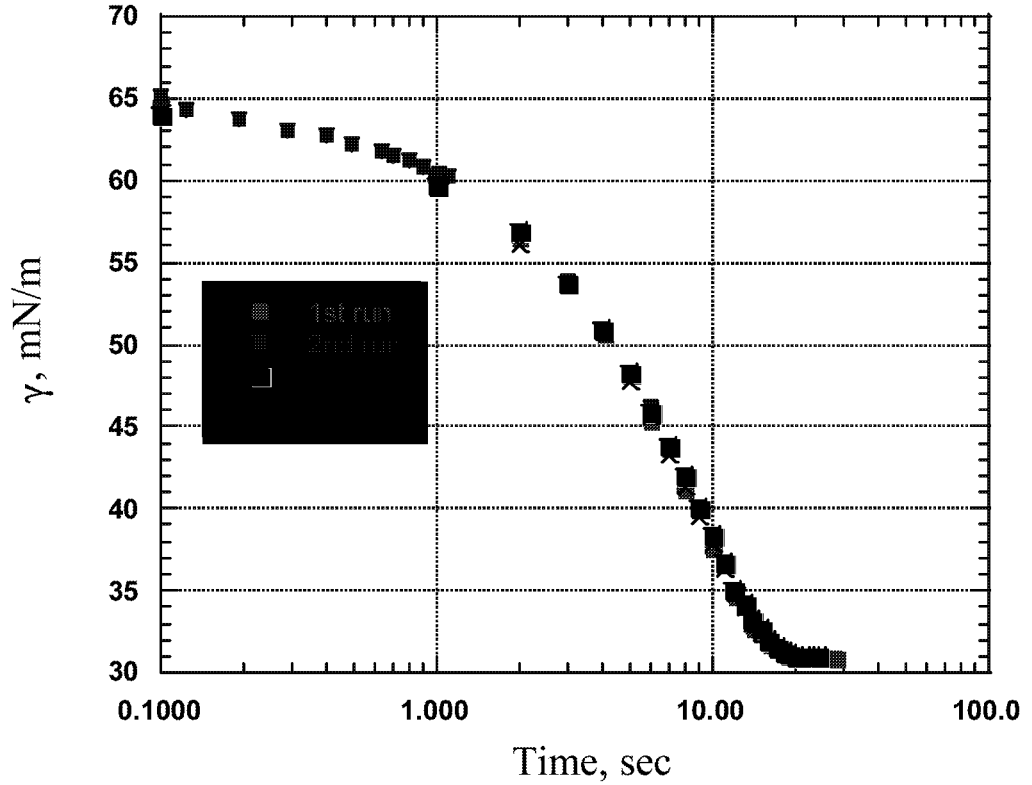


**Figure 85 Surface tension of $C_{14}E_6$ solution ($7.719 * 10^{-5}$M) as a function of time**

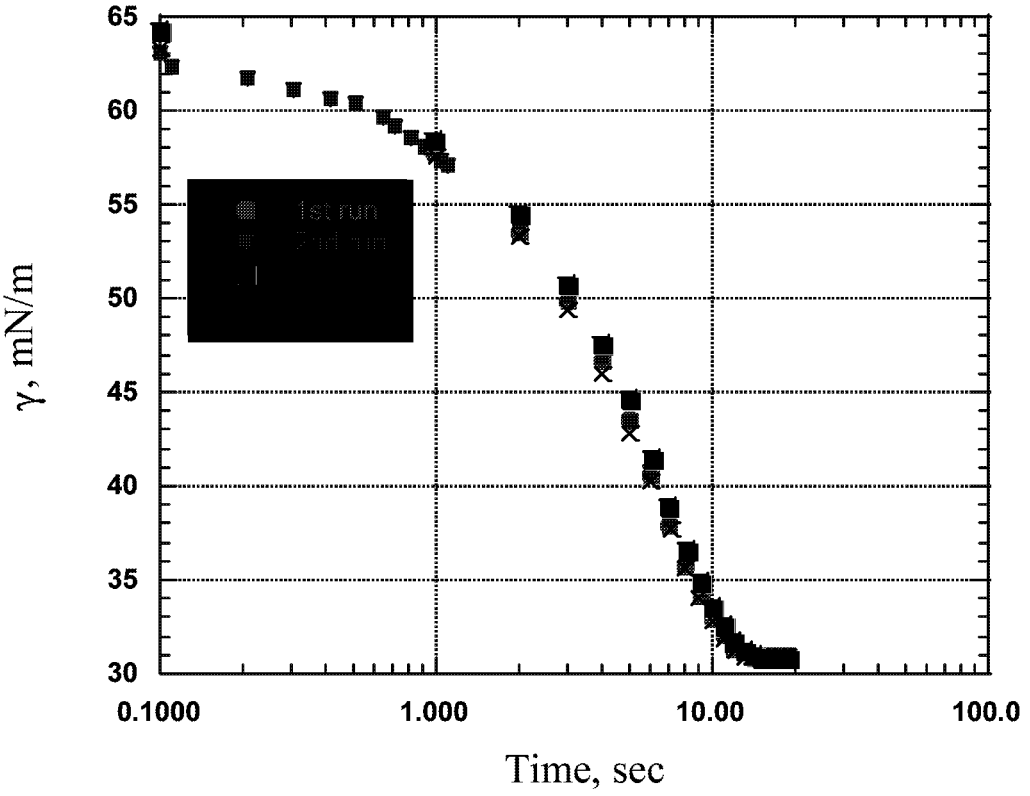


**Figure 86 Surface tension of $C_{14}E_6$ solution (9.666 * $10^{-5}$M) as a function of time**

It is clear from these results that a valid theoretical model can be developed for surfactant adsorption. The model will indeed need modifications for it to be applicable to real conditions involving mixed micelles and solid particles.

## IV. SUMMARY AND CONCLUSIONS

In this project, micro and nanocharacteristics of alkyl pyrrolidones and sugar-based surfactants in solution and at interfaces, especially in mixtures with other components, have been systematically investigated as a function of various parameters relevant to enhanced oil recovery (EOR). The major findings of these comprehensive studies are summarized with scientific significance and industrial importance highlighted.

### Phase Separation, Surface Activity and Micellization in Mixtures of N-hexyl 2-pyrrolidone And Water

In the study of phase behavior and surface activity of N-hexyl 2-pyrrolidone (HP), it is found that HP and water are partially miscible above a lower consolute temperature (LCT) of 19.1 °C. HP is surface active at the air/solution interface and forms micelles in solution at all temperatures ranging from the freezing point up to the LCT and up to 25 °C in the water-rich phase above the LCT. At low water contents, water is positively adsorbed at the air/solution interface. These results are very important for designing the interfacial behavior of the surfactants during the process of enhanced oil recovery.

### Micellization Behavior of N-cyclohexyl-2-pyrrolidone

To better understand structure-performance relationship, the aggregation of another pyrrolidone surfactant, N-cyclohexyl-2-pyrrolidone (CHP), in aqueous solution and its adsorption at the air/solution interface were also studied, using surface tension, pyrene solubilization, fluorescence, viscosity, freezing point, and calorimetric techniques. It was found that CHP molecules

form small micelles in water at a relatively high c.m.c. (0.45 M). The interior of the micelle is more polar than that of the common long-chain surfactants such as sodium dodecyl sulfate (SDS). This compares with the behavior of hexyl pyrrolidone micelles. At high CHP/$H_2O$ ratios the large exothermic heats of mixing suggest hydrate formation. The partial molar heats of dilution in the micellar range indicate that the micellar structure changes significantly with concentration. The two-dimensional second virial coefficient of the adsorbed monolayer of CHP at the air/water interface, estimated using the surface pressure data at low CHP concentrations, becomes more negative with increase in temperature and the standard heat of adsorption is endothermic. Surprisingly, this suggests increasing attraction between chains with increase in temperature. Implications of increase in temperature in enhanced oil recovery (EOR) on adsorption due to this should be noted.

Sugar-based Surfactant at the Solid/liquid Interfaces

Adsorption of n-alkyl-β-D-glucosides and maltosides on solids was investigated. The adsorption is proposed to be due to interactions between the solid surfaces and the hydrophilic groups of the surfactant, and at high surfactant concentrations hydrophobic interaction between the surfactant chains. The adsorption of surfactant on hydrophilic solids such as alumina is divided into three regions. At lower concentrations, the surfactant adsorbs on the solid surface individually due to interactions between the surfactant head and the solid surface. At higher concentrations interactions between surfactant chains take place leading to a steep rise in adsorption. Above the cmc of the surfactant the adsorption reaches a plateau. The structure of the saturated adsorbed layer is close to that of a bilayer with hydrophobic chains interpenetrating each other.

The adsorption on hydrophilic solids showed the surfactant to absorb on alumina, hematite

and titania, but much less on silica. The shapes of the adsorption isotherms for alumna, hematite, titania are quite different from that for silica, either. This behavior of alkyl maltoside on hydrophilic solids is opposite to that of alkyl polyethylene oxide surfactant, and this unique behavior of the sugar-based non-ionic surfactant has practical implications. Effect of salt on the adsorption is attributed to the salting out of the surfactant hydrophobic chain. The adsorption is not affected by the pH changes in the solution. Temperature also has a small effect on the adsorption, suggesting that there is no chemical interaction between surfactant and alumina.

On these solids the final adsorption state is the one in which the surface becomes hydrophilic. This is supported by the results obtained for the wettability and stability changes of the solids upon surfactant adsorption. These properties enable the n-dodecyl-β-D-maltoside to be utilized in wetting, oil recovering processes.

Adsorption Mechanism of n-dodecyl-β-D-maltoside on Alumina

Adsorption of sugar-based n-dodecyl-β-D-maltoside on alumina has been studied in more detail to reveal the mechanisms of adsorption. Through systematic studies, it was concluded that neither electrostatic interaction nor chemical interaction is the single governing force for the adsorption of n-dodecyl-β-D-maltoside on this oxide. The adsorption isotherm of n-dodecyl-β-D-maltoside on alumina has a relatively small slope in the low concentration range, indicating weak driving force for adsorption. The sharp increase in adsorption density at higher concentrations is attributed to the hydrophobic chain-chain interactions. This is indicated by the concave shape of the isotherm. It is therefore proposed that hydrogen bonding between hydroxyl groups on the surfactants and alumina surface hydroxyl species is the primary force for the adsorption of alkyl polyglucosides

on alumina. This has been verified by studying the adsorption/desorption of this surfactant in the presence of urea and DMSO (dimethyl sulfoxide), both hydrogen bond breakers, and FTIR analysis.

Mixtures of Sugar-based Surfactants with Other Types of Surfactants in Solution

Mixtures of the sugar-based n-dodecyl-β-D-maltoside (DM) with the cationic dodecyltrimethyl ammonium bromide (DTAB), the anionic sodium dodecylsulfate (SDS) and the nonionic pentaethyleneglycol monododecyl ether ($C_{12}EO_5$) in solution, with and without the supporting electrolyte, was studied by surface tension measurement and fluorescence spectroscopy. The interaction parameters, as measures of surfactant interactions, were calculated for these systems. Sugar-based surfactants upon mixing with cationic and anionic surfactants show strong synergy, because the mixing of an ionic surfactant with a nonionic surfactant will cause a decrease in the surface charge density of the micelles. As a result, the mixed micelles of ionic and nonionic surfactants are more stable. This effect is further accompanied by a depression of the steric repulsion between the headgroups at the micellar surface. All these effects cause synergism. On the other hand, behavior of mixtures of nonionic surfactants is close to ideal mixing since there is no change in the electrostatic interactions in these micelles. Salt is found to reduce the synergy between surfactants, mainly due to charge neutralization effect of counter ions.

The magnitude of interactions between n-dodecyl-β-D-maltoside with other surfactants follows the order anionic/nonionic > cationic/nonionic > nonionic/nonionic. The weaker interaction in cationic/nonionic systems is possibly due to the fact that DTAB has a bulky headgroup that can hinder the formation of compact micelles. This order is also in accord with the general trend observed for some large numbers of mixed surfactant systems.

Polarity parameter, as studied by the fluorescence, shows the interior of all the above mixed micelles to be mildly hydrophobic (value of 0.82-0.84 in comparison to 0.78 obtained for ionic micelles and 0.85 for nonionics). Similarities in value for mixtures with the cationic and the nonionic surfactants suggest the predominating effects of the nonionic surfactants.

Adsorption of Mixtures of Nonionic Sugar-based Surfactant with Anionic Surfactant on Alumina

To explore possible synergism or antagonism in mixed surfactant systems, the adsorption of nonionic-anionic mixtures of dodecyl polyglucosides (C12-APG) and sodium dodecyl sulfate (SDS), as well as n-dodecyl-β-D-maltoside (DM) and sodium dodecyl sulfate (SDS) on alumina have been studied at pH 6 where alumina is positively charged and pH 11 where it is negatively charged. At pH 6, marked synergistic effects between DM/APG and SDS were observed, especially in the region where hydrophobic chain-chain interaction dominates the adsorption process as long as the surface is not saturated. In the plateau region, clearly there is competition for adsorption sites. At this pH, SDS and DM/APG promote adsorption of each other and there exists mainly synergism. The strongest synergism was found when DM:SDS was 1:1. At pH 11, the adsorption of APG/SDS, or DM/SDS mixture is less than those of APG or DM alone. The presence of SDS in the systems reduces the sugar-based surfactants adsorption except in the rising part, although the SDS adsorption itself is increased due to hydrophobic interaction with sugar-based surfactants. Generally there is mainly antagonistic effect between DM/APG and SDS at this pH. Since weak adsorption of surfactants is essential for them to be cost effective in chemical flooding operations for enhanced oil recovery (EOR), these results have useful implications for the oil industry.

Adsorption of Mixtures of Nonionic Sugar-based Surfactant with Cationic Surfactant on Silica

The adsorption of the nonionic-cationic mixtures of n-dodecyl-β-D-maltoside(DM) and dodecyltrimethyl ammonium bromide (DTAB) on silica has been studied at various mixing ratios. DM does not adsorb on the silica by itself. However, in the mixtures, DM adsorbs on silica through hydrophobic chain-chain interactions with the adsorbed DTAB species. The DM adsorption is characterized by a sharp increase in density at a given concentration.

In mixed systems, DTAB acts as anchor for DM. Its adsorption is markedly affected by the presence of DM. As long as the surface is not saturated, DTAB adsorbs more because of the presence of DM. When the surface is saturated, DTAB adsorption is reduced due to competition from DM for adsorption sites. The ratios of DM/DTAB in the adsorbed layer are found to be a function of the adsorption density. The ratios start low at low concentrations, increase rapidly in regions where chain-chain interactions dominate, reach a maximum at the onset of plateau region, and then decrease. These results have implications for designing surfactant combinations for controlled adsorption for optimum wettability and dispersion.

Adsorption of Mixtures of Nonionic Sugar-based Surfactant with Nonionic Ethoxylated Surfactant on Silica

The adsorption of n-dodecyl-β-D-maltoside (DM) in mixtures with the nonionic nonylphenol ethoxylated decyl ether (NP-10), on silica has been studied at various mixing ratios. In these systems, DM does not adsorb on the silica by itself. However, in the mixtures, DM adsorbs on silica through hydrophobic chain-chain interactions with the adsorbed NP-10. The DM adsorption is characterized by a sharp increase of DM adsorption density at a given concentration. Again, NP-10

acts as anchors for DM, like in the case of DTAB/DM mixtures.

In mixed systems, NP-10 adsorptions are markedly affected by the presence of DM. As long as the surface is not saturated, NP-10 adsorbs more than when alone in the presence of DM. When the surface is saturated, NP-10 adsorption is reduced due to the competition from DM for adsorption sites. The ratios of DM/NP-10 in the adsorbed layer are found to be a function of the adsorption density. The ratios start low at low concentrations, increase rapidly in regions where chain-chain interactions dominate, reach a maximum at the onset of plateau region, and then decrease.

Adsorption/desorption behavior of surfactants in packed columns

To relate results of equilibrium tests to field operations, and to provide information on the kinetics of surfactant adsorption/desorption under situations close to oil recovery operations, kinetics of surfactant adsorption/desorption was investigated with packing columns. On silica gel, adsorption of NP-15 reaches equilibrium within a few minutes. The deaggregation of NP-15 hemimicelles from silica surface can enhance the desorption of NP-15 and this phenomenon might be utilized in designing efficient chemical flooding schemes. The adsorption of nonionic NP-15 on alumina is facilitated by the co-adsorbing anionic dodecyl sulfate and this co-adsorption can be a prolonged process. All such co-adsorption as well as desorption can have marked effects on surface properties such as wettability.

Theoretical and Experimental studies of the Adsorption of Surfactant at Interfaces

A theoretical model for the adsorption of surfactant molecules at the air-liquid and solid-liquid

interfaces both below and above the critical micelle concentration has been developed. This model was developed for the kinetics of surfactant adsorption, i.e., surfactant adsorption from the bulk solution as a function of time, to an initially clean interface above the critical micelle concentration (CMC). The model can be applicable to both solid-liquid and air-liquid interfaces. At the air-liquid interface, the surface concentration is related to the surface tension using the equation of state. In order to test this model, dynamic surface tension of $C_{14}E_6$ solutions above the CMC has been measured using a pendant bubble setup. The experiment results were correlated with theoretical predictions.

# REFERENCES


1. Salka, B. "Alkyl Polyglucoside-Properties and Application" *Cosmetics & Tolletries*, 108, 1993(3), 89

2. Balzer, D. "Alkylpolyglucosides, their Physico-chemical properties and their Uses" *Tenside Surf. Det.*, 28, 1991, 419

3. Drummond, C. J., Warr, G. G., Grieser, F., Ninham, B. W., Evans, D. F., "Surface Properties and Micellar Interfacial Microenvironment of n-Dodecyl-β-D-Maltoside," *J. Phys. Chem.*, 89, 1985, 2103.

4. Hill, K., von Rybinski, W., Stoll, G., *Alkyl Polyglycosides, Technology, Properties and Application*, VCH Publishers, Inc., New York, 1996.

5. Anjing Lou, B.A. Pethica and P. Somasundaran, "Surface and colloidal properties of cyclic amides. 1. Two-Dimensional virial coefficients for adsorbed monolayers of N-Alkyl-2-pyrrolidones at the air/water interface"Langmuir,12, 1996,5845.

6. GAF Corporation Chemical Division, M-Pyrol, N-Methyl-2-Pyrrolidone Handbook, GAF Corporation, 1972.

7. Z. Li and M.J. Rosen, *Analytical Chemistry*, **53**, 1981, 1516.

8. Dubois, M., Gilles, K. A., Hamilton, J. K., Rebers, P. A., Smith, F., "Colorimetric Method for Determination of Sugars and Related Substances", *Anal Chem*, 28, 1956, 350

9. Koenigs, W., Knorr, E., "Ueber einige Derivate des Traubenzuckers und der Galactose," *Berichte*, 34, 1901, 957

10. Noller, C. R., Rockwell, W. C., "The Preparation of Some Higher Alkylglucosides," *J. Amer. Chem. Soc.*, 60, 1938, 2076

11. De Grip, W. J., Bovee-Geurts, P. H. M. "Synthesis and Properties of Alkylglucosides with Mild Detergent Action: Improved Synthesis and Purification of β-1-Octyl-, -Nonyl-, and -Decyl-Glucose. Synthesis of β-1-Undecylglucose and β-1-Dodecylmaltose," *Chemistry and Physics of Lipids*, 23, 1979, 321

12. Rosevear, P. VanAken, T., Baxter, J., Ferguson-Miller, S., "Alkyl Glycoside Detergents: A Simple Synthesis and Their Effects on Kinetic and Physical Properties of Cytochrome *c* Oxidase," *Biochemistry*, 19(17), 1980, 4108

13. Shinoda, K., Yamanaka, T., Kinshita, K., "Surface Chemical Properties in Aqueous Solution of Non-ionic Surfactants: Octyl Glycol Ether, α-Octyl Glyceryl Ether and Octyl Glucoside," *J. Phys. Chem.*, 63, 1959, 648

14. Nickel, D., Nitsch, C., Kurzendorfer, P., von Rybinski, W., "Interfacial properties of surfactant mixture with Alkyl polyglucosides," *Prog. Colloid Poly. Sci.*, 89, 1992, 249

15. Platz, G., Thunig, C., Policke, J., Kirchhoff, W., Nickel, D., "Phase behavior of alkyl polyglucosides in combination with fatty alcohols and alkyl sulphates," *Colloids and Surfaces*, 88, 1994, 113

16. Kameyama, K., Takagi, T., "Micellar Properties of Octylglucoside in Aqueous Solutions," *J. Colloid Interface Sci.*, 137(1), 1990, 1

17. Brown, G. M., Dubreuil, P., Ichhaporia, F. M., Desnoyers, J. E., "Synthesis and properties of some α-D-alkyl glucosides and mannosides: apparent molal volumes and solubilization of nitrobenzene in water at 25 °C", *Canadian Journal of Chemistry*, 48, 1970, 2525-2531.

18. L. Zhang, P. Somasundaran, and C. Maltesh. "Electrolyte Effects on The Surface Tension and Micellization of n-Dodecyl-β-D-Maltoside Solutions", *Langmuir*, 12, 2371-1273, 1996.

# PUBLICATIONS AND PRESENTATIONS

Publications

1. Brian A. Pethica, Zhenghe Zhu, Anjing Lou and P. Somasundaran, *"Surface and Colloidal Properties of Cyclic Amides. 4. N-cyclohexyl-2-pyrrolidone/water Mixtures Aggregation in solution and adsorption at the air/solution interface"* Submitted to Journal of Colloid and Interface Science.

2. P. Somasundaran and L. Huang, "*Adsorption/aggregation of Surfactants And Their Mixtures at Solid-liquid Interfaces"* Advances in Colloid and Interface Science, Vol. 88. P. 179-208, 2000

3. P. Somasundaran and L. Huang, *"Adsorption of Polymers at Solid-liquid Interfaces"* Submitted for the book entitled "Polymer in Personal Care, Phamaceutical, and Industrial Applicatin", To be published by Marcel Dekker Inc..

4. L. Zhang, P. Somasundaran, J. Mielczarski and E. Mielczarski, "*Adsorption Mechanism of N-dodecyl-β-D-maltoside on Alumina"*, submitted to Journal of Colloids and Interface Sciences.

*Presentations*

1. S. Hazair, P. Somasundaran, C. Maldarelli, "Model for Dynamic Surface Tension above the Critical Micelles Concentration" AICHE Meeting presentation, Los Angeles, Nov. 2000

2. P. Somasundaran, "Role of Conformation of Surfactants and Polymers in Controlling Interfacial Processes" Chemical Engineering, Chemistry and Material Science Colloquium,

Polytechnic University, New York. Dec. 2000.

3. P. Somasundaran "Application of Surfactant/Polymer Interaction With Solids in Deposition, Biosurfaces & Flocculation" Presentation at Unilever Research, Pune, January, 2001

4. Lei Zhang, P. Somasundaran. "Mixed Surfactant Systems: Sugar-based Surfactants in Mixtures". Presented at I/UCRC annual IAB meeting, Columbia University, May 30-31, 2001

5. Lei Zhang, P. Somasundaran. "Adsorption of Nonionic Sugar-based Surfactants and Anionic Sodium Dodecylsulfate Mixture on Alumina" Presentation at 75$^{th}$ ACS Colloid and Surface Science Symposium, Carnegie Mellon, June 10-13, 2001

6. Rui Zhang, Lei Zhang, P. Somasundaran. "Properties of Nano-structured Solloids on Solid and Surfactant Micelles in Solution and Their Application in Industry". Presented at *2001 International Symposium on Nano-material and Technology*, Beijing, China, July 2-5, 2001